Task selectivity in mouse parietal cortex

Julie J Lee

A thesis submitted for the degree of

Doctor of Philosophy

University College London

I, Julie J Lee, confirm that the work presented in this thesis is my own. Where information has been derived from other sources, I confirm that this has been indicated in the thesis.

Abstract

A challenge for the brain is to flexibly deal with the vast variety of potential situations encountered in a lifetime. One way to deal with this challenge is to distribute multiple representations across the same neurons, another is to allocate distinct subpopulations for different contexts. Posterior parietal cortex (PPC) has been implicated in motor planning, decision making and navigation. Are the same PPC neurons involved in these diverse functions, and if so, how are these processes shared across the population? I recorded from neurons in PPC using two-photon calcium imaging and compared their activity in mice trained to perform two different visual detection tasks. In one task, the mouse turned a steering wheel to report whether a visual grating was on the left or right side. In the other, the mouse navigated through a virtual T-maze using a spherical treadmill and turned at the end to report whether a grating appeared on the left or right wall. Both tasks involved visual detection, choice, and motor execution, but many neurons were selectively active only in either task. Running could not fully account for task selectivity. Instead, selectivity was related to context more generally: activity during the task was well-predicted by activity during passive conditions on the same apparatus. Finally, I related each neuron's task event-related activity to ask whether neurons active in both tasks shared choice and stimulus preferences. Neurons did not share choice preferences across tasks, suggesting that choice selectivity is not represented abstractly in single neurons, however, there was some evidence that stimulus representations were shared across tasks. These results indicate that PPC allocates distinct neuronal populations for different purposes, determined by the context in which a task is performed. Within each task, event-evoked activity of individual neurons may be governed by multi-dimensional characteristics specific to each context.

Impact statement

The impact of the following work can be viewed with regards to two domains, one for the neuroscience of decision-making, and the other for the design of intelligent artificial systems.

While all animals encounter a multitude of potential tasks in our lives and easily switch between them, most studies of decision-making study only one task at a time. The choice of task design can complicate interpretation of the neural signals associated with each task. Instead, here I train the same mice to perform two variants of decision-making tasks and employ large-scale neural recordings at single neuron resolution to directly compare the activity of the same neurons during behavioral performance of these tasks. In doing so, I am able to explicitly test to what extent hypothesized roles attributed in the past hold up when comparing two tasks which supposedly require the same cognitive processes. In doing so, these experiments can test key assumptions of how I assume a given brain region is involved in a particular process, and reveal which aspects of previous findings were reducible to the specific task design and related confounds. Further implications are addressed in the General Discussion.

With regards to machine learning and artificial intelligence research, research in these areas take inspiration from findings from neuroscience as an inspiration of how a biological system — namely, the brain — has "solved" a given problem. A key aim of recent work in this field has been along themes known as "task flexibility/switching", "continual/lifelong learning" and "transfer learning". The key proposition is that in order to design truly "intelligent" artificial systems, neural networks need to be able to wield a key element of "higher" animal cognition, that of flexibility and generalization over tasks. Deep/recurrent neural networks have shown remarkable performance in various benchmarks, but are often specialized to perform one task at a time, and fail dramatically when tested on another task that would be expected to be very similar. When trained to learn the second task, the phenomenon of "catastrophic forgetting" occurs such that the ability to learn the first task is forgotten. Humans and other mammals are capable of juggling multiple tasks and switching between them much faster than neural networks can, so it is instructive to examine the activity of the same population of neurons across tasks to see how in a biological system, individual neurons change their activity as a function of task, in order to instruct how to design better neural networks to acquire the same capacities.

Finally, work here has been shared with the scientific community at various conferences including Cosyne, Federation of European Neuroscience Societies, Society for Neuroscience and Champalimaud Research Symposium.

Acknowledgements

These acknowledgements suffer from a recency bias, and I apologize to those I might have missed. We've had a global pandemic in between, forgive me.

These acknowledgements would not be complete without a sincere acknowledgement to those who started me on this journey as an undergraduate student. Particular thanks to my wonderful former undergraduate tutor, Josie Briscoe, my first supervisor ever Jeff Bowers, and Nina Kazanina and Colin Davis who started me on the path to computational anything. The most warmth goes to the kindness and patience beyond measure of Dawn Eagle for being my first supervisor to introduce me to rodents and "real neuroscience", and who taught me to truly care for my rats. Plus I must thank the Camgens for friendship and growing through our PhDs together. Thanks to the hilariously deadpan Risto Kauppinen for supervising me in more "real neuroscience". Finally special thanks to Conor Houghton who believed in my capabilities even when I didn't (plus allowing me to sneak into your compneuro lectures, which were the highlight of my degree despite being off-curriculum — I'm not sure you knew I wasn't enrolled!).

If the PhD is a coming-of-age story, my rotations were my formative years. The sincerest of thanks to those in my first rotation, first of all Wittawat and Barry without whom I might not have talked to anyone the entire rotation, my dance partner/office-mate Sze Ying, and the rest of the Gatsby unit during my rotation. Special thanks to my supervisors who led me through my first complete research project and publication, the friendliest person in science Mehdi, and the incredibly sharp and kind Peter D. I was also incredibly grateful to have met and received since the mentorship of my postdoc colleagues from my other rotations, Anushka and Catherine, whose clarity of understanding, awareness of the academic world and friendship were invaluable to navigating this PhD. Thank you also to Henry and Mona for helping me into this journey.

Without question I must thank my lab, whose presence I chose (despite not rotating - sorry David!) based on their wonderful ability to balance rigorous discussions of science, intense conversations on topical issues and lighthearted joking around. The lockdown has made the absence of our lab camaraderie very felt. Special mention in no particular order to Carsen, Miles, Lauren, Thomas, Anwar, Kevin, Pip, Rossi, Sylvia, Mika and of course Charu for holding the ship together. Thanks to Carsen also for giving me a cookie when I had my first paper accepted :) For guidance, thanks to Krumin for always having a deadpan comment at hand and a magical ability to bail anyone out of technical issues at any hour (including in the eleventh hour for this thesis!). For supervision and support, thank you to Matteo, who together with Kenneth have created a

wonderful example in championing the ability to express yourself simply yet clearly, to admit when you don't know an answer and of course always bring up the tail-tickling/toothache hypothesis in journal club!

The most fervent of acknowledgements goes to ice hockey, whose "moments of zen" were much-needed sanity resets, and much missed during quarantine. In particular, thank you Bobby for your tireless work with the Dragons and genuine care for the team helped me grow immensely as a hockey player. Special mention to my D-partners Martina and Leslie, friend Dom, the Dragons, Streatham Storm and the coaches, and the Bunker Boys (& Girls) including Jason and Anne. This paragraph is not long enough for how essential this was to staying sane in my PhD. Equally necessary thanks are to the summer schools I've attended, which were always such brilliant fun and always provided a much-needed reset and many more new friends, particularly CAMP, which was my first time programming a proper script.

For friendship in my PhD years, thank you to my labmates past and present above and additionally in no particular order to Harsha, Feryal, Gwen, Daniel, Kim, Svetlana, Arthur, Catherine, Sophie, Dorothea and many others I'm surely forgetting. Everyone says a PhD is a journey but a worldwide pandemic made this PhD an even crazier journey. Special mention to my virtual companions from morning coffee with Kirstie, the writing club (Rachel, Dan, Melissa), and Feryal, Sophie, Harsha and Anwar.

For making this thesis better (or giving me a scapegoat for the bad parts) thank you sincerely to Lauren, Peter, Rossi, Tai Ying and Krumin for being there at a moment's notice.

Finally, in the spirit of Daniel Colón-Ramos, I would like to dedicate this thesis to those that could have done a better job than me, but did not get the same opportunities.

Last but not least:

To the mice, without whom this thesis would be blank.

Table of Contents

ABSTRACT **5**

IMPACT STATEMENT **7**

ACKNOWLEDGEMENTS **9**

GENERAL INTRODUCTION **14**

HISTORICAL OVERVIEW OF PPC 14

THE ROLE OF PPC IN DECISION-MAKING 16

THE ROLE OF PPC IN NAVIGATION 17

The use of virtual reality environments *18*

THE CAUSAL ROLE OF PPC 19

TASK-DEPENDENT FUNCTIONS OF PPC 20

OUTLINE **23**

GENERAL METHODS **25**

BEHAVIORAL METHODS 25

Shared task structure *25*

Steering-wheel task specifics *27*

T-maze task specifics *28*

Training and testing protocols *29*

Testing within a session *29*

Behavioral quality control: Inclusion and exclusion criteria *30*

NEURAL DATA METHODS 33

Calcium imaging *33*

Retinotopy for determining the field of view for imaging *33*

Two-photon imaging acquisition methods *35*

Two-photon imaging processing methods *36*

Analysis procedures *40*

CHAPTER 2: COMPARING ACTIVITY ACROSS TASKS **41**

METHODS 41

Isolation distance *41*

Across day comparison *43*

RESULTS 45

Validation across days *46*

DISCUSSION 48

Explanations by other factors *48*

Limitations ... *49*

CHAPTER 3: THE ROLE OF MOTOR CONTEXT ... **50**

3.1: ACTIVITY DURING PASSIVE CONDITIONS ... 50

Methods ... *50*

Results ... *51*

3.2: THE INFLUENCE OF RUNNING IN EXPLAINING SELECTIVITY ... 54

Introduction ... *54*

Methods ... *55*

Results ... *57*

DISCUSSION ... 58

Interpretation of context selective subgroups ... *59*

Stationarity vs disengagement ... *60*

Limitations ... *60*

CHAPTER 4: SHARED SELECTIVITY IN ACTIVE NEURONS ... **61**

INTRODUCTION ... 61

METHODS ... 62

Receiver operating characteristic analyses ... *62*

Significance tests ... *64*

Session inclusion criteria ... *64*

4.1: SHARED CHOICE SELECTIVITY ... 65

Methods ... *65*

Results ... *70*

4.2 STIMULUS SELECTIVITY ... 76

Methods ... *77*

Results ... *77*

DISCUSSION ... 83

Within-task assessment of choice selectivity ... *83*

Across-task comparisons of choice selectivity ... *84*

Dependent stimulus and choice selectivity ... *86*

Limitations ... *86*

SUMMARY ... **88**

GENERAL DISCUSSION ... **89**

THE EXTENT OF ABSTRACTION MAY BE TASK DEPENDENT ... 89

COMPARISON TO PRIMATE STUDIES ... 90

CONTEXT-DEPENDENT SENSORIMOTOR PROCESSING ... 91

Silent cells in cortex ... 92
Implications ... 93
The importance of unbiased sampling ... 93
Spontaneous behaviors are context-dependent ... 94
Non-independent sampling of neurons across sessions ... 95
Limitations ... 95
Differences in definitions of PPC ... 95
Projection-specific differences across layers ... 96
Activity does not imply causality ... 96
Future directions ... 98
Population decoding ... 98
The influence of learning on task selectivity ... 98
Outlook ... 99
APPENDIX A ... 100
Anatomical organization of task-selective neurons ... 100
Alignment of imaging fields of view across days ... 100
Results ... 100
APPENDIX B ... 102
Comparison of isolation distance to other measures ... 102
APPENDIX C ... 103
Influence of rotational modulation ... 103
APPENDIX D ... 105
Extended methods ... 105
Surgery ... 105
Behavioral details ... 106
REFERENCES ... 108

General Introduction

Perceptual decision-making requires a series of processes from sensation to decision to action. Sensory inputs can be infinitely variable from moment to moment, but organisms are still able to extract meaningful commonalities from sensory inputs in order to generate a stable percept. In decision-making tasks, subjects are able to employ knowledge of the structure of the task to make a decision on the basis of this percept, and report this decision in the form of an action. These steps involve different layers of generalization and discrimination, and through experience and training, subjects can extract meaningful regularities and discard irrelevant details.

The posterior parietal cortex (PPC) has been argued over the years to be a key locus in sensorimotor processing, in part due to its anatomical location neighbored by visual and somatomotor cortices, and its reciprocal connectivity to those regions. On the basis of this historical characterization, diversity of reported signals therein, and some evidence for its capacity for remapping based on task demands, PPC could thus be a region which converts arbitrary sensory input into an abstract representation of choice, one that is divorced from both the minutiae of the sensory input and the particulars of the motor output.

Historical overview of PPC

The role of posterior parietal cortex (PPC) in decision-making has been attributed to a wide range of proposed functions. Early reports supported the view of as a sensorimotor "association" area, finding that humans with parietal lobe damage did not have primary sensory or motor deficits, but issues specifically connecting the two (Bálint, 1909). This impairment was called "optic ataxia", characterized by deficits in making visually-guided reaches to targets that were not reducible to visual deficits per se, as patients were still able to judge the spatial location of visual objects in the impaired hemifield (reviewed in Kerhkoff, 2001). The proposed function of the parietal cortex in making visually-guided movements was corroborated by later work in recording from neurons in the macaque parietal cortex. Neurons in this area responded during eye movements to visual targets, but importantly these responses were not engaged by passive visual stimulation or spontaneous eye movements (Mountcastle et al., 1975). Later work found that this activity was not just reflective of ongoing motor activity but also preceded it, after finding that neurons maintained activity during the delay period of a delayed saccade task when no visual stimulus was present (Andersen et al., 1987). This activity was interpreted to be reflective of an intended motor plan to act (Gnadt & Andersen, 1988). Further studies have found this

"intentional" activity to be effector-specific, with different neurons showing activity preceding reaches vs saccades; specifically, saccade plans were located in the lateral intraparietal area (LIP) and reach plans in an adjacent area named "parietal reach region" (Snyder et al. 1997).

Pioneering work that followed found that in a sensory evidence accumulation task, LIP did not just reflect the intended plan to move, but seemed to integrate noisy sensory evidence in support of the subject's eventual choice with the slope of the "ramping" activity increasing with the strength of evidence (Shadlen & Newsome, 1996; 2001). From these works, decision-related activity was interpreted in an intentional framework, by which decision-related activity employs the very neurons involved in the eventual motor action (reviewed in Shadlen et al. 2008). This view would argue that decision-related activity in PPC can differ depending on which form the action takes. Although thus less flexible to different types of actions, particularly those that have not yet been mapped to a specific motor form, this setting would be efficient for action, as abstract choices do not need to be "held in mind" to map to different actions depending on task. This interpretation predicts PPC might show different activity depending on task requirements, i.e. whether the relevant action is known beforehand.

Another line of work has attempted to discern whether decision-related activity in LIP is modulated by (visuo)spatial sensory information per se. Soon after initial studies finding neural correlates of motor plans, a different study reached the opposite conclusion, finding parietal neurons that had sensory responses in the absence of movement (Robinson et al. 1978). In the evidence accumulation work above, the saccadic targets are visual stimuli, and the spatial location of one of the saccadic choice targets was chosen as the location in which the recorded neuron showed the most persistent activity during the delay period of their task. Activity built up for choices into the neuron's receptive field and did not for choices to the other target out of its receptive field (Shadlen & Newsome, 2001). However, in this study, the choice targets were visual stimuli, and thus neurons may have shown activity due to classic retinotopic preferences. Further studies have shown that by placing the sensory stimulus to be integrated in the neuron's receptive field, LIP neurons also show modulation by this stimulus (reviewed in Freedman & Assad, 2016). In particular, a clever design that dissociated perceptual decision and motor plan related processes revealed that neurons were modulated by direction of the stimulus motion and not direction of the saccade (Bennur and Gold 2011). Lastly, more recent work has reported "mixed selectivity" in PPC: that decision-relevant activity is superimposed with decision-irrelevant activity responsive to visual stimuli (Meister et al. 2013; Park et al. 2014).

In any case, initial studies of evidence accumulation in LIP have been hugely influential in inspiring a wave of studies into decision-making in rodents. The similarity of primate and rodent PPC is unclear given the large evolutionary gap between these two species (Belmonte et al., 2015, Sereno et al., 2014). Nevertheless, even if these regions should not be inferred to be anatomically homologous, studies in macaque LIP have been instructive in shaping the direction of research in rodent PPC, to investigate whether the same functions can be found there. As in other species, posterior parietal cortex in rodents is defined according to its proximity with respect to visual and somatosensory cortices and its connectivity to other regions, particularly the lateral posterior nucleus of the thalamus (Hovde et al. 2019; Olsen and Witter 2016). Here I briefly review the existing literature on the function of PPC.

The role of PPC in decision-making

Inspired by neural correlates of evidence accumulation in parietal cortex in macaques, a wealth of studies have recorded in rodent PPC during decision-making tasks to look for neural correlates of decisions there as well. These tasks used a range of sensory modalities, including visual (e.g. Goard et al. 2016; Raposo et al. 2014; Pho et al. 2018; Pinto et al., 2019; Scott et al., 2015), auditory (e.g. Song et al. 2017; Zhong et al. 2019; Raposo et al. 2014; Runyan et al. 2017; Hanks et al. 2015; Akrami et al. 2018), tactile (e.g. Nikbakht et al. 2018; Mohan et al. 2018), and combinations of the above. Recently, many studies have also employed virtual reality techniques to study navigation-based decision tasks, the most common being some variant of a visually guided two-alternative forced-choice (2AFC) decision task embedded in a virtual "T-maze". Across studies using different task designs, authors have indeed reported choice signals in PPC, with some finding choice-selective "sequences" in VR (Harvey et al. 2012) or ramping accumulation of evidence (Hanks et al. 2015; Pinto et al. 2019; Koay et al. 2019). However, reminiscent of macaque LIP studies, many studies have also observed decision-relevant visual sensory activity (Itokazu et al. 2018; Goard et al. 2016; Pho et al. 2018), although some sensory responses persist in passive conditions (Steinmetz et al. 2019; Pho et al. 2018). The occurrence of visual-related activity may not be a surprise given that PPC in rodents overlaps with higher visual areas A, RL and AM (Wang and Burkhalter 2007; Wang et al. 2011), which have been shown to have retinotopic visual responses (e.g. de Vries et al. 2020; Andermann et al. 2011). In any case, within decision-making tasks, visual sensory activity is often present in tandem with motor choice related activity (Goard et al. 2016; Steinmetz et al. 2019; Itokazu et al. 2018). These results suggest in rodents, like in macaque LIP above, there is also reason to believe that in perceptual decision-making, PPC is involved in neither sensation nor action alone, but sensorimotor interactions.

The role of PPC in navigation

In parallel, several studies have probed the role of PPC in freely-moving rodents in navigation. In these studies, primarily conducted in freely-moving rats, activity of single PPC neurons was found to reflect self-motion signals such as egocentric heading and movement motifs, such as turns and forward running (Wilber et al. 2014; McNaughton et al. 1994; Whitlock et al. 2012; Chen et al. 1994) or movement sequences (Nitz, 2006). These signals are usually interpreted to aid in route planning.

In light of apparent choice signals in PPC, the relationship between choice signals and self-motion signals in navigation experiments is initially unclear. There may be common ground; Calton and Taube (2009) dissociated navigation as consisting of three processes, (1) orientation in space; (2) manipulation of spatial representations to enable route planning and (3) execution of the plan. This process has many parallels to how many would break down the decision process: sensation, choice and action, i.e. motor execution (reviewed in Schall, 2001). In both cases, the animal must sense the world, including relevant visual cues, and act based on this information. Navigation can indeed be interpreted as a sequence of decisions; even in the open-field, rodents are goal-oriented, guided by randomly scattered rewards in the environment. Further, when faced with a bifurcation point in a maze, rats show characteristics of deliberative decision-making, in behaviors called "vicarious trial-and-error" whereby the rat will look one down one possible path then the other, before committing to a choice (reviewed in Redish, 2016). Thus, perhaps self-motion signals can also be viewed as a decision-related motor plan for where to move next, and indeed some reports have found that self-motion activity precedes the movement by several hundred milliseconds (Whitlock et al. 2012).

In support of mixed sensorimotor processing in PPC, the self-motion signals reported above are modulated by sensory factors as well. Movement-related activity sometimes persists during navigation in the dark (Nitz 2006; Nitz et al., 2012; Chen et al. 1994), but many found an interaction between these signals and visual stimulation (Wilber et al. 2014) or the spatial location of the animal within the environment (McNaughton et al. 1994), which changes the relative positions of visual cues. In support of the role of PPC in using visual cues for navigation, rats were unable to navigate to a submerged platform in a Morris water maze using proximal landmarks after parietal lesions — although their use of distal landmarks was spared (Save and Poucet, 2000). However, in terms of self-motion vs. visually-modulated signals in these navigation studies, it is generally difficult to pinpoint whether differences in movements at

different spatial locations (such as different locations within a maze eliciting different body movements) accounts for apparent (visuo)spatial-selective activity, or vice versa.

The use of virtual reality environments

Virtual reality (VR) techniques can help make sense of these results by being able to more precisely measure, and thus relate, details of the visual scene and motor behaviors. Compared to real reality (RR) experiments, one evident difference with VR is the absence of vestibular signals; some have observed degraded hippocampal place fields in VR (Aghajan et al. 2015) but, generally, place cell responses are still present (Aghajan et al. 2015 and others e.g. Harvey et al., 2009; Dombeck et al. 2010). The extent of the mismatch likely depends on the setup, such as the immersiveness of the VR and ability to move the body and/or the head (reviewed in Aronov and Tank 2014). In VR, studies have found decision-related correlates (e.g. Harvey et al. 2012; Pinto et al. 2019) but also selectivity for the virtual spatial location in virtual reality that is not reducible to visual differences (Diamanti et al. bioRxiv; Krumin et al. 2018)

The prime advantage of VR over RR is the ability to manipulate the visual scene. In particular, in VR, it is possible to break the natural congruence of visual and motor information, through "open loop" experiments. One caveat of these manipulations is that the very act of severing this congruence might break a circuit that otherwise expects the visual scene to move with self-motion, and produce degraded responses simply as a result of the unethological nature of the manipulation. With this disclaimer in mind, the findings from these studies are still instructive. Task-relevant responses are usually reduced in "open loop" conditions (Harvey et al. 2012; Diamanti et al. bioRxiv; Krumin et al. 2018; Minderer et al. 2019) and degrade further when the mouse is stationary rather than running (Diamanti et al., bioRxiv). These results can be interpreted to confirm that PPC is not a "pure" sensory region given that sensory signals are not sensitive to congruent locomotion and/or engagement. When preference for virtual (visual) speed vs actual speed is directly compared in incongruent "open loop" segments, medial areas of parietal cortex better decode running speed than virtual speed (Diamanti et al., bioRxiv; Minderer et al., 2019). However, "open loop" periods, as discussed, are intentionally unnatural manipulations; perhaps PPC may still favor integrative sensorimotor information, with primacy for self-motion information if this congruence breaks — that is, when visual flow becomes an unreliable source of information to guide movements. Still, the precise nature of the interplay between potential sensory, motor, decision and navigation processes in PPC is confusing; instead, causal manipulations have been instructive in narrowing down the space of potential explanations for the function of PPC.

The causal role of PPC

On the whole, findings from perturbation studies are largely consistent with the hypothesis that PPC has a visual sensory or visual sensorimotor role. First, the effect of causal perturbations of PPC in rodents seems to be specific to the sensory modality, with studies finding behavioral deficits of perturbations in most visual decision tasks (Harvey et al. 2012; Driscoll et al. 2017; Zatka-Haas et al. 2020; Goard et al. 2016; Licata et al. 2017; Minderer et al. 2019; Pinto et al. 2019; Coen et al., SfN Abstract 2019; Odoemene et al., 2018), but not deficits in unisensory auditory (Erlich et al. 2015; Akrami et al., 2018; Coen et al., SfN Abstract, 2019) or tactile (Guo et al. 2014) tasks. In some of these studies, subjects performed the same motor choice for uni- or multisensory audio/visual stimuli, yet the effects of perturbation were restricted to a visual impairment (Licata et al. (2017); Raposo et al., 2014; Coen et al., SfN Abstract, 2018). In general, the modality specificity of PPC suggests that the region cares more about sensory or sensorimotor information, rather than motor information per se, given that despite the same motor actions, these studies observed different effects of inactivation with different sensory modalities.

Indeed, studies which inactivate PPC at distinct epochs within a trial implicate the involvement of PPC in early stages of the decision process where sensory information is more likely to be used (Driscoll et al. 2017; Goard et al. 2016; Zatka-Haas, Steinmetz et al. bioRxiv). In a visual Go/No-Go task with a delay, Goard and colleagues (2016) found an effect of bilateral inactivation in the stimulus period, but not delay or choice period. In the virtual T-maze decision task with a memory delay, bilateral PPC inactivation across the whole trial or first half of the trial resulted in behavioral impairments, but not inactivation of the second half of the trial. Pinto et al (2019) recapitulated this first-half effect with results showing very slight but significant impairments in a visual evidence accumulation virtual T-maze task (Pinto et al. 2019). Differences in the effect size between these studies are likely a consequence of the relative requirement for continued visual monitoring. In the visual evidence accumulation task, correct choices depend on integration of visual evidence across the whole trial, including after the halfway mark. Conversely, in the visually-guided memory task, the correct choice is known as soon as the mouse perceives the stimulus, occurring within hundreds of milliseconds at most — the time to visual perception in mice has been suggested to be even as fast as 40-80ms for large, high contrast gratings Resulaj et al. (2018). Therefore, the behavioral deficit likely depends on the time window needed to maintain a stimulus representation in PPC before sending that information to downstream regions. Finally, in a two-alternative unforced choice contrast discrimination task, Zatka-Haas, Steinmetz and colleagues (bioRxiv) used unilateral optogenetic inactivation of different cortical

areas and were able to infer a relationship between the amount of stimulus information in a cortical region and the behavioral effect of inactivating the same region. They found that the resulting bias away from contralateral choices as a result of inactivation was directly proportional to the extent to which they could decode contralateral visual stimulus information in wide-field activity in the same area. On the whole these results are consistent with PPC engaging in the sensory component of the decision-making process in a manner useful for the eventual choice.

However, not all results from inactivation studies are clear cut. Erlich et al. (2015) did not observe behavioral impairments in freely moving rats following unilateral or bilateral muscimol inactivation in either a two-alternative visual detection task (go to the side with a light) or in an auditory evidence accumulation task (judge which side has more auditory clicks). The latter lack of effect is likely attributed to the modality specificity mentioned earlier, but the lack of an effect in a visual detection task is puzzling given the otherwise consistent conclusions from other studies mentioned above. Perhaps relevantly, the same authors observed that inactivation of downstream secondary motor area (M2 or FOF) did have an effect, and bilateral inactivation of this region *with* unilateral inactivation of PPC then produced an impairment on both auditory evidence accumulation and visual detection tasks. Notably this result was not attributable to the bilateral FOF inactivation alone as the effects of bilateral inactivation were symmetric, yet the combined unilateral inactivation of PPC produced asymmetric biases for trial types depending on whether the stimulus was in the contralateral hemifield. Together these results suggest that PPC is responsible for directing sensory activity to downstream secondary motor regions (M2) to carry out relevant motor plans, a hypothesis corroborated explicitly by Itokazu et al. (2018) who found that while PPC neurons as a whole contained both sensory and motor information, M2-projecting PPC neurons preferentially contained sensory information. This view was also confirmed by inactivation studies and modelling in Zatka-Haas, Steinmetz et al., (bioRxiv).

Task-dependent functions of PPC

There may be differential involvement of PPC depending on task demands. Using unilateral PPC inactivation only, Erlich and colleagues (2015) did find a selective effect on interleaved free choice trials, in which the rat could choose either side with a light to get a sure reward. Interestingly, the selective deficit mirrored findings in humans and macaques (Wilke et al., 2012; Katz et al., 2016; and others). Thus, there may be a specific effect of unilateral parietal inactivation affecting internally-guided engagement with contralateral stimuli but that does not affect the ability to report the side of a visual stimulus. This possibility is reminiscent of contralateral neglect arising from parietal lesions in humans, which has been reported in macaques and

rodents as well (reviewed in Kerkhoff, 2001); however, it should be noted that these studies may have mistargeted the PPC and contralateral neglect may have been an outcome of lesions of nearby regions instead. In any case, the selective deficit in internally-guided decisions but not visually-guided decisions observed in Erlich et al. (2015) might link back to self-motion signals in the open field navigation even in the dark (reviewed above). That is, rodents primarily navigate through whisker feedback (reviewed in Diamond et al. 2008), so perhaps when they do not need to make use of visual information, PPC may be influenced more by motor plans. Interestingly, this strategy seems to exist behaviorally in rats; that is, when visual cues are present, rats are guided by them, when they are not, they prefer odor and self-motion cues (Maaswinkel and Whishaw 1999). Indeed, this hypothesis — that PPC privileges sensory- vs choice/motor-related information based on relative reliability or necessity of visual cues — may contextualize the aforementioned "open loop" VR results where PPC was found to favor motor information over visual information when the two are independent (Minderer et al. 2019; Diamanti et al. bioRxiv). In any case, understanding parietal activity as a function of different goals, contexts and internal states are all likely key to understanding PPC as a whole.

Indeed, inactivation results support that the role of PPC, and its relative involvement compared to other regions, is likely dependent on task. In VR, studies have reported differential effects of PPC inactivation depending on the nature of the task (Pinto et al., 2019; Harvey et al., 2012; Driscoll et al., 2017). Specifically, in these studies, bilateral inactivation impaired performance on a memory-guided detection task but not a visually guided detection task without a delay. In Pinto et al. (2019), the influence of inactivation across distributed cortical areas depended on whether mice performed a visual evidence accumulation task, a visually-guided task with a memory delay, or a visually-guided task without a memory delay, with more distributed engagement of cortical regions with more complex tasks. The lack of effect in visually-guided decision tasks in VR is difficult to interpret in light of the clear behavioral deficit in visually-guided tasks outside of VR, as discussed above albeit in unilateral inactivation studies (e.g. Zatka-Haas et al. 2020; Licata et al. 2017). In the VR tasks, the visual cue was presented as a landmark at the end of the corridor and might be interpreted as a distal cue, processing of which was observed to not be impaired in lesioned rats as discussed above (Save and Poucet 2000). A recent study suggests higher visual area rostrolateral ("RL"), which overlaps with parietal areas in mice, encodes near binocular disparities, potentially suggesting a role in selective processing of proximal visual cues (La Chioma et al. 2019). However, this area is different from the anteromedial ("AM") area used in the VR studies. One speculative interpretation is that despite PPC inactivation, the mouse could be aware of the distal cue and execute their choice before the distal cue becomes proximal.

However, thus far there is only tangential evidence to this possibility. It may be instead that visual detection in VR is qualitatively distinct from visual detection outside of VR.

Few studies have explicitly examined PPC activity within the same population of neurons as a function of task, but existing literature is supportive in suggesting some element of flexibility. In two studies, neurons in PPC were found to have shared selectivity for choice across two modalities — in one case, visual vs auditory (Raposo et al., 2014); in another case, visual vs tactile (Nikbakht et al., 2018). However, given that inactivation studies privilege the causal influence of the visual sensory information, including in the same visual/auditory study (Raposo et al., 2014), this choice selectivity could have reflected feedback activity from downstream areas. Additionally, in a visual Go/No-Go task in which the mouse had to report its choice with a lick, more PPC neurons were found to switch selectivity to the new target stimulus when contingencies were changed (Pho et al. 2018). However, in their case, different stimuli were presented as visual gratings at horizontal or vertical orientations, which might not be as selective as in stimuli in different hemifields. The diversity of task designs and the different functions interpreted as a result is already a hint that PPC may be sensitive to task. Many of these studies find that activity respects the motor action in studies where the motor report is kept the same, but no studies have looked for shared task variables in different contexts with different motor actions within PPC.

Outline

Here I wanted to test whether I could find abstract representations of task information in two tasks which are similar in abstract structure, but vary along dimensions which have been shown to modulate PPC activity and involvement differently. Namely, one task involves visually-guided decisions in VR, and the other involves visually-guided detections by motor reports in a steering wheel. Differential effects in visually-guided detection tasks above provide an interesting prediction that despite both tasks apparently involving the same sorts of processes of perceptual decision-making, PPC might be engaged differently across these tasks. An analogy might be made here to the intentional framework, in which decisions are subserved by separate motor circuits involved in separate actions. Here the means of motor report might matter for task-specific responses in PPC. Studies using different motor reports all apparently find choice selectivity in PPC; in the studies reviewed above, decisions can be reported by lever-pressing, licking, nose-poking, turning a steering wheel, running on a spherical treadmill running and even making lateral eye movements. The question of interest here is whether these choice signals are abstract, in that the internal representations of "left" and "right" choices can be found in the same neurons despite different literal motor actions of "wheel" vs "run" to report the same choice.

Both tasks involve visual information, so inactivation studies would suggest that PPC should be invariant to differences of motor report across tasks; however, other studies suggest a mixed picture with potentially interactive processing of stimulus and motor information. How specifically might PPC be involved across two tasks with similar abstract task requirements? There are two potential hypotheses. First, neurons could be entirely task-general, such that the means of motor report is independent of apparent selectivity to task features. Note that this option would not be incompatible with single neurons showing overlapping "mixed selective" activity for multiple task features if neurons are selective for the same mixtures e.g. stimulus and choice, across tasks. Alternatively, neurons could be task-specific, such that different neurons encode the same task features across tasks, but in a manner that is predictable and repeatable, that would suggest PPC is sensitive to the different task contexts and adjusts its activity accordingly.

The extent to which representations overlap across tasks will elucidate how general (and thus, perhaps how truly attributable to PPC's true function) apparent task related activity is within PPC across two implementations of the same abstract task. If task-related activity exists in the same

neurons, apparent abstract representations of task-relevant features can be supposed to be really that which is abstracted from the sensorimotor details of how different choices are instantiated.

To compare neural activity across tasks, it was essential to record the *same* neurons across tasks, so I first needed to train the same mice to perform both tasks. Then, I employed two-photon calcium imaging to record from hundreds of neurons simultaneously. Following this, I then compared the activity of the neurons I recorded in these tasks, to determine to what extent activity in PPC is task-specific or task-general.

General methods

All experiments were conducted according to the UK Animals Scientific Procedures Act (1986).

Behavioral methods

Head-fixed, water-deprived mice were trained on two variants of a two-alternative forced-choice (2AFC) visual detection task for water reward (schematized in Figure 1). One involved virtual navigation by running on a spherical treadmill, and the other involved turning a steering wheel to move a visual grating.

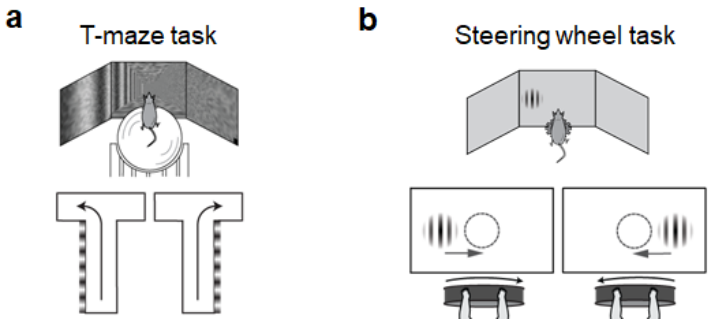

Figure 1. Two visual decision tasks. (a) Schematic of the T-maze and (b) steering wheel task. In both cases, the mouse is required to detect a visual grating of one of several visual contrasts (0, 6, 12 or 50%) on the left or right side. (a) In the T-maze, the mouse runs on an air-suspended Styrofoam ball through a virtual reality T-maze and turns left or right according to whether the grating is present on the left or right side. (b) In the steering wheel task, the mouse moves a visual grating by turning a steering wheel according to whether the grating is on the left or right of the center. The dotted circle is for visualization only and indicates the location the mouse must move the grating to register a choice.

Terminology: Session refers to a given set of all experimental conditions within a given day. These conditions were consecutive but could constitute separate head-fixations. Condition refers to one unique type of condition within a session, of which types include the behavioral tasks or passive experiments.

Shared task structure

Both tasks had a vertical Gabor grating on either the left (-30 degrees azimuth) or right (+30 degrees azimuth) side of the visual field, at approximately central elevation. On each trial, a grating was uniformly randomly chosen among 0%, 6%, 12%, 25% and 50% contrasts.

These tasks were designed to have the same kinds of trial events, namely, to follow the following structure: appearance of a visual grating, prompting an immediate motor response, with constant visibility of the stimulus until the response and no delay period. Mice received a reward (2µl of

water) for correct choices and a short auditory noise burst for incorrect choices. There were no other punishments. Extraneous task cues such as the onset tone, reward tone, and an initial freeze period for at least 200ms of the stimulus on the screen — where the mouse could move but physical movement did not move the stimulus — were present in both tasks. Between trials, there was an inter-trial interval (ITI) where a gray screen was presented. The ITI duration varied across sessions (0.5-3s), with later sessions increasing the ITI to better separate calcium activity across trials.

Importantly, the direction of movement for the same choice was maintained across tasks. In both cases, mice had to orient in the same direction to bring the stimulus (centered at approximately 30 degrees azimuth) to the center of their visual field to make a correct response. Orienting in the opposite direction, pushing the stimulus away from the center, was an incorrect response (see Figure 2). The direction of movement was meant to be "ecologically likely". Specifically, a counter-clockwise rotation of the apparatus always oriented the visual scene counter-clockwise and vice versa for clockwise rotations, as if the (head-fixed) mouse turned to orient *towards* the stimulus.

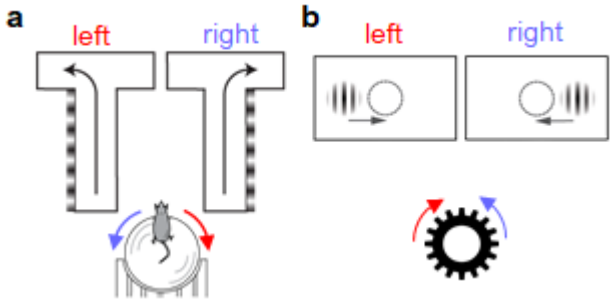

Figure 2. Illustration of choice movements used in the (a) T-maze and (b) steering-wheel task. In both cases, “clockwise” movements are used to select stimuli on the left (contralateral hemifield), as if orienting towards the stimulus to bring it to the center.

Both tasks were performed in the same rig; for neural recordings, every condition was in the same two-photon rig across all sessions and mice. The mouse was surrounded by three computer screens at right angles, with the central monitor located ~20cm in front. The three screens spanned the mouse’s visual field approximately 270 degrees horizontally and 70-75 degrees vertically. Further experimental details are described in Appendix D.

Other than the visual scene displayed on the monitors, the only difference across the two tasks was the apparatus underneath the mouse. All other environmental cues, such as peripheral visual objects in the environment (i.e. outside of the screens), olfactory sensations, environmental sounds, etc., should in principle be identical across the two tasks, which were consecutive and at maximum had a gap of a few minutes within a given day’s session.

Timeouts were introduced in some sessions but, in practice, fully trained mice in the current dataset rarely timed out until satiation near the end of the task. The length of the timeout ranged between 10 seconds and no limit, typically 60-120 seconds.

Steering-wheel task specifics

In the steering-wheel task, mice use a set-up described in Burgess et al. (2017). Specifically, the mice sit on a raised platform within a "half-pipe"-shaped well (Figure 3). Their forepaws rest on a Lego steering wheel which they are able to freely turn in one dimension (rotating in a clockwise or counter-clockwise direction).

Figure 3. Picture of a mouse in the steering-wheel setup, showing the position of the mouse with respect to the steering wheel. Picture taken by Christopher P Burgess.

At the beginning of a trial, a visual grating appears on the left or right side of the screen at +/- 30 degrees azimuth. The mouse is able to move the wheel to move the grating along the horizontal direction, either an additional 30 degrees to the periphery (+60 or -60 degrees azimuth) or 30 degrees to the center (0 degrees azimuth). Wheel positions are recorded using a rotary encoder attached to the axle of a Lego wheel. The mouse is able to move immediately, but at the start of the trial there was a “freeze period” or “interactive delay” of 200 or 500ms (differing across sessions) where the stimulus was frozen in place and would not move even if the mouse moved the wheel in that time period. In the 500ms interactive delay, by design, the mouse usually started to move the wheel before the stimulus would move concurrently. Median RT within a session ranged from 200-350ms, although the distribution could be skewed if the mouse became disengaged and depended on the length of the timeout. If the session included timeouts, at the end of allowed time, the trial would end with an incorrect white noise burst. If the session did not include timeouts, the stimulus remained on the screen until the mouse eventually made a choice to either end point. During the trial, the stimulus was always visible.

In later sessions, I adjusted some experimental parameters to facilitate better task similarity and help with temporally separating different task events. The grating initially spanned 9 visual degrees sigma, but in later experiments the stimulus was made larger (20 visual degree sigma),

though centered at the same azimuth and elevation. The change was made to cover a larger portion of the visual field in this task, to make the visuospatial extent of visual stimulation more similar to the other task. The inter-trial interval (ITI) was typically 0.5-3 seconds. In later experiments, I increased the ITI (to 3s) after observations that the mouse sometimes over-eagerly started the next trial with an identical wheel turn. A longer ITI was also chosen to dissociate neural activity between adjacent trials given the slow decay of the calcium indicator. This increase in ITI did not affect analyses as no analyses were performed in the ITI. Further, a pre-trial "quiescent period" was introduced in later sessions where the mice had to maintain a certain degree of stillness in the wheel before the trial began. This duration was randomized across trials, meaning the effective ITI on each trial was variable, but with a maximum of 3 seconds.

Due to a bug, 0% contrast trials in the steering-wheel task were rewarded only for timeouts in the majority of sessions. On average, the median proportion of trials that were zero contrast was 17% +/- 4% median absolute deviation (m.a.d) of the total number of trials (including time-outs if any). Mice on average still responded fairly equally in either direction at a median proportion of leftward vs. rightward choices at exactly 50% +/- 17% m.a.d., across sessions. Mice rarely timed out; median proportion of zero contrast trials that resulted in timeouts was 1.5% +/- 8.9% m.a.d. across sessions. The response window was variable across sessions but was designed to be long enough to only end if mice were extremely inattentive (usually 60 seconds, with a minimum 30 seconds to a maximum of infinite length i.e. no timeout). In comparison, median RT within a session was usually 0.4-0.8s. In two sessions, 0% contrasts were changed to be rewarded randomly as was intended.

T-maze task specifics

In the T-maze task, mice use the same setup as described in Krumin et al. (2017), similar to that first described in Dombeck et al. (2007). Physically, the mice sit on a spherical treadmill consisting of a styrofoam ball (20cm in diameter) which is lightly suspended in pressurized air. Movements of the spherical treadmill were measured using two optical computer mice to control a virtual reality scene. Mice are able to control the ball by running on it and turning with their forelimbs and hindlimbs. The rotation of the ball “forward”, i.e. around the axis perpendicular to the animal, was responsible for forward movement in virtual reality, and the rotation of the ball around the vertical axis was responsible for turning in virtual reality (at 20% gain). The lateral displacement of the ball (rotation around the axis parallel to the animal’s orientation) was ignored.

At the start of each trial, mice are shown a virtual reality T-maze consisting of a long corridor, and two directions to turn at the end perpendicular to the initial corridor. In the T-maze, the visual

stimulus is now a feature of the entire left or right wall of the initial corridor but is still centered at approximately 30 degrees azimuth. The “freeze period” or interactive delay was 200ms in the T-maze. To make their choice, mice needed to run down the central corridor and turn left or right down the arms of the T, at which point the trial would end and they would receive a reward for a correct choice, or auditory white noise burst for an incorrect choice. Like the steering-wheel task, a clockwise rotation was needed for left choices in order to turn "left" in virtual reality, and vice-versa for right choices. There was a 3s ITl. 0% contrast trials were rewarded randomly.

The virtual scene was controlled using a custom virtual reality engine implemented in MATLAB utilizing OpenGL through the Psychophysics Toolbox (Brainard, 1997; Pelli, 1997). The initial corridor was 110cm long including the juncture of the T, and 20cm wide, with the two arms of the T spanning 60cm in width, i.e. an additional 20cm to the left and right. The grating was superimposed on a noise texture of 20% visual contrast and there were noise textures at 40% visual contrast on the floor to provide a more immersive environment.

Training and testing protocols

Details about training and habituation are in Appendix D.

During training, for practical purposes, mice were usually trained to asymptotic performance on one task before they were introduced to the other. Some mice started with the T-maze and others started with the steering-wheel task. This training protocol was to ensure mice were capable of performing either task before taking time to start training the other task, given the time-consuming nature of training. This "blocked" training could have implications for differing neural representations, which is addressed in the General Discussion.

Testing within a session

As it was necessary to switch the apparatus across tasks, mice were tested serially in two blocks, with full performance of one task before performance on the other. The gap in between tasks was usually no more than a few minutes.

To maintain equal numbers of trials in each task, mice were switched to the other task when they reached approximately half of their daily water weight, typically 100-300 trials depending on performance. The second task was stopped when mice reached their water minimum, or stopped performing trials or made many consecutive errors, whichever came first. Mice typically performed 100-300 trials/task/session with a total duration per task of 20-60 minutes.

During testing, mice usually performed the T-maze first, but to check for order effects, occasionally the order was switched so that they performed the steering-wheel task first.

Behavioral quality control: Inclusion and exclusion criteria

I included n = 6 mice in all analyses, as these were the same mice to be later included which had good neural data. Mice which had learnt but developed physical degradation of the cranial window, increasingly poor performance in either task or extreme biases in behavior were dropped from the experimental pool. Sessions were included in the dataset when mice had good psychometric performance on both tasks, with at least 100-200 trials on each task. All mice included in the dataset had fully learnt and reached asymptotic performance in both tasks. However, day-to-day, mice could show more lapses or changes in sensitivity.

To plot behavioral performance, psychometric curves were fitted using maximum likelihood estimation (Busse et al. 2011). Mice were able to learn both tasks to proficiency and showed good performance in both tasks within a session as evidenced by their psychometric curves (Figure 4, psychometric curves over all included sessions in this dataset in Figure 5). At 50% contrast, mice performed at nearly 100% correct.

Training time for acquisition of the second task was mouse-dependent but mice were typically quicker to learn the second task. It is tempting to interpret the rapid acquisition of a second task as a result of "scaffolding" based on learning a similar task structure; however, it is equally likely that pre-existing factors contributed to this observation. Namely, mice proficient in one task already may be already a "smarter" subset of mice. Alternatively, factors extraneous to the task *per se* such as comfort being handled and head-fixed may be the dominant contributing factors to this effect.

In practice, mice seemed to prefer performing the T-maze first over the steering wheel task first perhaps as the former was more physically demanding and thus resulted in more disengagement. Therefore, to optimize behavior, in practice most sessions involved presenting the T-maze first. However, two sessions were included where the steering-wheel task was performed first, and later analyses which potentially depended on this ordering were examined to ensure that these two sessions fell within the expected distribution of observed effects compared to the more common ordering.

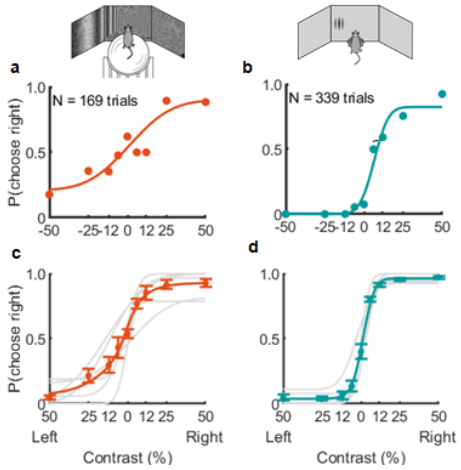

Figure 4. Mice are able to perform both tasks in a single day. Example sessions from one mouse showing psychometric performance on the (a) T-maze and (b) steering wheel task. Smooth curves indicate the fitted psychometric function. (c,d) Average psychometric curves for each mouse, and the summary over all mice (thick line) for n = 6 mice.

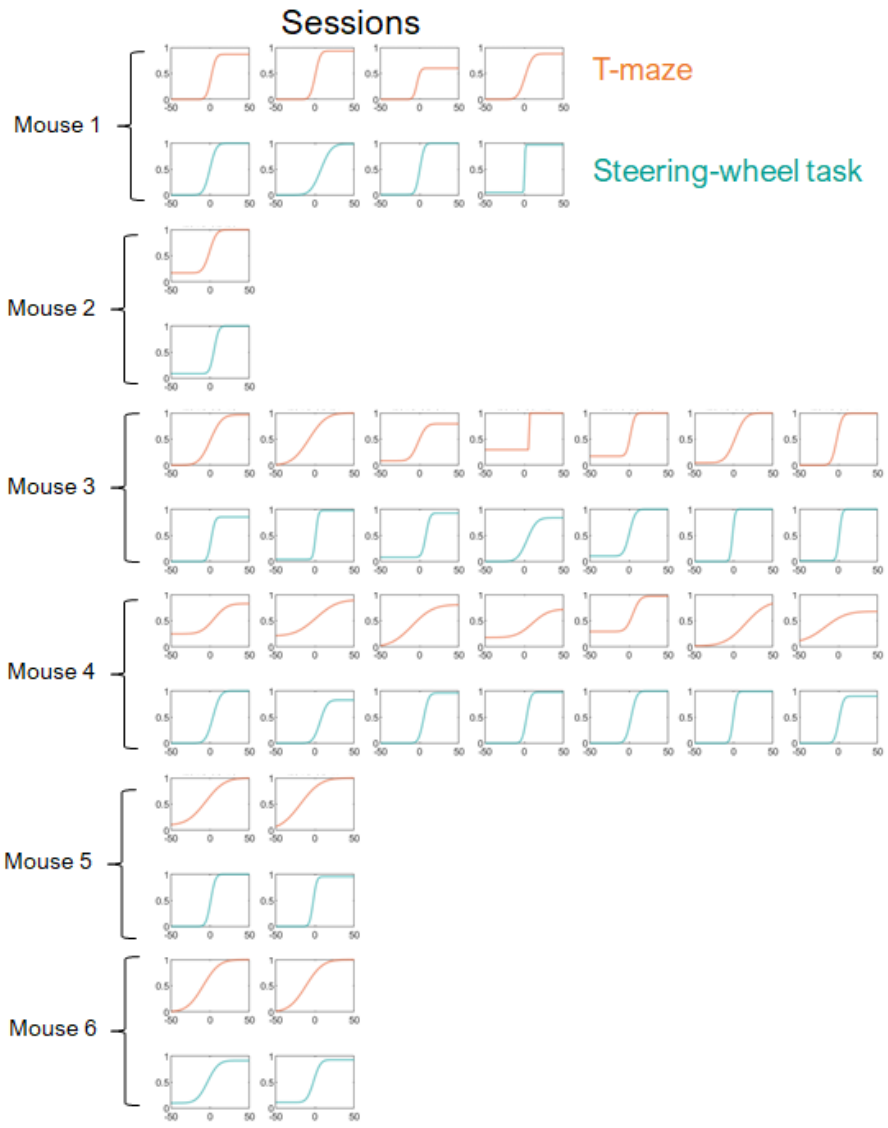

Figure 5. Psychometric fits for each task within each session across all six mice. Each column is a different day (not aligned across mice), whereby the pair of tasks is performed consecutively, but not necessarily in the presented order.

Neural data methods

Given that mice were able to perform both tasks within a single day with good behavior on both, I was then able to record the same neurons within days to provide a within-session comparison. I recorded from hundreds of neurons simultaneously using two-photon calcium imaging while mice performed the aforementioned tasks.

Calcium imaging

Genetically-encoded calcium indicators (GECIs) are commonly used to record activity of neurons using calcium release as a proxy for neural activity. In these datasets, calcium imaging was performed using variants of the GCaMP6 family, fast (GCaMP6f) and slow (GCaMP6s) described in Chen et al. (2013), which have high sensitivity to single action potentials, fast kinetics and little saturation.

Transgenic mice were used which ensured uniform expression of GCaMP across excitatory neurons and stability of expression across time. One mouse in the current dataset was a GCaMP6f mouse (double transgenic Ai95(RCL-GCaMP6f)-D x Slc17a7-IRES2-Cre-D) with GCaMP in glutamatergic neurons. All others (n = 5) were GCaMP6s mice (double transgenic tetO-6GCaMP6s x Camk2a-tTA; Wekselblatt et al., 2016) with GCaMP in Camk2a-positive (excitatory) neurons. Neither of the two transgenic mouse lines used were found to have interictal spikes in a survey of transgenic mouse lines that initially highlighted aberrant epileptiform activity in a triple-transgenic mouse line (Steinmetz et al. 2017).

Although I used two different strains, the greater difference that is relevant for this study is likely the speed of the calcium indicator (GCaMP6f vs GCaMP6s). However, the GCaMP6f mouse was also imaged more superficially. To my knowledge the results at large here are not affected by these differences.

Retinotopy for determining the field of view for imaging

Stereotaxic coordinates can be misleading for identification of brain regions, as the location of bregma on the mouse cortex can vary from animal to animal, as a function of age, and according to laboratory convention. In particular, areas such as PPC are closely bordered by neighboring areas primary visual and somatosensory cortices, which are expected to have different response properties. Further, PPC spans only ~500um in anterior-posterior breadth, so accuracy is essential when the imaging field of view for two-photon imaging is only 500x500um. Therefore,

I mapped known retinotopic areas under wide-field imaging in order to more precisely target my two-photon imaging field of view.

Wide-field imaging

Protocol for wide-field imaging followed standard procedure from the lab and elsewhere (Garrett et al., 2014; Zhuang et al, 2017). I imaged the entire 4mm cranial window under a "wide-field" macroscope with dual illumination. A sCMOS camera (PCO Edge 5.5) was used to image the brain. Illumination was generated using an LED (Cairn OptoLED) using alternating frames of violet (405nm, excitation filter ET405/20x) and blue (470nm, excitation filter ET470/40x) light (at 35fps each) to capture calcium-dependent fluorescence and calcium-independent hemodynamic activity respectively.

Retinotopic mapping using wide-field imaging (Zhuang et al. 2017; Garrett et al. 2014) is now fairly routine and involves presenting retinotopically-specific visual stimuli at different visual azimuth and elevation. In my case, I presented "sparse noise" to map retinotopy. In this stimulus protocol, black and white squares appear and disappear asynchronously on a gray background. Since these squares appear and disappear independently, this visual stimulus is reliable even with relatively short recordings (5-20 minutes here) for inferring visual retinotopy.

Movies were averaged at 2x2pixel or 4x4 pixel resolution in order to better estimate retinotopic maps. Following imaging, movies were compressed using singular value decomposition to decrease the file size. The movies were then processed to filter out hemodynamic artefacts: both purple- and blue- wavelength signals were band-pass filtered at the “heartbeat” frequency 7-13Hz, and the purple wavelength signal was regressed out. For estimating retinotopic maps, stimulus-triggered averages were computed to find the wide-field calcium response corresponding to different retinotopically-located stimuli. Then, according to standard procedure (Garrett et al. 2014), I computed a "visual field sign map" (Sereno et al. 1994) by taking the difference (sine of the angle) between the gradients of the azimuth and elevation maps for every pixel. Sign reversals in the gradient maps correspond to traversals across visual areas, and so the visual field sign map is useful in locating visual areas across species (Sereno et al. 1994).

Defining PPC from the retinotopic map

The area described in all experiments as PPC was chosen to be an area anterior of primary visual cortex and posterior of primary somatosensory cortex potentially overlapping with areas A and RL (Figure 6). This area was chosen according to definitions by the Allen Mouse Brain Common

Coordinate Framework (Wang et al. 2020) which calls this area one of a set of "parietal" regions. I chose this location as it seemed to minimally overlap with potential somatosensory regions to the anterior side of parietal areas.

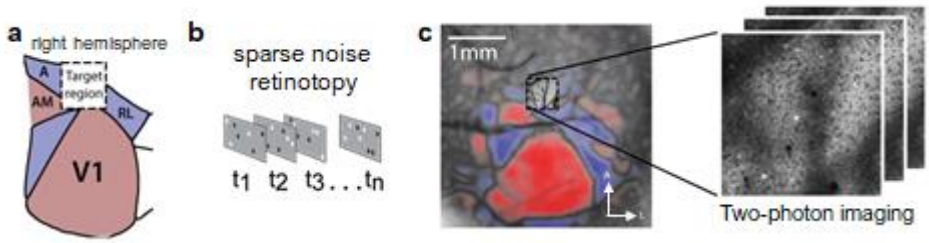

Figure 6. Processing pipeline for imaging in PPC. (a) Schematic of visual and higher visual areas in posterior cortex, adapted from the Allen Common Coordinate Framework. (b) Schematic depiction of the sparse noise retinotopy protocol. Asynchronous black and white squares appear on a gray background and are independent across time. (c) Example retinotopic "visual field sign" map from one example mouse, showing it is possible to identify areas V1, AM, A/RL and some other secondary visual areas. Inset, example field of view for two-photon imaging in this example mouse.

The precise location of PPC can be a matter of debate, with some recording more anterior-medially, in area AM. However, recent work from other labs have argued that posterior cortex is fairly uniform in representation at the gross scale, in terms of activity and effects of inactivations, in the sorts of tasks employed here (elaborated in the General Discussion). To discuss one example, Minderer and colleagues (2019) recorded throughout posterior cortex using two-photon calcium imaging during a visually-guided locomotion task and were not able to find unique clustering of feature encoding among parietal subregions; instead, AM was functionally indistinct from areas such as the one I image here. Therefore, I do not expect differences, if any, in the results here to other work in parietal cortex simply as a result of recording region. I address this topic further in the General Discussion.

Two-photon imaging acquisition methods

I performed neural recordings using multi-plane two-photon (2p) calcium imaging in layer 2/3 excitatory neurons. The sessions in this work were typically 2-3 hours in duration.

Mice were imaged under the 2p microscope after they had habituated to head-fixation. For testing sessions, mice in this dataset were imaged after they reached asymptotic performance in both tasks in training. There was a further acclimatization period to ensure habituation to 2p procedures and re-acquisition of good psychometric performance.

Two-photon calcium imaging was performed over PPC as defined above. Imaging was performed using a ThorLabs B-Scope with a Nikon 16x 0.8 numerical aperture (NA) water immersion objective. A Ti:Sapphire (Coherent Chameleon) laser provided excitation at 920nm, with depth-

adjusted power level controlled by an electro-optic modulator, i.e. pockels cell (M350-80LA, Conoptics Inc.). Light isolation was mitigated using a custom metal cylinder, cone and black cloth to prevent light contamination from the illuminated screens.

Acquisition was controlled using ScanImage (Pologruto et al., 2003), and frames were acquired continuously at 30Hz over an imaging window of 500x500um, at a resolution of 512x512 pixels. Multi-plane imaging was performed using a piezo motor over two planes in layer 2/3, starting at 90-130um below the surface, separated by 60-70 um, spanning a total of 180-210um. The piezo motor takes a fraction of time proportional to 30fps * 1/number of planes to "fly back" to its initial position and therefore for two planes, the effective imaging rate is 10fps per plane.

I only imaged excitatory neurons as GCaMP is only expressed in excitatory neurons in the transgenic mouse lines used. All recordings were made in the right hemisphere as the cranial window was only over this location.

Two-photon imaging processing methods

The resulting raw movies were processed in Suite2p (Pachitariu et al., bioRxiv) to provide registration to correct for motion artefacts, cell detection, signal extraction and further analyses including neuropil correction and spike inference, also known as "deconvolution".

Registration

There are two forms of drift that could artefactually affect neural responses in two-photon, "slow drift" and "fast drift" (Pachitariu et al., Cosyne Abstract, 2018). The former is non-rigid but can be corrected for by subtracting a running baseline. The latter is rigid, so while fast, can be corrected using rigid frame-by-frame registration techniques as is default in Suite2p.

Motion artefacts are well known to present an issue for neural recording techniques including two-photon calcium imaging (Stringer, PhD Thesis) and electrophysiology recordings (Pachitariu et al., 2018, Cosyne). It is known that running and active behaviors drives brain-wide activity (e.g. Stringer et al. 2019; Musall et al. 2019; Niell and Stryker 2010; Ayaz et al. 2013; Saleem et al. 2013), but these behaviors can also cause cells to move quickly in and out of the imaging plane, causing artefactual apparent evoked activity. Artefacts from fast motion are particularly evident during high-effort active behaviors such as running, but can even occur during subtle behaviors like licking (Chen et al. 2013). In most tasks in rodents, choices are made by an overt motor action, so motion artefacts can also lead to spurious "task-evoked" activity. Slow drift can also be an issue in long recordings, whereby the plane may slowly move out of focus such as due to slight

thermally-induced brain expansion, to the extent that there may be entirely independent groups of cells imaged at the beginning and end of the imaging session. Therefore, it is essential to correct for this movement, both computationally using registration algorithms and by careful manual inspection to discard sessions in which the problem is too severe.

Raw movies are aligned in Suite2p by default using 2-D "rigid registration" which parsimoniously assumes the entire plane shifts in unison. The implementation in Suite2p uses phase correlation with subpixel registration for greater accuracy (1/10 of a pixel) by interpolating the resulting phase correlation map. Following registration, cells are detected in Suite2p by clustering temporally correlated pixels; this method classifies cells by "functional" measures of temporal activity, rather than morphological measures of ROIs that have a "cell-like" shape.

Neuropil correction

Then, neuropil correction is performed which corrects for "contamination" by signal other than generated by the cell itself. So-called “neuropil” signals consist of out-of-focus fluorescence from other processes such as dendrites and passing axons, since standard calcium indicators are not soma-localized. The point-spread function of two-photon calcium imaging — while less sensitive than one-photon imaging to fluorescence that originates beyond the intended source — means that the focal point can still contain some signal from nearby locations in anatomical space.

It is important to correct for neuropil as the contribution from neuropil can be stimulus-locked, adding to apparent evoked activity that in fact disappears upon correction (Rossi, PhD Thesis). Neuropil correction is also necessary particularly when the mouse is likely to move and thus introduce potential movement artefacts as discussed above (Stringer, PhD Thesis). It now routine to subtract an estimated neuropil surround, commonly inferred by taking a fixed ratio of pixels forming a "donut" surrounding each cell, and subtracting the temporal activity of these pixels according to a fixed multiplicative factor. I used a neuropil ratio which estimates the neuropil as a radius of size 5x the number of pixels defined for the cell, as is the default in Suite2p. As well, as per convention, I used a neuropil multiplicative coefficient < 1, which is estimated per cell by default, and ends up being $\sim$0.6-0.8.

Spike deconvolution

Finally, spike inference (i.e. deconvolution) was performed using the OASIS algorithm (Friedrich et al. 2017). Although efforts are constantly made to improve the temporal resolution of calcium sensors, the long tail of decay of calcium signal means that signal can be "blurred" depending on

the spike rate. Rather than using the calcium itself, deconvolved calcium activity is often estimated, using spike inference algorithms. These algorithms assume or learn a spike-to-fluorescence transfer function or "kernel", and invert (deconvolve) the fluorescence signal given this kernel to obtain the spikes that likely generated the observed calcium signal. Deconvolution does not give spikes per se, but rather spike probabilities.

Each deconvolution algorithm incorporates its own design choices, but in practice performance across popular existing deconvolution algorithms was not shown to differ dramatically (Berens et al. 2018). In the SPIKEFINDER challenge, deconvolution in Suite2p was benchmarked against ground-truth electrophysiology data along with other popular algorithms of the time (Berens et al. 2018). Performance was similar across different algorithms despite some taking a biophysical modelling approach and others using more parsimonious methods such as constrained non-negative matrix factorization. Furthermore, in their own work, Pachitariu et al. (2018) found that in practice, accuracy of deconvolution in Suite2p is robust to different choices of the kernel compared to ground truth electrophysiology. In particular, accuracy was not significantly improved when using the "ground-truth kernel".

Deconvolution in Suite2p accounts for fluctuations in baseline — such as resulting from fast or slow drift, neuropil contamination, or bleaching — by using a running minimum over a long interval, here 60 seconds. Figure 7 shows the outcome of deconvolution and running baseline subtraction in correctly correcting for spurious slow drifts in the signal.

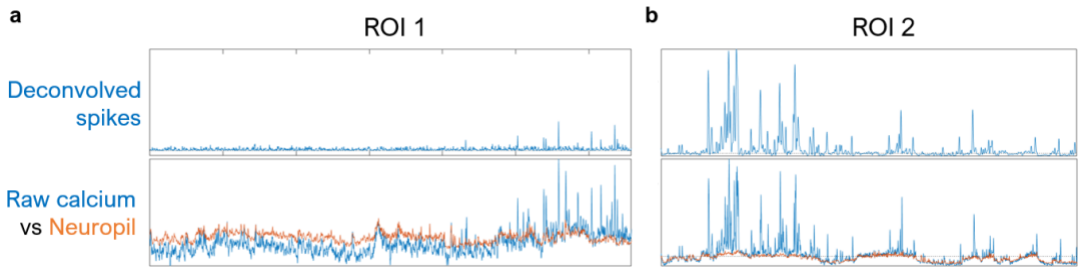

Figure 7. Illustration of the effects of deconvolution for two example ROIs. (a) ROI 1 suffers from large fluctuations in the baseline, evidenced by comparison to the co-fluctuating neuropil. This fluctuation is removed after subtracting a running baseline during the deconvolution step. (b) ROI 2 also has fluctuations in the baseline which affect the raw calcium intensity, again as evidenced by neuropil that closely tracks the underlying change in baseline. In this case, true calcium activity is superimposed on this fluctuating baseline, so subtraction of the baseline recovers true activity.

Manual curation

ROIs detected by Suite2p were manually curated using the Suite2p GUI. I classified ROIs as cells according to spatial and temporal criteria. For the former, this procedure meant that the extracted ROI reasonably resembled a disc-like soma at the size expected at the imaging zoom I used

(approximately 15 pixels). For the latter, the activity trace was examined to evaluate the signal-to-noise of the ROI, particularly relative to the respective neuropil (as also illustrated in Figure 7 above). Manual curation was performed blind to the time at which the task transition occurred.

Alignment across tasks

The apparatus needed to be switched across tasks, necessitating two distinct head-fixation sessions (albeit with a gap of no more than a few minutes). Evidently, this procedure could introduce errors in alignment. Therefore, I was extremely careful to align recordings across tasks both at the rig and after processing the two-photon movies. At the rig during acquisition, the mean image over several frames of the previous task's recording plane was used as a reference plane, and I manually aligned the "live" movie of the current imaging plane in z, x, and y, to match the previous task's mean image until the difference was indistinguishable to the eye. Although the microscope allows for rotation, this axis was not adjusted, as the angle of the headplate was fixed within a session and often across days. Following acquisition, the raw movies were then examined by eye, with particular attention before and after the switch in task, to ensure that the same population of cells was visible.

During data processing, the raw two-photon movies comprising all the conditions in that day's session were temporally concatenated before processing in Suite2p. In doing so, I took advantage of the registration algorithm inherent in Suite2p to adjust for small errors in 2-D. This procedure is therefore biased to assume that the same neurons are present in both tasks. Given prior careful manual inspection of raw movies and exclusion of sessions which seemed to have clear misalignment, this procedure is valid and indeed preferred in order to be more conservative given later findings.

However, similar results were achieved (not shown) when instead processing separate head-fixations separately in Suite2p, and then post-hoc classifying overlapping ROIs to be the same cell based on the union of their pixels across the two head-fixations within a session. This procedure was the same as described below for across-day alignment, where alignment is less certain due to more likely morphing of the brain and misalignment in the axes of x, y, z and roll/rotation.

Finally, I visually examined the activity traces in Suite2p for differences in signal across head-fixations which could be due to an error in alignment in z. Specifically, an error in z would bisect the soma at a different depth — or miss it entirely — and result in an apparent difference in the acquired signal. It is hard to dissociate the contribution of this artefact vs. real changes in signal in the cell. Therefore, I based my judgement on the activity of the neuropil surround (Figure 8).

While a broad increase in neural activity, including in the neuropil, can be triggered by a change of behavioral state, a stepwise change in an otherwise low-mean, high-variance signal likely means the imaging plane in fact was recorded at a different depth across head fixations. In particular, when jumps in neuropil signal occur across many ROIs, including ROIs that are evidently not cells, this temporal signature motivates discarding the respective session.

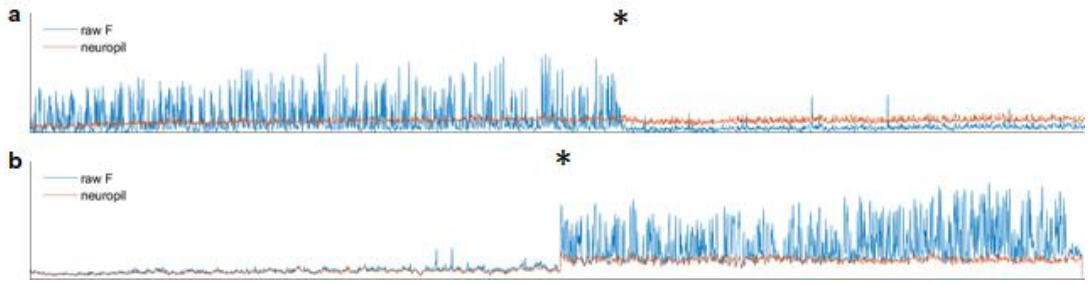

Figure 8. Example of visual inspection of calcium traces of the cell and neuropil for determination of alignment quality. (a) A neuron with good alignment from an example session vs (b) a neuron with poor alignment from a session that is not used. The asterisk illustrates the timing of the task switch. The neuropil signal goes up sharply at the moment of the task switch, but this is likely erroneous due to misalignment.

Imaging sessions were discarded if a large proportion of neurons were no longer visible by the end of each task, and/or if a large proportion of neurons were not visible across both tasks. There were 26 sessions that remained after these strict criteria.

Analysis procedures

Neurons in these sessions are often deliberately dependent across days as I often attempted to record the same neurons over several days. Therefore, I only carried out analyses on a session-by-session basis, and aggregated summary statistics across sessions. I did not want to "double count" neurons that appeared often, as these could be neurons which are systematically biased to be feature selective (or non-selective) in some way.

Aligning behavioral data

Behavioral data was aligned to neural data using timing software developed in the lab. Punctate variables such as timing of events and continuous variables such as steering wheel rotation velocity were down-sampled to match the calcium imaging frame rate (10fps). A photodiode measured screen refresh rates which were used to confirm stimulus onset times. For the steering wheel task, wheel movements were detected using the "findWheelMoves3" function described in other work (Steinmetz et al. 2018) and available on GitHub.

Chapter 2: Comparing activity across tasks

This chapter examines coarse-level "participation" of single neurons across the two tasks. As a minimum standard for determining whether the same set of neurons carry the same abstract representations across tasks, I test whether the same set of neurons is active during both tasks, which is a necessary precondition for sharing task feature event-evoked activity. I describe measures for summarizing the activity of a neuron within a task, independent of task-evoked activity. I then validate results by taking advantage of the ability to return to the same imaging plane to compare activity within- vs across-tasks.

Methods

Isolation distance

Cells which fire rarely, e.g. no more than a handful of times over a 20-60 minute task session, are conventionally considered inactive. Certainly a cell which does not fire consistently to a repeated experimentally-defined task event cannot be considered to be "behaviorally relevant" for at least those experimentally-defined task events that occur at much more frequent rate.

To summarize average neural activity in the whole session, I used a measure called “isolation distance” (Figure 9), previously described in Stringer & Pachitariu (2019). Isolation distance is inspired by a metric of the same name and motivation that is commonly used for spike sorting in principal components analysis (PCA) space. This measure is similar to any other common scalar summary of an activity trace (such as mean firing rate) in the information it conveys about the cell's activity over a time period.

As described in the previous chapter, in non-soma-localized GCaMP indicators, GCaMP is present not just in the cell bodies but also other cell processes such as dendrites and passing axons. Out-of-focus fluorescence from this “neuropil” can erroneously contribute to the signal averaged within the pixels that define a cell. A standard procedure is to “correct” for this neuropil by subtracting a scalar multiple of the average activity in a radius around each cell. Here the "neuropil coefficient" was estimated per cell but is usually <1, around ~0.6-0.8. Meanwhile, standard cell extraction procedures for two-photon data involve estimating pixels which are correlated within themselves but not with respect to the surrounding pixels in the background, i.e. the neuropil. Given these are well-established assumptions in the literature about what constitutes a cell and what constitutes extraneous noise to be subtracted out, it is reasonable to

assume the neuropil can be treated as an estimate of baseline “noise”. Isolation distance uses this assumption to compute single-neuron “activity” as the difference between activity within the ROI and activity in the neuropil surround — in effect a measure of signal-to-noise ratio (SNR). There is some precedent for this approach as applied to calcium imaging, in a study (in which this procedure was not the focus) that classified neurons as inactive if their activity did not differ from the neuropil signal (Chen et al., 2015).

I computed isolation distance for each neuron as follows. For every cell, I identified the pixels defining its ROI, and the pixels defining its donut-shaped neuropil surround (both estimated in Suite2p), and then extracted a matrix of pixel intensities x time from the registered raw two-photon movies. On each matrix I performed a mean-subtracted singular value decomposition (SVD), i.e. principal components analysis (PCA) and extracted the first left singular vector (similar to the first principal component (PC)), to get a vector of loadings per pixel, which summarizes its activity over the entirety of the analyzed time period (here during the entire task). Importantly, I repeated the procedure for the pixels defining the neuropil surround for that cell, generating two distributions of pixel activity (one for ROI, one for neuropil) that could then be compared (as illustrated in Figure 9 below). The isolation distance is then how "isolated" these two distributions are from each other, according to the Bhattacharyya distance metric. Intuitively, if these two distributions are overlapping, the ROI is very similar to the neuropil and so has low SNR. If the distributions are more distant, the cell is instead distinct from the neuropil, which is likely because the cell has fluorescence peaks that deviate from the shared baseline. The procedure is shown for two principal components for illustration, but here I only use the first PC as it is sufficient for distinguishing activity, as evident in these examples.

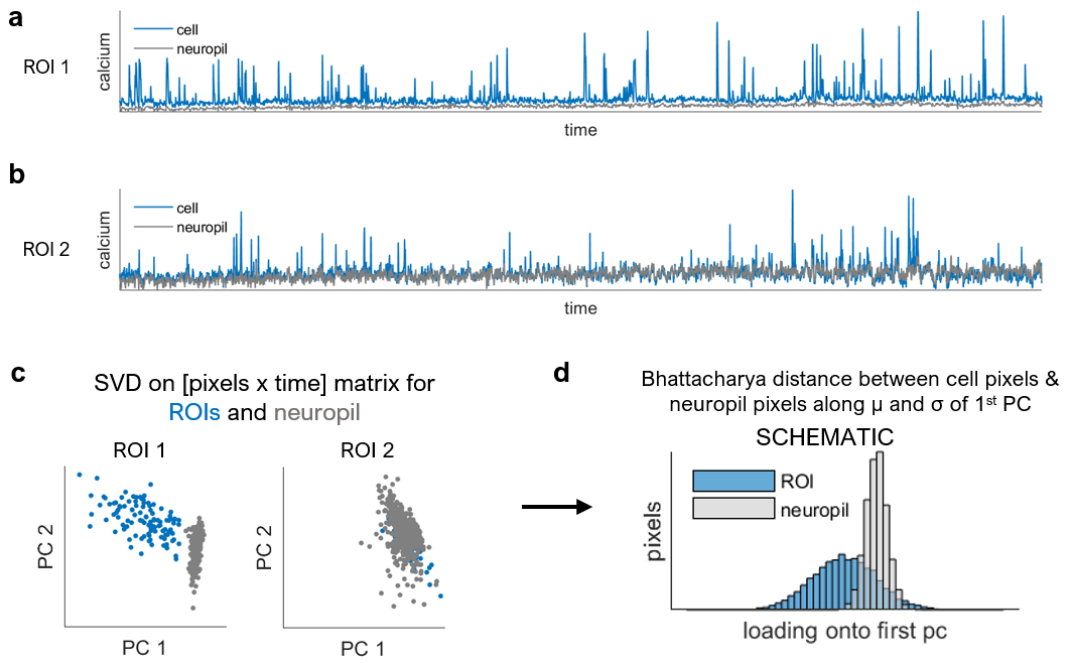

Figure 9. Procedure for computing isolation distance as a measure of activity for a cell throughout an imaging condition. (a,b) Two example ROIs detected in Suite2p and the activity of their neuropil surround. (c) Singular value decomposition (SVD) is performed on the matrix of pixels x time, to compress time from the number of frames to a lower number of dimensions. Each dot is a pixel of either the ROI (blue) or neuropil (gray). ROIs which are "well isolated" from the neuropil are likely cells, as they show high variance over the session beyond the noise range of the neuropil. ROI 1 is likely a cell due to this property. Conversely, ROI 2 is likely not a cell as the distributions overlap. (d) A schematic of the logic of comparing the ROI and neuropil distributions for a hypothetical ROI. The distance metric, the Bhattarcharya distance, measures the similarity between two distributions (one- or multi-dimensional). Only the first PC is used as it is sufficient to distinguish the quantity of interest.

Isolation distance produced results qualitatively similar or better than common measures such as average firing rate (see Appendix B for comparisons in a GCaMP6f and GCaMP6s mouse). Importantly, of all tested measures (mean, standard deviation, skewness, coefficient of variation) isolation distance produced estimates of "activity" that were closest to intuitions in manual inspection of traces and most robust to noise. This last requirement was especially important as a high noise floor is observed in the strain of GCamP6s transgenic mice that contributed to the majority (5/6 mice) of the present dataset (as observed in Huang et al. 2019).

Notably, isolation distance is used on pixel intensities of the raw movies, so is not sensitive to subtleties of different deconvolution algorithms or other choices for normalization.

Across day comparison

I used RegisterS2p to detect cells across days, which uses the mean fields-of-view image and processed ROIs from Suite2p (Pachitariu et al. 2018) between pairs of sessions (Figure 10). After manually defining control points on each image, affine registration is performed to spatially align

two imaging fields, and any ROI whose pixels substantially overlap (at least 60%) between the two fields is classified as the same cell. Importantly, this process only uses the spatial location of ROI pixels in the imaging field to link cells between sessions, and does not utilize cell activity as a marker of similarity. Therefore, although cross-day registration is another manual step, it cannot introduce any biases toward including cells that are or are not task selective as it is completely agnostic to the actual activity (i.e. isolation distance) of each cell being aligned.

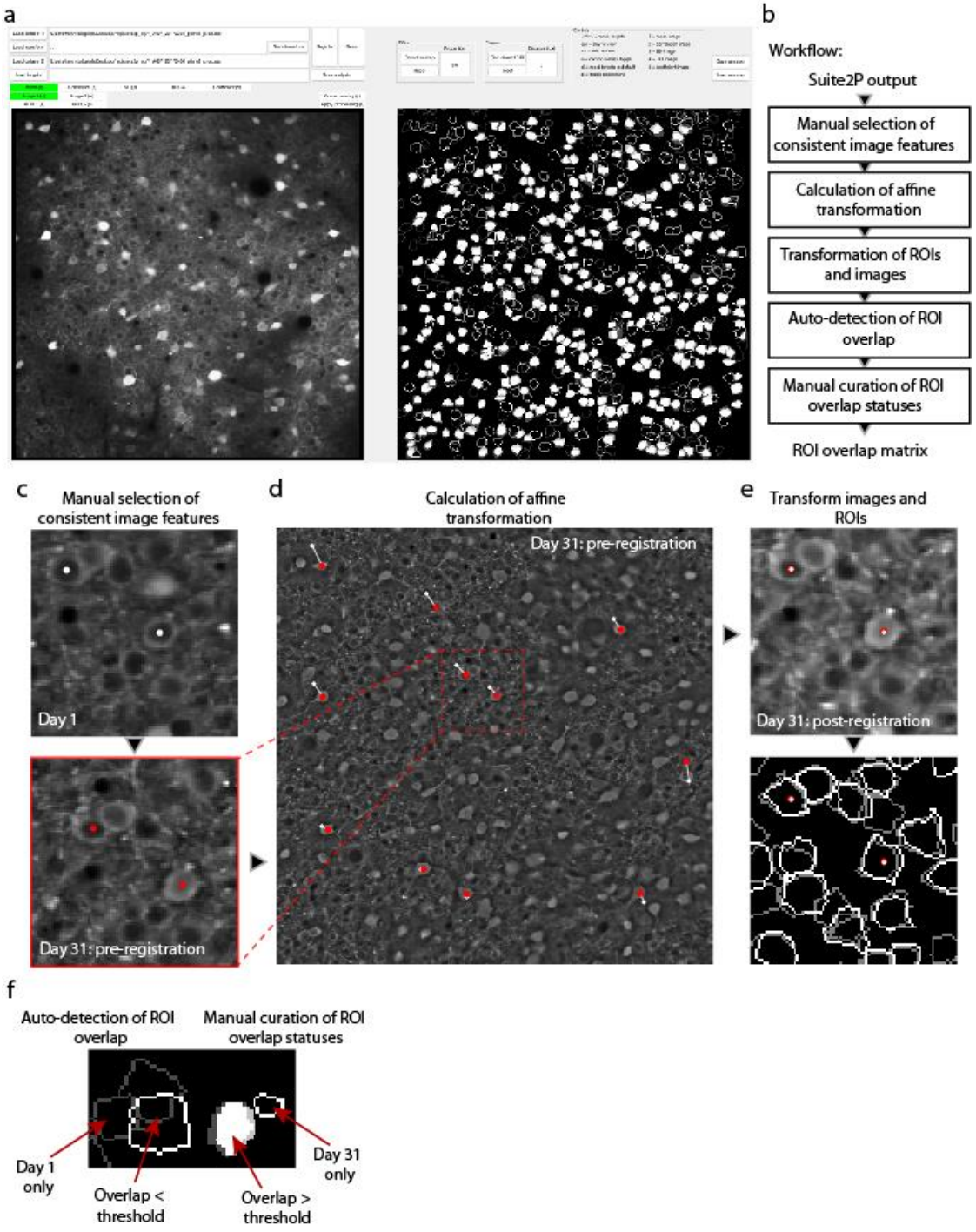

Figure 10. Pipeline of "Register S2P". (a) GUI used to match imaging planes and ROIs across days. (b) Workflow of the registration steps (c) Manual selection of control points using the normalized mean image to select likely pairwise matches across days. (d) Illustration of the affine transformation used to warp the two sessions. (e) Following affine transformation, the ROIs are well-matched between the two days (bright white vs gray). (f) Illustration of the overlap heuristic used to classify ROIs as belonging to the same cell. (g) Validation of the usefulness of affine registration over rigid registration in recovering the same cells, as measured by pixel correlation. Figure created by Henry Dalgleish, published in the Suite2p preprint (Pachitariu et al., bioRxiv).

Results

The majority of neurons recorded in the two tasks were not active throughout performance of both tasks, but rather were selectively active during either task. Figure 11 shows example neurons which show activity in one task but not the other. Using isolation distance to compute a single value for each neuron's overall activity level in each task, I found that most neurons tended to be active in either task only. Within each task, neurons show apparent activity or inactivity, as shown by the marginal histograms in Figure 11-c. When comparing the activity of a population of neurons across the two tasks, most neurons are active in one task but not the other, with relatively few that are active in both, as evidenced by the observation that most points lie near the ordinate axes and relatively few on the diagonal. This observation was highly consistent across sessions and mice.

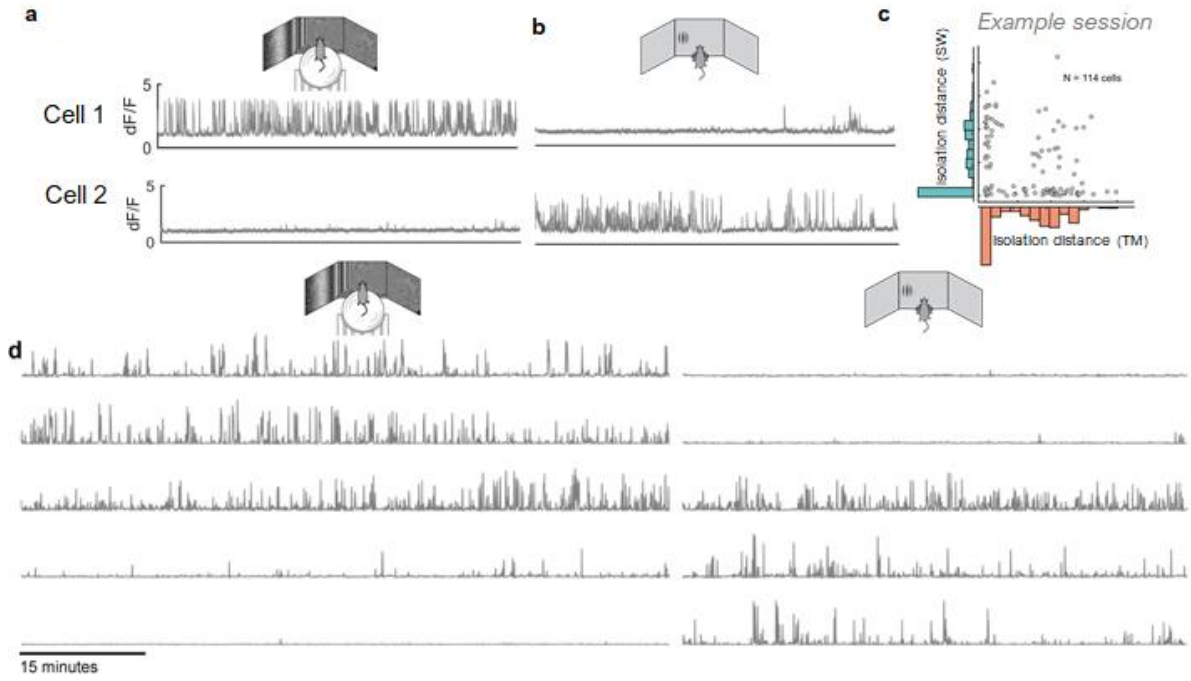

Figure 11. Many neurons are selectively active during either task. (a,b) Two example cells showing activity in one task but not the other. (c) Example session which shows the distribution of isolation distance across the T-maze (TM) and steering-wheel (SW) tasks. (d) More example neurons, including a neuron active in both tasks.

Validation across days

Although tempting, it is not valid to make statistical inferences on the proportion of task selective neurons without access to all neurons in PPC. The ideal test asks whether there are greater numbers of task selective neurons — neurons that are *active* in *one* task, but *inactive* in the *other* — than expected based on the number of neurons active or inactive in each task separately. For example, given that there are 50 active and 10 inactive neurons in the T-maze, of those 50 active neurons, how many are then inactive in the *steering-wheel task*, and is it more than expected? However, this test is not valid here, as the sample of neurons under analysis is already biased by this stage, influenced by which neurons express GCaMP, which neurons are picked up by two-photon calcium imaging, which neurons are extracted by Suite2p, and which neurons the experimenter eventually selects during manual curation. These factors could all influence the set of active neurons and relative activity and inactivity across tasks in unpredictable ways; this possibility undermines the ability to extrapolate the results broadly to PPC.

Even more concretely though, tests of the statistical significance of observed frequencies, such as the Chi-squared test, also depend on there being a representative number of neurons inactive in *both* tasks. The "true" number though is not known, and likely smaller in practice than in PPC generally, as neurons inactive in both tasks (i.e. the whole session) could be missed by Suite2p, and then further not chosen for inclusion at the manual curation stage — either confused for noise, or purposely omitted.

Therefore, instead of asking "given the number of active neurons in one task, do we expect the observed number of inactive neurons in the other task?" (i.e. the number of task selective neurons), I instead ask "given the similarity of activity across days within tasks, do we expect the observed *dissimilarity* of activity across days *across* tasks?".

Specifically, I used the ability to return to the same imaging plane across days and calculated the isolation distance in each task for the same population of neurons on pairs of nearby days, then calculated the Spearman rank correlation of the distributions of isolation distance for each task across days, either within tasks or across tasks. This comparison also compensates for differences in activity that might be expected by changing head fixation. I required that both sessions (days) in each comparison passed the strict criteria of behavioral performance and imaging quality described above, resulting in n = 4 pairs of days for cross-day analysis.

Using this analysis, I confirmed the presence of task selectivity. There was a lower correlation of isolation distances *across* task across days, than expected given the correlation *within* task across

days (Figure 12). In each pair of days under comparison, within-task consistency between days was very high, while the same population of neurons had either no significant correlation, or a significant negative correlation, when compared *across* tasks between the same days.

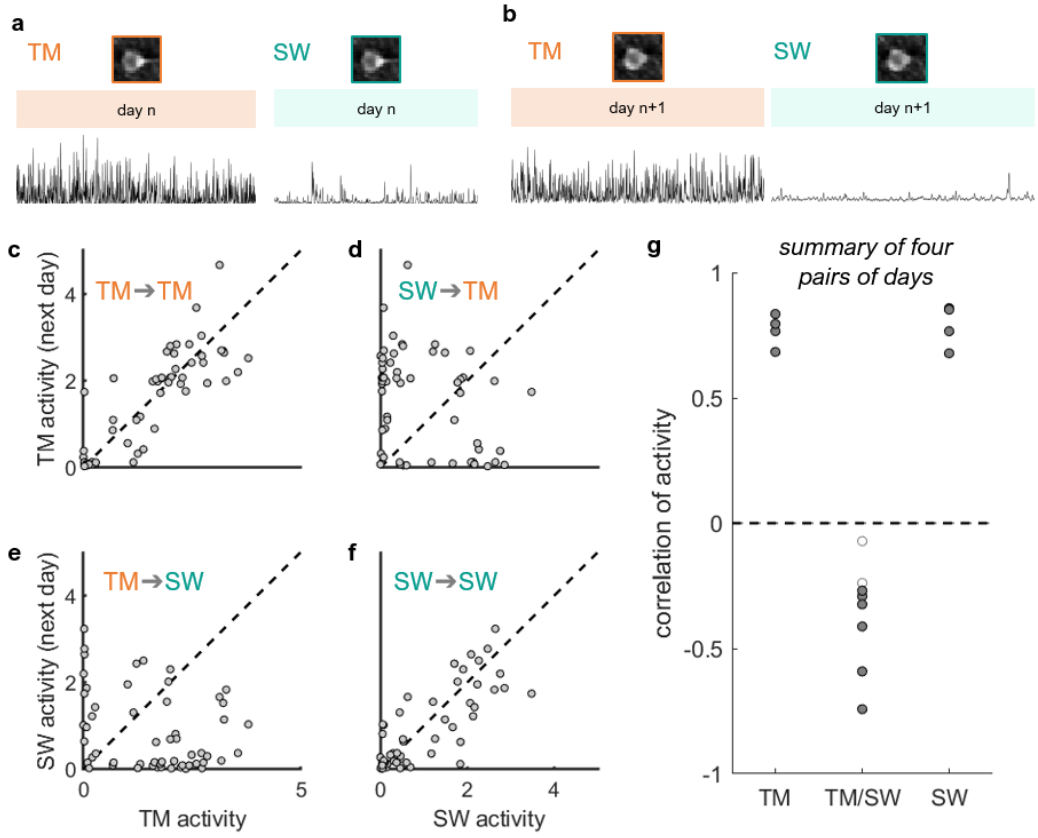

Figure 12. Comparison of activity across days. (a,b) Example neuron showing a crop of its ROI (inset) and its activity over two neighboring days. (c) On day n, this neuron is active during performance of the T-maze, but relatively inactive in the steering-wheel task (T-maze (TM) in orange; steering-wheel task (SW) in blue). (d) The selective activity during the T-maze is consistent on the next day. (e-f) Example pair of sessions comparing isolation distance of the same population of neurons either (c,f) within task or (d,e) across tasks. (g) Summary over four pairs of days. For summaries across tasks, there is *no a priori* reason to distinguish the two combinations across tasks, so the combinations TM to SW and SW to TM (e.g. d, e) were combined (middle column). According to a Spearman rank correlation of each combination as in (c-f), activity across task is significantly negatively correlated or not significantly correlated across days, while activity within task is highly positively correlated. Filled circles indicate significant correlations at $p < 0.05$.

Discussion

By using each cell's isolation distance as a measure of overall activity, I found that the majority of neurons in PPC participated in only one of the two tasks, even though these tasks were designed to be similar in structure. The number of neurons selected for analysis is a subset of the overall number of neurons in PPC; that is, there is a further set of neurons in PPC that are not functionally engaged to any extent across all task conditions. Suite2p can detect some of these, but there are still even more potential neurons that do not fire at all that remain undetected by Suite2p altogether, as Suite2p estimates ROIs based on temporal activity not morphology. Therefore, the proportion of neurons in all of PPC that are active in both tasks or either task is likely much less than reported here.

Notably, this measure is a coarse criterion of whether a cell is active at any point during performance of each task. Whether these cells demonstrate behaviorally relevant activity can be assessed by examining whether event-evoked task-feature selectivity is shared between both tasks (addressed in Chapter 4). The proportion of neurons that share task-feature selectivity across tasks cannot be larger than the proportion that show calcium transients in both tasks to any extent; given this fact, I speculate that the proportion is much smaller.

Explanations by other factors

Besides the effect of task, there could be other potential explanations for differences in neural activity across tasks, either due to artefacts or true preference for confounded factors. I address these concerns below.

Drift and misalignment. Differences in activity across tasks are not due to artefacts of misalignment or drift, as I excluded any sessions that showed evidence of drift or misalignment from the dataset. The raw movies are concatenated across tasks and registered before extracting ROIs in Suite2p, so the same pixels are tracked across tasks. Therefore, if activity were to be found across tasks, this method would pick it up.

Running. It is well known that running drives brain-wide activity modulation of neural activity (Niell & Stryker, 2010, and many others since). As such an important question is whether differences in running activity account for the difference in activity across tasks, given that one task involves running and one does not. However, I observe that differences in running modulation do not seem to account for these results (discussed next in Chapter 3.2).

Visual dissimilarity. It is known that neurons in PPC are visually responsive (as discussed in the General Introduction). As such, it is possible that different neural activity observed across tasks is due to the different amount of visual stimulation in each task. If mouse PPC is highly retinotopic, one prediction is that neurons active in the steering-wheel task are a subset of neurons active in the T-maze task, given that task stimuli in the T-maze task are accompanied by a richer peripheral visual environment than those in the steering-wheel task at the same visual location. However, I did not observe this sort of clustering. Rather, there seem to be many neurons which are active in the steering-wheel task only, a prediction that would not be made by this hypothesis. Further, the next chapter addresses this concern with additional experiments which tests for similarity within conditions of equivalent visual stimulation. These results are thus unlikely to be a consequence of differences in visual stimulation across the two tasks.

Time and satiation. In practice, mice often performed the T-maze first, so task identity is often confounded with elapsed time and overall satiation. Irrespective of which task was performed first, the accumulating effects of time or water would not be expected to produce a stark change in neural activity at the exact point of the task switch. Moreover, since the effect of task-specific neurons is robust on different days despite different trial counts, elapsed time in each task, or even times of day, it is highly unlikely that these results are due to these environmental factors.

Limitations

It is possible that two-photon calcium imaging is inherently limited in missing rare, below-threshold neural activity, and thus I observe "inactive" neurons due to technical limitations of the calcium sensor or imaging parameters. Although the GCaMP sensor itself is sensitive to detecting single action potentials (APs) at high zoom (Chen et al., 2012), Huang et al. (2019) found that measured calcium activity at low zoom is driven primarily by activity consisting of > 2 APs within 100-500ms. In effect, if a cell fired only a handful of APs within a short time window, that activity would not be visible in two-photon imaging. However, if some cells have very few spikes at a very low firing rate throughout the task period of 20-60 minutes, it is probably fair to assume they cannot contribute “meaningfully” to behavior. In any case, later results that depend more on precise timing (Chapter 4) were qualitatively similar to recordings in overlapping higher visual areas performed using Neuropixels probes (Steinmetz et al., 2018), so this limitation is unlikely to nullify findings of inactive neurons as an artefact of the spatiotemporal resolution of the recording technique.

Chapter 3: The role of motor context

I wanted to determine what elements specific to each task could drive selective “participation” of different populations of neurons. Tasks were designed to be similar in abstract structure but varied in the sensorimotor details within, most evidently in terms of means of motor report (the apparatus: a spherical treadmill or steering wheel) and visual scene (virtual T-maze vs Gabor). Thus, to establish whether activity was aligned to the dimension of the means of motor report, I recorded the same neurons in the absence of a task in both apparatuses. In Section 3.1, I discuss results from these experiments. I also discuss results from some conditions in which I present the same visual context as either task but on the opposing apparatus.

Further, as discussed in the previous chapter, a major difference across tasks is the presence or absence of running. Therefore, in Section 3.2, I check that differences in running modulation do not explain why I observe “task selective” neurons.

Here, “context” is used intentionally broadly to refer to the conjunctive association of all sensorimotor features and abstract associations present in either task. “Motor context” is defined to be specific to the motor-related aspects of each task context; conversely, "visual context" here would refer to the visual scenes of each task, which could involve differences between virtual navigation and the absence of a spatially-embedded scene.

3.1: Activity during passive conditions

Methods

Following each task, I continued to record the same neurons while mice viewed a "blank screen" for 5-60 minutes, resulting in two additional conditions: “blank screen treadmill” for when the mouse was on the T-maze motor apparatus, and “blank screen wheel” when the mouse was on the steering wheel apparatus. In these conditions, mice could move (i.e. run or turn) or stay still according to their desires. In practice, mice often ran in the “blank screen treadmill” condition; thus this condition was used later as a "task-agnostic" condition to test for running modulation in the neural population (in Section 3.2). In contrast, mice only infrequently turned the wheel during the "blank screen wheel" condition, and occasionally in concert with grooming behaviors.

In three sessions, I also played elements of the task performed back to the mouse to assess the role of visual context. Each of these were unique, and so are used for illustration. In one session, I replayed a full playback of the T-maze that had just been performed on both apparatuses. In

another session, I replayed a "scrambled" T-maze which contained sequences of disjointed segments from the T-maze (a few seconds each) that was just performed. The objective of this condition was to determine the effects of the visual scene independent of continuous optic flow. I replayed this condition on both the T-maze and the steering-wheel task. Finally, in a third session, of which I only had one example, I replayed the opposite task on both apparatuses. The steering-wheel stimuli was shown to the mouse on the ball ("open loop"), and the T-maze was played back to the mouse on the wheel.

Like in the previous chapter, I measure a neuron's activity throughout each experimental condition using a scalar measure of "isolation distance". I extract the isolation distance four times: during the two tasks and the two "blank screen" conditions. I then correlate the same population's isolation distance across conditions that share the same apparatus vs across conditions that do not, resulting in 2x2 combinations.

Results

The activity of neurons was highly similar within the same motor context (T-maze vs blank screen treadmill; Steering-wheel task vs blank screen wheel), and uncorrelated across motor context (vice versa), mimicking cross-day observations from Chapter 3.2. I conclude on this basis that neurons which participate in either the T-maze or steering wheel task are largely the same as those that participate in passive conditions in the respective motor context in the absence of a task (Figure 13). These results should not be interpreted to suggest that PPC activity is limited to binary participation in a "motor context", only that motor context seems to be a dominant dimension that is highly predictive of the participation of different subsets of neurons across tasks. There are numerous possible differences across the two blank conditions beyond simply the apparatus — such as arousal state, amount of movement, etc. — so results should be interpreted with caution and only considered in light of aforementioned results from task conditions.

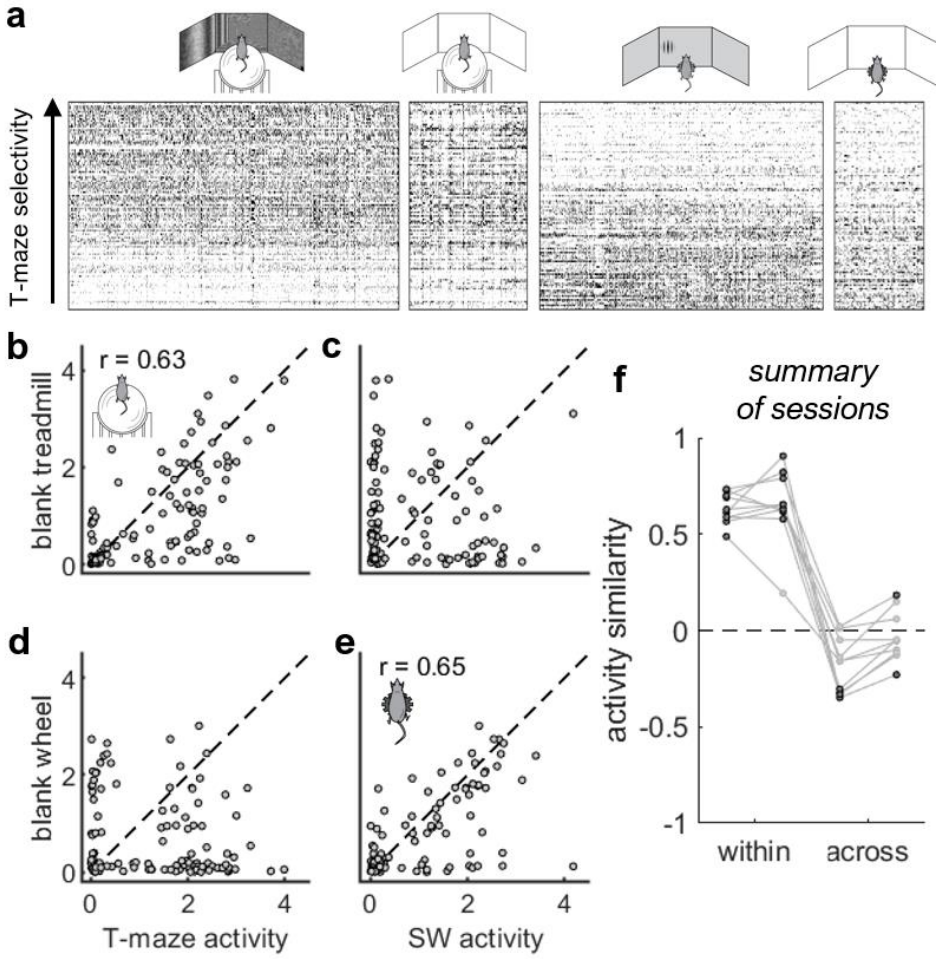

Figure 13. Comparisons of task and blank screen activity. (a) Example session in a "raster" format where pixel intensity reflects amplitude of deconvolved activity (which can take positive real values). Each neuron is a row; neurons are sorted by T-maze vs steering-wheel task selectivity, with the same sorting across conditions (each column). (b-d) Scatter plot summaries of isolation distance for the same population of neurons across different combinations of the four conditions. (b,e) Within the same motor context, activity is highly correlated, but (c,d) across different motor contexts, activity is not significantly correlated. (f) Summary of all sessions with blank screen conditions, compared within session. Filled circles indicate significant Spearman rank correlations. From left to right: within treadmill context, within wheel context; T-maze vs blank wheel; steering-wheel task vs. blank treadmill.

To establish whether motor context was the prime driver of activity similarity or dissimilarity, I also compared a few sessions in which I had "replayed" the task visual scene on the same or the other apparatus. In two cases, the mouse viewed a playback of the T-maze visual scene on the steering wheel apparatus, and in one case, the mouse viewed a playback of the steering wheel task visual stimuli on the spherical treadmill. Again, in all three sessions, activity was shared within the same motor context but not shared across motor contexts, regardless of the visual scene present on the screen (Figure 14).

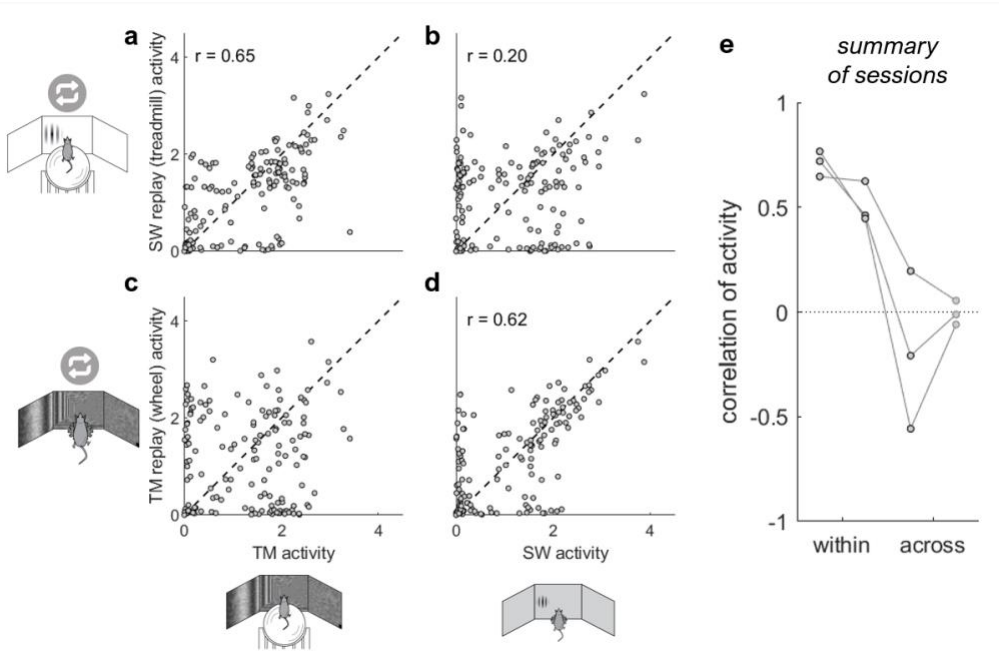

Figure 14. Replay of the task visual scene still shows that task activity preference follows the motor context. (a-d) One session where the "opposite task" was replayed on each apparatus. Within the same apparatus (a,d), neurons were highly correlated in their activity, while across apparatus, neurons were (b) less correlated or (c) not significantly correlated even with the same "visual context". (e) Summary of three sessions with replay, the other two where replay occurred on the usual apparatus. In all three sessions, neurons were still more correlated in activity within the same motor context than across motor contexts. From left to right, TM vs treadmill-based replay; SW vs wheel-based replay; SW vs treadmill-based replay; TM vs wheel-based replay.

3.2: The influence of running in explaining selectivity

Having observed that "task selective" cells are also selective within passive conditions in the same motor context, in this section, I perform control analyses to check whether differences in running explains why many neurons are active in only either task.

Introduction

Differences in participation across tasks may be explained by known brain-wide modulation of neural activity by running (e.g. Niell and Stryker 2010; Saleem et al. 2013; Stringer et al., 2019; Clancy et al. 2019 and many others, reviewed most recently in Parker et al., 2020). The hypothesis implied is that the neurons that are selectively active in either the T-maze or steering-wheel task may be exactly those neurons enhanced or suppressed by running, respectively. Studies finding a modulatory effect of locomotion warrant careful analyses, as such effects may be artifactually overestimated in both electrophysiology and two-photon calcium imaging data due to drift and neuropil contamination (Stringer, PhD Thesis) and wide-field imaging due to arterial dilation causing hemodynamic contamination prior to correction (Huo et al. 2015; Shimaoka et al. 2018). Nonetheless, it is now fairly accepted that there is some real contribution of locomotion on neural activity in non-motor areas.

Running modulation has been observed specifically in parietal areas and overlapping higher visual areas as well (Diamanti et al bioRxiv; Minderer et al 2019; Christensen & Pillow, bioRxiv). To test specifically whether virtual or visual speed better explained responses in PPC, Diamanti et al. (bioRxiv) and Minderer et al. (2019) used "open loop" replay in virtual reality, and found that the influence of running speed was greater than the influence of visual speed, particularly in more medial parts of PPC (areas A and AM). In "closed loop" virtual navigation though, Krumin et al. (2018) found that virtual spatial position fields explained PPC responses better than "real" variables of forward and rotational velocity on a spherical treadmill.

In any case, perturbations to test the causal influence of running-related activity are few. A recent study in mice performing visually-guided virtual T-maze tasks found that inactivation of several regions including parietal areas slowed down running (Pinto et al., 2019), an outcome also observed in a task where mice were required to monitor visual flow to maintain a straight trajectory (Minderer et al. 2019). However, in both cases, slowing down was likely a behavioral strategy due to increased uncertainty about visual evidence upon inactivation, which would be consistent with the broader interpretations of PPC perturbations as causing visual or visuo-motor impairments (as discussed in the Introduction). In both studies, effects were observed in parietal

areas, but also visual areas beyond PPC, corroborating the proposition that the causal effect was mediated by visual, not motor, impairments.

Given aforementioned findings of brain-wide modulation by locomotion, it would be unsurprising to find neurons apparently modulated by running in PPC. The question here is rather whether the existence of running-modulated neurons *fully explains* the delineation in participation of neurons across the two tasks.

There are varying hypotheses regarding the specific profile of the effects of running on neural activity (reviewed in Busse, 2018), with some suggesting there is a continuous relationship between running speed and neural activity in V1 (e.g. Saleem et al., 2013; Ayaz et al., 2013) and others arguing that there is a qualitative difference between stationarity and running (e.g. Niell & Stryker, 2011). Therefore, I also ask whether specifically activity in stationary periods is most similar to activity in the steering-wheel task.

Methods

In the task, running is behaviorally relevant" because mice cannot complete trials without running and they are motivated to collect water reward as they are water-deprived. As well, running traverses the mouse actively through portions of the T-maze which are known to invoke "firing fields" of virtual heading angle and position (Krumin et al 2018) and/or neurons that tile the corridor in choice-specific sequences (Harvey et al. 2012; Koay et al. 2019). Therefore to check for “pure” running modulation, I used the blank screen condition in the treadmill context as a task-agnostic method for assessing running modulation.

I compared each neuron's "running modulation" (rRun) in the blank screen treadmill condition to its “task selectivity index” (task SI) compared between the two tasks, as illustrated in Figure 15. rRun was computed using the correlation between forward running speed on the spherical treadmill and its deconvolved calcium trace. Task SI was the difference between isolation distance in the T-maze vs. the steering-wheel task, divided by the sum to normalize the value to lie between -1 and 1:

$$\frac{(\text{TM isolation distance - SW isolation distance})}{(\text{TM isolation distance + SW isolation distance})}$$

Task SI reflects the relative participation by the neuron in the T-maze vs the steering-wheel, where positive values reflect T-maze preference and negative values reflect steering-wheel task preference (see Figure 15b-c for an example). To compare running speed and neural activity, I

downsampled the running speed to match the imaging frame rate, then smoothed both the neural activity and running speed by convolving the traces with a 1-second s.d. Gaussian filter. Smoothing allowed more opportunity to discover running-related effects that were not instantaneously apparent in calcium activity, such as due to slower GCaMP dynamics, or that may precede rather than directly follow an increase in running speed.

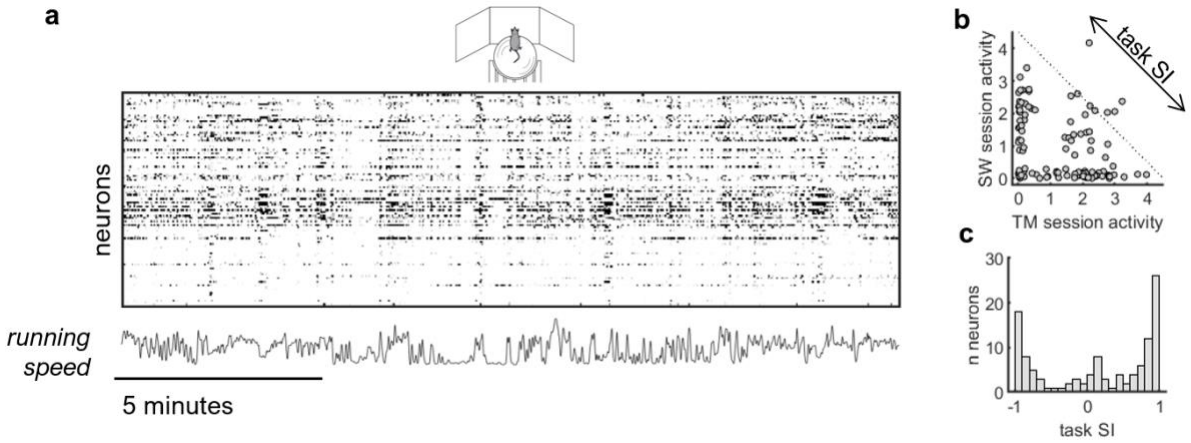

Figure 15. Schematic showing the procedure for comparing running modulation and task selectivity. (a) Example "raster" representation of neural activity across the blank screen treadmill condition. Each row is a neuron and pixel intensity reflects the amplitude of deconvolved calcium. The running speed of the mouse is shown below. Running modulation is the correlation between each neuron's activity and the mouse's running speed. (b,c) Explanation of task selectivity for an example session. (b) Task selectivity takes the normalized difference between activity in the T-maze vs steering-wheel task (where T-maze selectivity was chosen to have a positive sign and steering-wheel task selectivity to have a negative sign). (c) The distribution of task selectivity as taken from the data in (b).

For each neuron, I assessed significance of running modulation by circularly shifting the running speed relative to the neural activity 1000 times by a randomly-selected number of frames. Significance tests are crucial given that spurious apparent running modulation is very likely even with best attempts to correct for artefacts, given that running causes fast z-drift (Stringer, PhD Thesis; Pachitariu et al., Cosyne Abstract, 2018). Circular shifting is preferable to randomly shuffling frames, as circular shifts provide a more stringent null hypothesis that accounts for autocorrelation such as due to slow GCaMP decay.

Stationary analyses

If running and stationarity are qualitatively distinct states, it may be unfair to check for running modulation using a measure that tests for a monotonic relationship of running speed as in the rRun correlation measure. So, I further tested how activity (isolation distance) was related across two "stationary" (with respect to running) periods: the steering-wheel task and stationary periods in the T-maze.

Blank screen recordings were often fairly short (usually 10-20 minutes), and mice often ran during these, so I did not have enough time points when the mouse was stationary to use this condition. Instead, I used stationary periods in the T-maze. As mentioned, interpretation of neural activity during running in the task (i.e. the T-maze) is problematic. Further, the cessation of running during a task context likely reflects disengagement or satiation (if it occurs near the end of a session). So, these results should be interpreted with caution.

To calculate "activity" during stationary periods, I re-computed isolation distance using the same ROIs as previously but only including the frames when the mouse had a running speed <1.2cm/s and was stationary for at least 3s — the latter to avoid contamination by preceding running periods due to slow decay of GCaMP, and also to ensure the stationarity was not a brief pause during, for example, a change in angular velocity. Now, instead of one calculation of isolation distance to summarize activity during the whole task epoch, there is another calculation of isolation distance within stationary periods only.

As before, I wanted to compare across days as a baseline. Since mice usually performed the task and rarely stopped for very long, in the end I only had one pair of days in which both sessions had a sufficient duration to compare task selectivity across stationary periods. Comparing within session is not valid here as stationary epochs are likely to be contaminated by nearby signals from non-stationary periods and therefore stationary and T-maze epochs might be spuriously similar, and therefore both dissimilar to the steering-wheel task in the same session.

Results

Many neurons were significantly modulated by running, and many neurons were not. Neurons with significant running modulation were modulated both positively and negatively by running, consistent with previous reports from primary visual cortex and throughout the brain (Stringer et al., 2019; Musall et al., 2019). To check if task selectivity could be explained by running, I compared each neuron's running modulation and task selectivity. If running modulation purely explained the presence of selective neurons, there should be a high positive correlation: all T-maze neurons would have positive running modulation, and all steering-wheel neurons would have negative running modulation (purple off-diagonal quadrants in Figure 16). However, I did not find this relationship; the correlation between these two measures was not significant in the example session in Figure 16, nor across any of the 10 sessions in which there was a blank running condition, median $r = 0.09 +/- 0.09$; $p > 0.05$ for all 10 sessions.

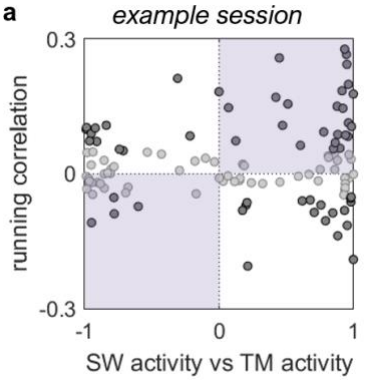

Figure 16. Testing for the relationship of task selectivity and running modulation. (a) Example session showing running modulation as a function of T-maze vs steering-wheel task preference (where positive values mean T-maze preference). Filled circles show significant running-modulated neurons according to the permutation test. The purple overlay shows hypothetical distributions of cells, if T-maze neurons were solely those modulated by running, and steering-wheel task neurons were solely those suppressed by running. In this example session, the Spearman rank correlation was not significant, using all neurons, r = 0.04, p = 0.67, or just significantly running-modulated neurons (filled circles), r = 0.06, p = 0.65.

To check if a neuron's activity during stationarity was shared during the steering-wheel task, in which the mouse is also stationary, I then looked at activity during stationary periods. Within the T-maze, activity went down during stationary periods; this decrease in activity was expected due to the task-relevant nature of running in the T-maze and previous findings in the literature regarding decreased activity during stationary periods and disengagement in general (although slightly debated). However, there was still not a significant correlation between activity measured only in the stationary period in the T-maze, and activity in the steering-wheel task (Figure 17). This result indicates that differences in participation across motor contexts are not likely a direct byproduct of neurons which are active only during either a running or stationary state.

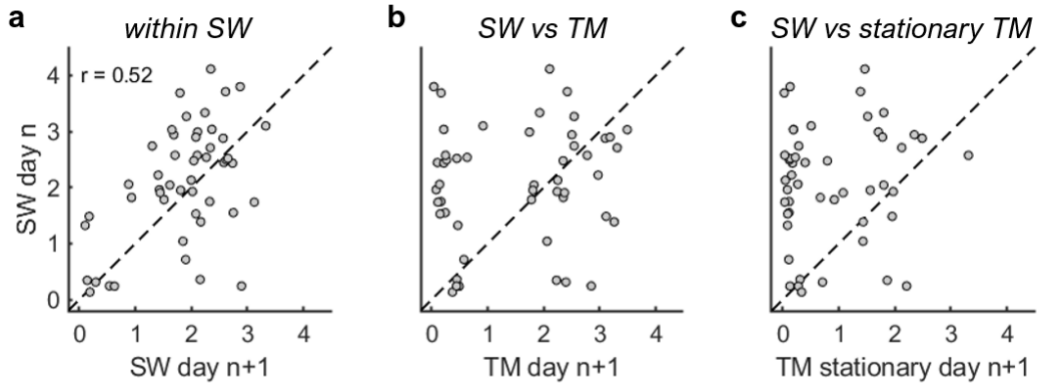

Figure 17. An example session comparing steering-wheel task activity to T-maze activity or stationary activity in the T-maze across days. (a) Baseline comparison of consistency of steering-wheel task activity across days, r = 0.52, p < 1e-3 (b) Comparison of activity across tasks; activity is not significantly correlated, r = 0.13, p = 0.39 (c) Comparison of steering-wheel activity to only stationary periods in the T-maze; activity is not significantly correlated, r = 0.12, p = 0.41

Discussion

In this chapter, I observed that the same neurons that are selectively active during performance of either the T-maze or steering-wheel task are also selectively active during passive conditions

on the same motor apparatus. Since I also had conditions showing the visual scene of each task, I was able to conclude that it is likely the motor context but not the visual context that mostly drives the occurrence of “selective participation”. Despite observations of shared activity within motor contexts that share running vs stationary states, I found that modulation by running did not account for task selectivity of neurons. This lack of effect was not obscured by stationarity having a qualitatively different effect on neural activity, as I observed activity was still dissimilar between the steering-wheel task and stationary periods in the T-maze.

While I find similarity in participation of single neurons across passive and active conditions in the same motor context, an important point to emphasize is that differences in event-evoked responses across active and passive states are completely consistent with the results here. There is reason to think differences in event-evoked activity across passive and active states are likely, although this topic is not a subject of this thesis (Diamanti et al. bioRxiv; Krumin et al. 2018; Steinmetz et al. 2019; Harvey et al. 2012; Pho et al. 2018).

Unless PPC is highly sensitive to miniscule visual aberrations, which is fairly unlikely, the observation that different sets of PPC neurons are engaged across the two blank conditions across apparatuses is fairly convincing that the neurons' selective participation is based on this "motor context" division. Notably, motor context here is used generally and can mean any conjunction of features unique to each motor context, including non-motor features such as olfactory or visual cues specific to each apparatus. The primacy of motor context over visual context is upheld even further given the observation that in one available session, the “opposite” visual scene was played, and neurons were still more selective in their activity within the same motor context. The results from this session also suggest that observations of different sets of neurons participating in the T-maze or steering-wheel task (from the previous chapter) are not due to differences in retinotopic preference.

Interpretation of context selective subgroups

Selective engagement of different sub-groups in PPC across motor contexts is reminiscent of works from Snyder and colleagues, who found effector-specific neurons selective to reaches vs saccades to a target (Snyder et al., 1997). This effector-specific recruitment of neurons may be analogous to the context-specific recruitment seen here across the steering-wheel and treadmill motor contexts. In their case, they mapped these effector-specific neurons into two subregions, lateral intraparietal area (LIP) where neurons largely encoded saccades, and an adjacent area, parietal reach region (PRR) where neurons largely encoded reaches. Interestingly, 32% of responsive neurons in their dataset were significant for both types of movements, a figure that

bears close resemblance to the proportion of neurons active in both tasks in this dataset. However, in their case, effector-specific neurons were largely anatomically separable, whereas here I observe that they are anatomically intermingled (see Appendix A).

Stationarity vs disengagement

It may not be possible to interpret neural responses during stationary states as stationarity is often associated with disengagement. There is evidence that neural activity in the brain becomes more correlated during disengaged periods, although locomotion is sometimes taken as a synonym for arousal (see literature on synchronized states, reviewed in Harris & Thiele, 2011). During stationary periods, an increase in correlation between neurons — in other words, neural activity becoming more low-dimensional — could potentially lead to spurious similarity in activity during stationary periods across apparatuses due to disengagement, not the absence of running. This topic is flagged as a possible caveat of analyzing stationary periods, but a comprehensive treatment of the nuances of whether attention, arousal state, and movement increase or decrease correlations is heavily debated and is beyond the scope of this thesis. To test for the effect of stationarity specifically, in the future it would be ideal to record for longer sessions in the "running treadmill" condition to encourage more stationary periods. In practice, I generally chose shorter durations (10-20 minutes) of blank screen conditions to not demotivate the mouse before performance of the next task. However, it would be useful to examine stationary periods in a task-absent condition as interpretation of stationarity in the T-maze is, as discussed, complicated by the task relevance of running in the T-maze.

Limitations

It is unclear given different methods of correcting for motor artefacts how much doing so removes "true" running contribution, vs. artefactual contributions; Stringer (PhD Thesis) observed that neuropil correction sometimes "aggressively" removes running correlations. Whether correlations are spurious or real is a question that perhaps is not possible to tell with existing recording techniques, given that motion artefacts affect both calcium imaging and electrophysiology (Pachitariu et al., Cosyne Abstract, 2018). However, since I could still find significantly running-correlated neurons, the ability to detect running modulation was not completely hampered in these analyses.

Chapter 4: Shared selectivity in active neurons

One of my initial aims was to discover whether single neurons shared selectivity for task-relevant features. If a given region is to reliably extract features of interest from specific sensorimotor details of a given experience, this property should be shared across different contexts in which the feature is encountered.

I already observed that many of PPC neurons do not “participate” in both tasks. But what about those neurons that do participate in both tasks? It may be that these neurons are the subset most relevant for behavior, and thus in this chapter I seek to first establish that there is task-related event-evoked activity within either task in general, and second, establish whether task-evoked activity is correlated across tasks.

Introduction

Decision-making can be summarized as consisting of several processes which may be distinct or overlapping. Given a sensory percept and a task, the subject needs to make a choice. Classic work suggests that neurons which are selective for evidence for choices of different directions are pooled for comparison to make a choice (Shadlen et al., 1996). This choice process can unfold as an ongoing monitoring of the sensory stimulus, as in the case of evidence accumulation tasks, or can be a unidirectional flow of information if the stimulus is immediate and perception is certain. The choice itself can either be "abstract", or specific to the eventual action needed to make the choice. In many task designs, these possibilities are confounded, but can be dissociated in designs where the “abstract choice” is made prior to the choice of specific motor action, with the selection of the side or effector possibly deferred until a later cue. The view that the choice is inherent to the means of action is known as the intentional framework, which argues that choices are “embodied” by virtue of recruiting existing motor circuits such as saccadic or reach regions (Shadlen et al. 2008; Andersen and Buneo 2002). After cueing to make a choice, or upon collecting sufficient evidence to be confident of a decision, a motor command must be sent on the basis of this selected motor choice in order for it to be literally carried out. While there can be choices that are not reported through any action, such as those relating to value comparisons, here I only discuss choices based on sensory evidence which result in an eventual motor report, such as those made in the tasks under study.

Early stage choice/action selection processes must precede the choice execution itself, and in a causally relevant and behaviorally plausible time window to drive a consequent action. When I

discuss choice, I mean that which could be predictive of upcoming movement direction, or reflective of ongoing movement direction — causally relevant, or a corollary discharge of either. In the case of the latter, the representation could be specific to the manipulandum or effector e.g. “turning the wheel left”, “saccading left”, or there may still be an ongoing representation of choice that is divorced from the specific manipulandum, perhaps for credit assignment, e.g. "I am making a left choice now" rather than "I am turning this wheel clockwise".

The involvement of different brain regions in different stages of this decision process predict different outcomes of inactivation. Inactivation studies reviewed in the General Introduction suggest that the causal involvement of PPC is likely early, and inactivation of PPC in rodents rarely causes motor errors directly.

Here, by changing the means of motor report that applies to the same abstract choice, I predict different outcomes according to different hypotheses of the function of PPC. Specifically, comparisons of choice selectivity across these tasks are able to address whether PPC contains an abstracted or embodied representation of choice. If choice selectivity is present in both tasks, and this selectivity is correlated, it can be concluded that choice representations are abstract with respect to the means of motor report. If choice selectivity is present in both tasks, but this selectivity is uncorrelated, choice representations may be embodied in the means of motor report. Finally, if choice selectivity cannot be decoded at all, it may be that PPC is not involved in decision-making in general.

Methods

Receiver operating characteristic analyses

The primary measure used to determine feature selectivity was receiver operating characteristic (ROC) analyses (described in Figure 18). This measure is motivated by signal detection theory (Green & Swets, 1966) which describes a theoretical framework for relating neural activity and behavior, specifically here the process of making categorical decisions based on noisy sensory evidence. In general, the ROC measures the difference between two distributions. In the case of the neural basis of decision-making, a neuron is considered able to discriminate between two task conditions (e.g. left-side vs. right-side choices) if the distribution of its activity during one condition is sufficiently non-overlapping with the distribution of its activity during the other condition (Britten, 1992). The "area under the ROC curve" (auROC) captures the ability for an “ideal observer” to correctly classify activity coming from different distributions (e.g. relating to

different choices), based on different criterion levels (*c* in Figure 18-a). If the distributions are completely non-overlapping, discrimination is perfect; if distributions are completely overlapping, discrimination is at chance level.

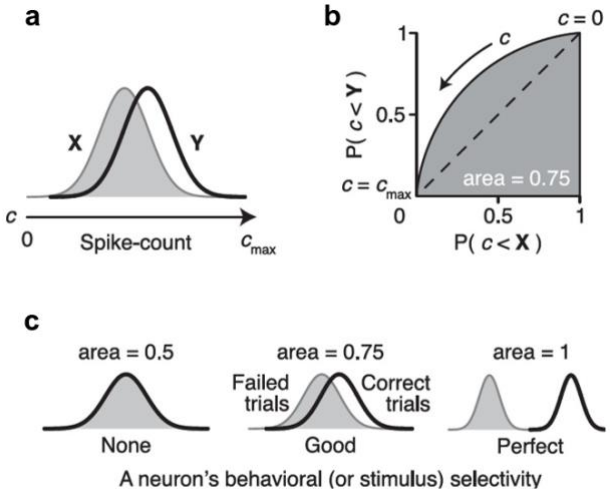

Figure 18. Schematic showing the logic of ROC analysis. Adapted from Smith et al. (2012). (a) Hypothetical example distributions of spike counts from one neuron over two behavioral conditions, X and Y, e.g. left and right choices. (b) The area under the ROC curve (auROC) for different threshold values of spike counts. (c) Relationship of the distance between distributions to the auROC value. If spike count distributions for both choices are completely overlapping (auROC=0.5), one cannot decode X and Y.

The auROC is equivalent to a Mann-Whitney U-statistic according to the following relationship:

$$\text{auROC} = \frac{\text{U}}{n_1 n_2}$$

where n1 and n2 are the numbers of trials for each comparison for the condition under consideration (e.g. number of left-side choices and number of right-side choices at 12% visual contrast stimulus on the left). AuROC is therefore equivalent to a non-parametric two-sample test of the distributions of neural activity for the conditions tested.

Whole trial analyses

Trial temporal dynamics could differ across the two tasks, i.e., the timings at which various task events occur, such as the interval between stimulus onset and choice, and the timecourses of execution of movements such as turning and licking. Therefore, I started by not making any assumptions about the timing of activity within a trial, and instead take the mean deconvolved calcium activity from stimulus onset to the end of response, which could include reward delivery if the choice were correct.

Significance tests

As two-sample tests can be sensitive to different sample sizes within each distribution of interest, it is important to perform a statistical test of these values that respects possible imbalances in sample size. This consideration is necessary in e.g. comparisons of choice selectivity for high visual contrast in a detection task, where there may be few errors compared to correct choices. That is, for a 50% left contrast stimulus, there may be many more left-side than right-side choices in a well-performing mouse.

To address imbalanced trial counts, I used a permutation test to assess significance of assessed feature selectivity. Namely, for every neuron I shuffled trial labels 1000 times, and recomputed the statistic, such as choice selectivity, for each new batch of "left"-labelled and "right"-labelled trials. As I kept the same number of effective "left" and "right" trials, the permutation test respects imbalanced samples of each condition and will recapitulate biases due to this imbalance in the permutations as well. The neuron was deemed feature selective if the actual statistic exceeded the 2.5% and 97.5% tails (i.e. alpha level 0.05, $p < 0.05$ in a two-tailed test) of the distribution resulting from the 1000 permutations.

Session inclusion criteria

I only included sessions if at least 10 trials of each comparison (e.g. 10 left-side choices and 10 right-side choices) remained after excluding invalid trials.

4.1: Shared choice selectivity

I first focused on analyses of choice selectivity, within and across tasks, given that choice signals have been an important subject of study in decision tasks in PPC.

Methods

Trial quality control: inclusion criteria

I always include both correct and error trials to dissociate between stimulus and choice. In some sessions, the same stimulus condition was repeated if the mouse did not respond correctly, to encourage engagement. These "repeated" trials were excluded from analyses here, as mice could know with certainty the correct choice even prior to the trial, and thus may engage in a different strategy for choices that is not guided by sensory evidence.

For wheel tasks, I excluded “early moves” where the mouse first started to turn the wheel <125ms after the onset of the stimulus presentation time. Movements earlier than this period were assumed to be too early to be reactive to the stimulus and may have been coincidental movements. In a subset of mice for which I did not enforce a “pre-trial” quiescent period, many trials also had movements prior to trial onset; I excluded these as well.

Stimulus-independent choice selectivity

To evaluate choice selectivity per se, it is essential to compute choice selectivity independent of stimulus side. In sessions with good psychometric performance, as was selected for in the sessions here, stimulus side is highly correlated with choice side. Therefore I first used a variant of choice probability that is independent of the stimulus side called “combined conditions” choice probability (ccCP) which was introduced in Steinmetz et al. (2019) and Zatka-Haas, Steinmetz et al. (bioRxiv).

As mentioned above, choice selectivity is estimated using ROC, which is related to the Mann-Whitney U in the following way:

$$\text{auROC} = \frac{\text{U}}{n_1 n_2}$$

In traditional measurements of choice probability (Britten et al., 1996), for a given stimulus contrast, e.g. 50% contrast on the right side, a neuron's activity in one trial type (e.g. left-side choices) is compared to its activity in another trial type (e.g. right-side choices). Intuitively, the

U-statistic for each neuron counts the number of trials for which right choices had greater activity than left choices, and the denominator (n1*n2) reflects the number of trials for each condition, left and right choices.

In ccCP, choices are still compared within a given stimulus contrast, but instead of computing the fraction *per* stimulus contrast, which then only uses few trials, the measure *combines* choices across stimulus conditions, without conflating stimulus at the same time. Namely, as before, the U-statistic is calculated for each stimulus condition. However, now the U-statistics are summed over all stimulus conditions. The sum is the new numerator, and the denominator is now the sum of the n1*n2 trial counts for each of the nine conditions. Inherent to the method, contrast conditions are excluded if the mouse only makes choices to one side. In my dataset, I had nine stimulus conditions (0% and 6, 12, 25 and 50% contrast on the left and right) and thus nine U-statistics, but the method is illustrated in Figure 19 for an example where there are only two stimulus conditions (e.g. left and right stimulus at 50% contrast).

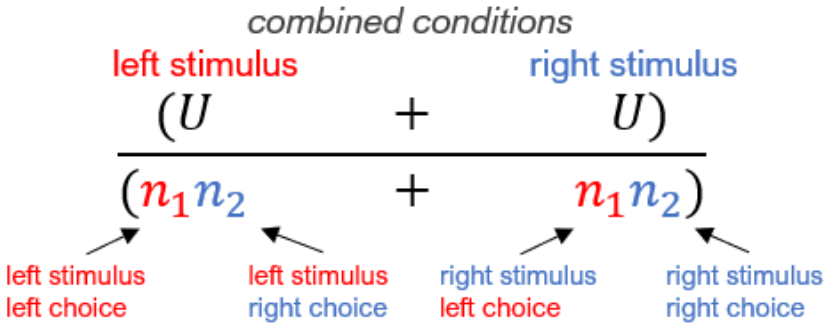

Figure 19. Illustration of the combined conditions choice probability computation for a case of two stimulus conditions. Rather than dividing U/(n1*n2) to get the auROC, the U and trial counts are individually summed. If n1 or n2 for either stimulus condition is 0, the trials do not appear in the denominator (the U-statistic is also 0 due to how the U statistic is computed algebraically).

The details are not essential, but important to the method is that the method still only makes comparisons *within* stimulus conditions when calculating each U-statistic, so is always independent of the stimulus side.

Finally, I normalize the value of the ccCP (which otherwise, as in the auROC, lies between 0 and 1) to lie between -1 and 1, where -1 means strong left choice preference, and 1 means strong right choice preference, using the following relationship:

$$normalized\ ccCP = 2 * (ccCP - 0.5)$$

Specific trial epochs

In addition to performing “whole trial” estimates of choice selectivity, I also looked at specific epochs within the trial. I therefore also checked for choice selectivity averaged only within the first 200ms (or 500ms in some cases) "freeze" period where the stimulus does not move, the "post-movement onset" period (see Figure 20), and the "pre-movement onset" period for the steering-wheel task only. In all cases I used the ccCP measure described above, but only averaged over activity within a specific window, rather than averaging over the whole trial from stimulus onset to response.

The "freeze" period was chosen to be comparable across the tasks, as I did not want to assume a "pre-move" period in the T-maze, given that trajectories therein can be fairly continuous and there is therefore not often a clear inflection point to define as the choice "movement" on every trial. This initial period could be thought to be a proxy for a period when the mouse might be gathering evidence for their choice. Note that in this case I perform "stimulus-side-independent" analyses, so although this period in general is likely reflecting perception of the stimulus, this measure is specific to sensory evidence *for the* (upcoming) *choice* as I compute it separately for each stimulus side, as per the whole trial ccCP analyses above.

For the steering-wheel task, the "move" time was the first detected wheel movement after 125ms from stimulus onset, detected using an algorithm used in other published analyses from the lab (e.g. Steinmetz et al. 2019) and used by the International Brain Laboratory. The pre-move window used here was 200ms before this time period, and the post-move was 200ms after this time period.

For the T-maze task, the freeze period was also the first 200ms. Again, there is no clear inflection point for "the choice movement" in the T-maze, so I used the time at which the mouse passed the 90cm mark in virtual reality, which is the junction where the main corridor meets the perpendicular turn segments (see Figure 20-c for an illustration). In many trials, the mouse would veer towards the wall corresponding to their eventual choice long before the juncture (potentially indicating their confidence or decision commitment) which was also observed in another study using this task (Krumin et al., 2018). Therefore the T-maze “post-movement” period is reflective of the turn in virtual reality, but may occur much later than the actual turn of the spherical treadmill that the mouse makes to select their choice.

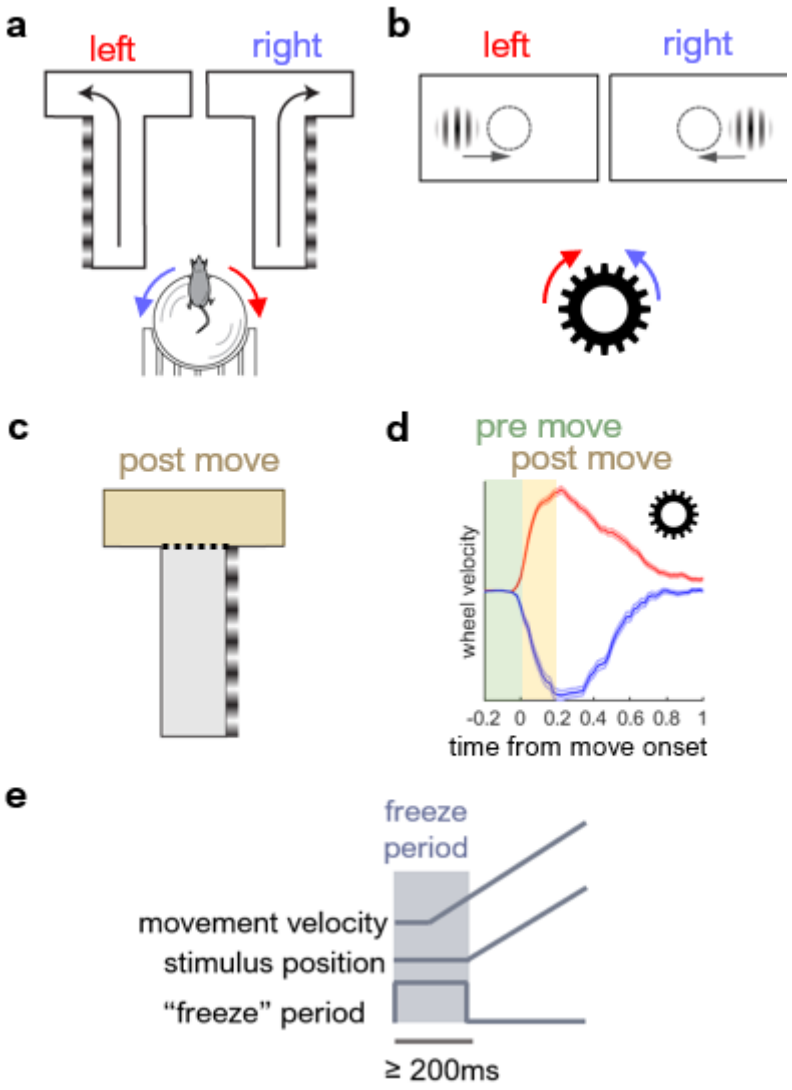

Figure 20. Illustration of choice directions and move epochs in the two tasks. (a,b) Schematic of how choices are carried out in both tasks. Both tasks involve a clockwise movement to "choose left". (c) Illustration of the relevant window used for the "post-move" in the T-maze (d) Illustration of the "pre-move" and "post-move" windows for the steering-wheel task. (e) Schematic of the logic of the "freeze period" in both tasks.

Event-triggered average

For visualization of task-evoked activity, some example neurons are plotted averaged to relevant task events. When calculating event-triggered averages, all relevant signals were aligned and resampled to a "common timeline" of the imaging frame rate, i.e. 10fps. For visualization purposes only, all signals were upsampled 150% before averaging, which allows for more precise visualization of event-evoked activity.

Across-task methods

It is not valid to compare all neurons across tasks, as a neuron's task responses are necessarily going to be absent if the neuron is silent. Therefore, I only look at the subset of neurons active — according to the measure of isolation distance — in both. To compare the distribution of choice selectivity across the same neurons, I required at least 10 neurons to be active in both tasks. This procedure excluded some sessions from analysis, depending on the isolation distance threshold used for classifying neurons as active.

I compared the choice selectivity (ccCP) value of the same neuron across tasks, in order to account for the choice side preference, which should be of the same sign (+/-, and ideally similar magnitude) if single neurons shared choice preference across tasks. Within-session, I correlated the ccCP values of the population of neurons (n >10 as above) across the two tasks using a Spearman-rank correlation to determine on a session-by-session basis whether in that session, the neurons active in both tasks shared choice preference.

Thresholding for activity

When analyzing activity concurrent with movement, such as "post-move" epochs that reflect ongoing choice, it is essential to employ the isolation distance to discard potentially inactive cells.

Figure 21 shows an example neuron that might be assumed to be truly choice selective on the basis of average activity across left and right choices, and in fact is deemed "significantly" choice-selective according to a permutation test. However, this cell has very low isolation distance during this task as judged using its entire trace throughout the task (isolation distance = 0.02, with typical thresholds being at least 0.05-0.8). Inspection of the neuropil surround of the cell reveals that even the neuropil shows separability by choices aligned to movement onset. As a consequence, supposed choice selectivity is likely a movement artefact, probably driven by minor but reliable differences in movement vigor across left vs right choices. It is possible that broad-scale activity at the spatial scale of neuropil could be used for representations of choice, but here I assume that the relevant unit of neural activity is at the level of somatic activity. While it is possible that nearby neuropil can be correlated and the cell can still have valid choice selectivity, it is not possible to distinguish this hypothesis from motor artefacts, so to be conservative I do not consider cells that are too similar to the neuropil (i.e. have a low isolation distance), in keeping with the assumptions made in the rest of the thesis.

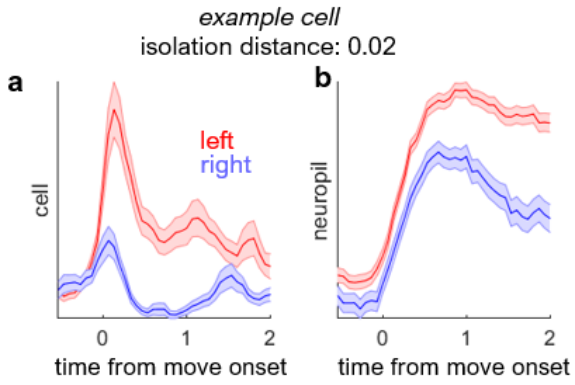

Figure 21. Apparent choice-specific event-aligned activity may be spurious in cells with low activity. (a) An example cell with very low isolation distance, aligned to movement onset and split across left and right choices, and averaged across trials (mean ± s.e.m.). (b) The respective neuropil surround of the cell in (a), averaged over the same events.

As before, I established baseline expectations of choice selectivity across tasks by comparing choice selectivity across days, either within the same task or across different tasks. Comparing selectivity within-task across days accounts for session-to-session variability in choice biases, motor errors and arousal that may differ artifactually across choices within a session. Although such biases could also be consistent within a mouse across sessions, or even across mice, it is at least a more robust measure than only comparing within session. As well, comparing baseline within-task selectivity across days accounts for any "representational drift" in what the cells may encode (Driscoll et al 2017) although I do not expect that anyway at this timescale (i.e. sessions separated by one or two days at most).

Results

Validation of stimulus-independent choice selectivity

As mentioned, in the steering-wheel, task 0% contrast trials were accidentally not rewarded. Therefore, interpretation of activity in these trials could be problematic. However, in the T-maze, 0% contrast trials were correctly rewarded at random, p(reward) = 0.5. I use these sessions to validate the combined conditions choice probability (ccCP) measure, which is designed to be stimulus-independent. Indeed I find very good agreement between the choice selectivity auROC estimated on 0% contrast trials "0% auROC" and the ccCP in the T-maze. Fifteen sessions were eligible to compare 0% auROC and ccCP with at least 10 trials of each response type. Correspondence between these measures in the same neurons was extremely good with median r = 0.96 +/- 0.04 m.a.d. across sessions. In some cases, this close agreement was because the mouse performed so well that most trials bar the 0% contrast trials were performed perfectly, such that most high contrast conditions were not included due to only having one type of response (left only or right only choices) in the ccCP analyses (see Methods for why). The high correlation between 0% auROC and ccCP is reassuring that ccCP can be used as an accurate proxy

choice in the absence of a sided stimulus, in sessions without enough 0% contrast trials, which helps include many more sessions.

Evaluation of stimulus-independent choice selectivity within tasks

In each task, there were neurons with movement-aligned activity selective for left vs right choice. Figure 22 shows two example neurons which were significantly choice-selective in a stimulus-independent manner (ccCP). An example of the same kind is shown in Figure 23 for the steering-wheel task.

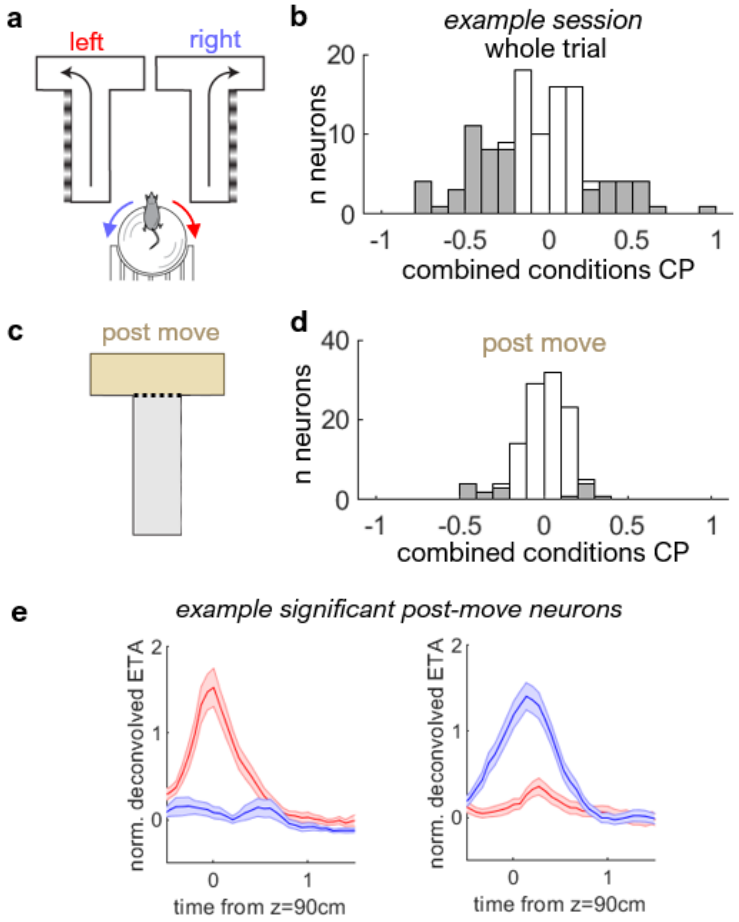

Figure 22. Neurons in the T-maze are selective for choice independent of stimulus. (a) Schematic of the T-maze. (b) Histogram of ccCP values estimated using the whole trial (-1 means left preferring and 1 means right preferring). Filled bars indicate statistically significant neurons according to the permutation test. For illustration, I include all recorded neurons, including potentially inactive ones. (c) Schematic showing the "post-move" period in the T-maze. (d) Histogram of ccCP averaged across the post-move period only. (e) Two example neurons of those that passed the significance test for ccCP in the post-move period, aligned to the start of the post-move period (the dotted line in (c)). The time corresponds to the time at which the mouse first passed the z=90cm mark down the corridor.

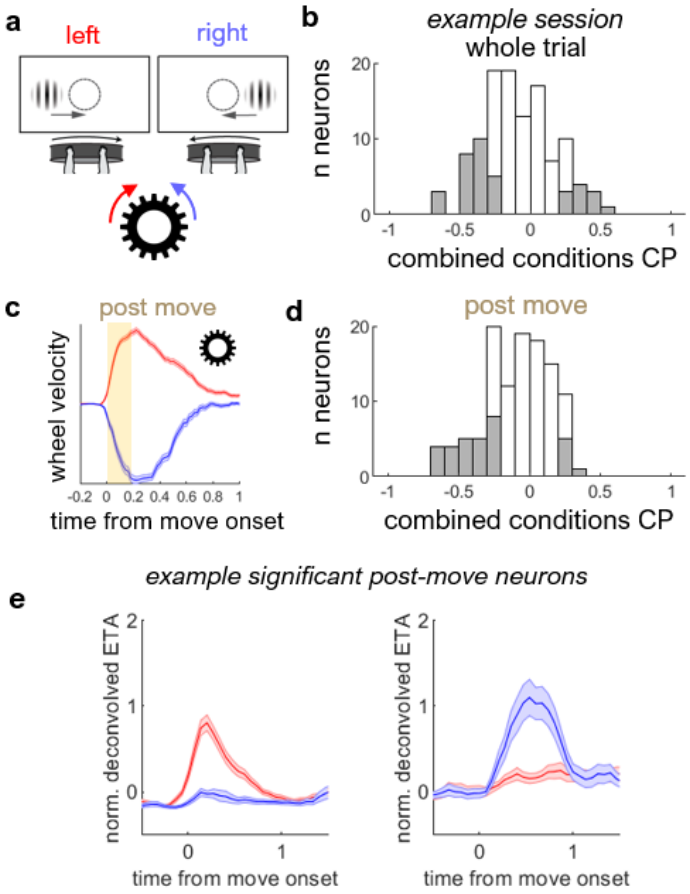

Figure 23. Neurons in the steering-wheel task are selective for choice independent of stimulus. (a) Schematic of the steering-wheel task. (b) Histogram of ccCP values for ccCP averaged across the whole trial. Filled bars indicate statistically significant neurons according to the permutation test. For illustration, I include all recorded neurons, including potentially inactive ones. (c) Schematic showing average wheel velocity for movements to the left and right, aligned to detected movement onset times, highlighting the "post-move" period used for the steering-wheel task. (d) Histogram of ccCP averaged across the post-move period only. (d) Two example neurons of those that passed the significance test for ccCP in the post-move period, aligned to detected movement onset times.

I then used the periods defined above and counted the percentage of neurons that were choice selective (based on ccCP) for every session. I used a low threshold to be liberal for including neurons which might not have high variance but may have been reliably active for certain choices, isolation distance > 0.05, so this procedure included many neurons that may have been inactive (as illustrated in

Figure 21). The percentage is thus the proportion out of the total number of neurons > 0.05 isolation distance. Results are shown in

Figure 24.

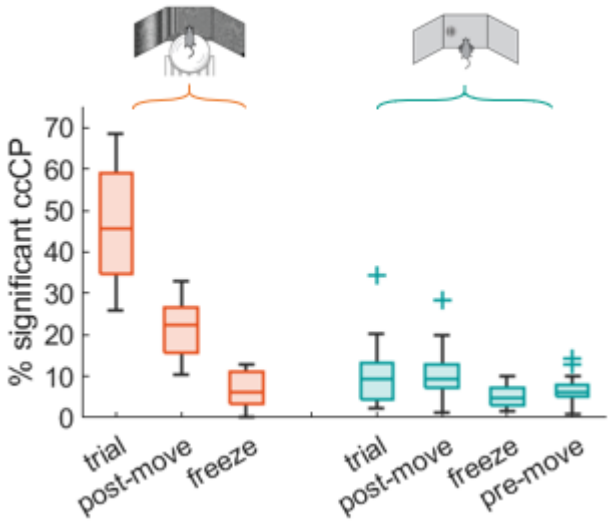

Figure 24. Percentage of neurons that are significantly choice selective over all included sessions. Median % significant were, from left to right, 45.5, 22.4, 6.2, 9.4, 9.2, 4.8 and 6%. A one-way ANOVA corrected for multiple comparisons found that the whole trial T-maze % significant and post-move T-maze % significant were higher than other types, and no other types were significant between each other.

In summary, I found that averaged across the trial or just after a choice movement, there was significant choice selectivity in the T-maze task but only a minimal amount of choice selectivity in the steering-wheel task. On average, about half of active neurons were significantly choice-selective, independent of stimulus side in the T-maze when averaged over the whole trial and about a quarter were choice-selective during the post-move period. In all other conditions, including for all epochs in the steering-wheel task, about a tenth of active neurons were choice-selective. The relative prevalence of choice selective neurons when considering the whole trial vs. just the post-movement period may reflect a preference for encoding of ongoing movement over just the onset. Consideration of the whole trial also better captures variation in the speed of the movement across trials that may then exceed the 200ms post-movement epoch due to the speed of the GCaMP indicator.

Since “freeze” and “pre-move” periods did not have as many selective neurons in the population, I do not analyze these periods further. Note that the set of active neurons in each task could include neurons that are or are not engaged in the other task. The greater percentage of neurons choice selective in the T-maze was not due to there being different numbers of neurons active in either task (i.e. the denominator for the percentage); a two-tailed rank-sum test found there was no significant difference between the distributions of the number of active neurons between tasks, $p = 0.3$. T-maze trials are longer than steering-wheel task trials, which could influence the whole trial analyses, however the epoch-based analyses use the same window duration, and still there are more T-maze choice-selective neurons in the post-movement period than steering-wheel choice-selective neurons in a post-movement period of the same duration.

Across-task comparisons of choice selectivity

After establishing which windows are most informative for choice in each task, I then ask the key question of interest, whether choice selectivity is shared in the same neurons across tasks.

Choice selectivity within the steering-wheel task was only mildly consistent on the next day within single neurons, while T-maze consistency was very good (Figure 25a-d for an example session). In 4/4 pairs T-maze choice probability was significantly correlated, in 2/4 pairs steering-wheel task choice probability was significantly-correlated, consistently across threshold values (Figure 25-e, left and right columns). The moderate correlation of steering-wheel choice selectivity in the same neurons across days is consistent with the low proportion of significantly choice selective neurons estimated within task and within session, from

Figure 24).

Across different threshold values (0, 0.05, 0.1, 0.2, 0.3, 0.5 or 0.8), either TM/SW or SW/TM combinations were significantly correlated in 0 or 1 of 4 pairs, with only one threshold value finding that both combinations were significant. In all cases the median across-task correlation was lower than either within-task correlation. Therefore, choice selectivity is not consistent across tasks.

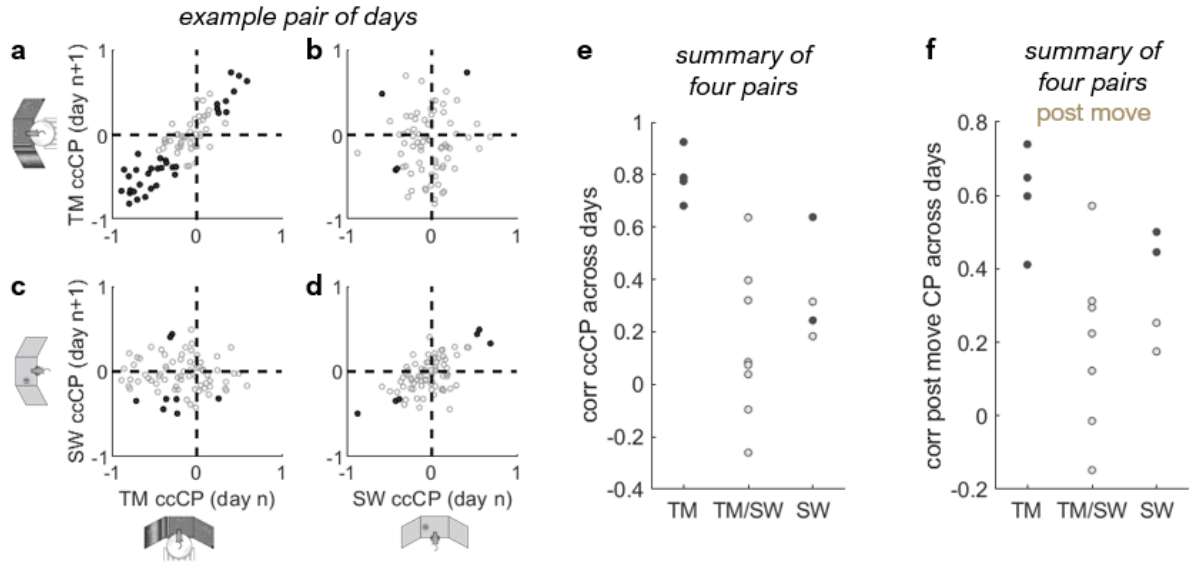

Figure 25. Choice selectivity is not correlated across tasks. (a-d) Example pair of days showing whole-trial choice selectivity values (where negative values means left choice preferring) for combinations of the T-maze and steering-wheel task on one day or the next. All neurons are shown for illustration, with no thresholding for inactivity. Filled circles indicate those neurons that pass the significance test on both days for the given comparison. (e) Summary of all four pairs of days. Each point is a Spearman rank correlation for a scatter plot such as shown in (a-d), such that each pair of days appears four times (one for each combination). As the T-maze vs steering-wheel comparison appears twice (i.e. (b) and (c)) I combined them, so the middle comparison has twice as many pairs, i.e. eight datapoints. Filled circles

indicate a significant correlation according to the Spearman rank correlation. I only correlate neurons active in both tasks, according to a threshold of isolation distance > 0.3. Different threshold values did not change the overall results. (f) Same but for ccCP estimated in the post-move periods of each task. Again I only used neurons active in both tasks.

As I only had four pairs of days, I expanded these analyses to across tasks, within a session, to provide a better estimate of whether any sessions had correlated choice selectivity. The procedure is identical to that computed for the middle columns of Figure 25e,f, but now is within-day, so I only have one comparison. Since this procedure no longer gives us a baseline for comparing within-task reliability (which I observed was low across days), interpretations of correlation values should be made with caution. I also varied the isolation distance threshold to see whether even thresholds which were very inclusive of potentially inactive neurons would result in any relationship, although the caveat holds from

Figure 21 that some of these choice selective neurons may be spurious. There was a tendency towards positive correlations of choice selectivity across tasks in the whole-trial analyses, but only a maximum of 3 of 20 sessions reached significance in the Spearman rank correlation of ccCP across tasks (Figure 26). Different isolation distance threshold values for defining active neurons did not change the overall conclusion, with at most three sessions showing a significant correlation of choice preference within-session for low threshold values, and no sessions were significant for "post-move" epochs. At the threshold used above in the cross-day analyses (activity > 0.3), only one session was significant.

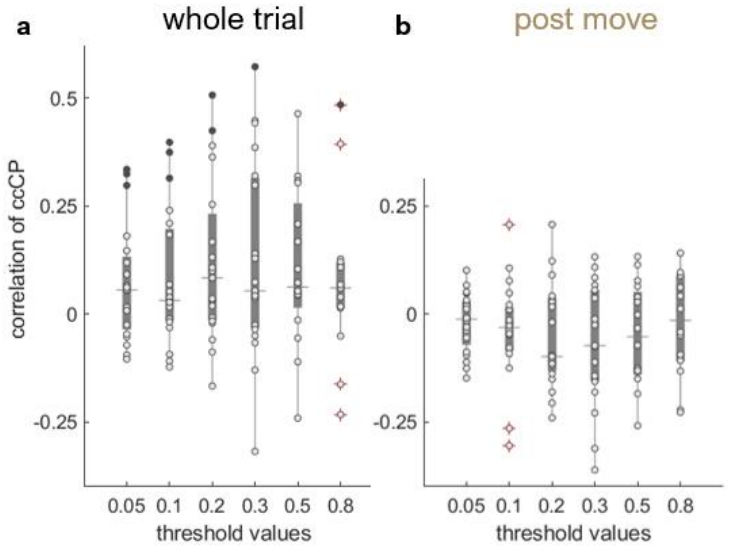

Figure 26. Correlation of choice selectivity across tasks, compared within days. (a) Spearman rank correlation of choice selectivity across tasks, as estimated over the whole trial (b) Correlation of choice selectivity across tasks, as estimated in the post-movement period only.

4.2 Stimulus selectivity

Given I could not find shared representations of choice, and that baseline levels of choice selectivity were low within the steering-wheel task, I wondered whether other task features played a larger role. Specifically, I wondered whether stimulus information was more likely to be shared across tasks.

According to some studies, lateral intraparietal area (LIP) in macaques is retinotopic with neurons having visuospatial receptive fields (Robinson et al. 1978), and is sensitive to decision-irrelevant visual cues such as flashes (Park et al. 2014; Meister et al. 2013) and visual evidence independent of choice (Bennur and Gold 2011). It is also known from rodents that PPC is sensitive to individual bouts of visual evidence such as flashes (Licata et al. 2017; Scott et al. 2017) and towers (Pinto et al. 2019), but also that this effect may be task-specific (Pinto et al. 2019). Visual information seems more prolific than movement- or choice-related information (Zatka-Haas et al. 2020; Steinmetz et al. 2019), and there seems to be a bias towards contralateral visual information (Koay et al. 2019; Steinmetz et al. 2019) for lateralized stimuli. Steinmetz et al. (2019) reported in their study that they found stimulus-triggered average responses in A, RL and AM as early as ~80ms from stimulus onset, which is before the onset of deliberate wheel movements; the observation that stimulus information is present even before the movement may suggest its role in sensory evidence *for* an upcoming movement plan.

Further, as discussed in the General Discussion, inactivation studies at large suggest a stimulus-related causal role, most relevant here from work in a two-alternative unforced-choice (2AUFC) contrast discrimination variant of the steering-wheel task (Steinmetz et al. 2019, Zatka-Haas, Steinmetz et al. bioRxiv), that was confirmed in a 2AFC variant (Coen et al., SfN Abstract 2019). Inactivation of regions overlapping with PPC decreased contralateral choices as if the contralateral hemifield had been blinded, and the extent of the effect depended on the stimulus decoding accuracy based on bulk wide-field calcium activity (Zatka-Haas, Steinmetz et al., bioRxiv). Note that both studies performed scanning inactivation across multiple sites across cortex, and did not target PPC precisely; the spatial extent of the inactivation thus likely exceeds PPC and affects visual areas as well. So, results should be interpreted with caution. Even so, Neuropixels recordings which are more precisely localized to higher visual areas A, RL and AM — that overlap with what is called parietal cortex — confirms that there are stimulus responses (Steinmetz et al. 2019). Therefore, I wondered if I would also see relative prevalence of stimulus information, and whether stimulus information would be shared across the two tasks.

Methods

In brief, I used the same logic described above for choice selectivity analyses. To probe stimulus selectivity, I used the converse comparison, now measuring choice-independent stimulus selectivity. Specifically I compared mean activity for left and right stimulus sides, within choices in the same direction, and pooled across left and right choice conditions. To increase the trial count, I now included all trials even if the mouse started to move before the trial, as "pure" stimulus responses should be invariant to these movements. I analyzed several different variants, comparing all contrasts, only high contrasts (25 or 50%), left vs right stimulus conditions, left vs zero stimulus conditions, and either over the whole trial or just within the first "freeze" period as described before. I still excluded sessions if they had fewer than 10 trials of each comparison. Many fewer sessions were available for comparison when only using high contrasts, so interpretation should be made with caution.

Results

First, I validated the measure of choice-independent stimulus selectivity. Figure 27 shows two example neurons from different sessions that were deemed to be significantly stimulus selective. Note that the rise time is extremely quick, with the peak occurring at 200ms, by the end of the freeze period, so the temporal profile is not due to stimulus movement. As well, it occurs independent of movement, in one session, I presented static gratings (for three seconds) to a mouse while it was running on a ball, and also had measurements of stimulus selectivity during the steering-wheel task. Even though the mouse did not move in compensation and could not move the grating (it was fixed at -30 or 30 degrees azimuth), this neuron showed a clear stimulus-evoked response, and was deemed in the task to be significantly choice-independent stimulus selective. However, it is the case that many neurons do show concurrent movement-related stimulus-evoked responses as well, which was observed in Steinmetz et al. (2019) in their wheel-based task.

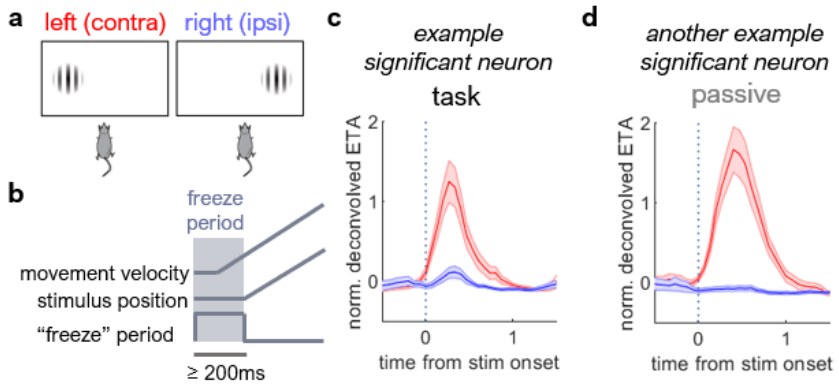

Figure 27. Stimulus selectivity in the steering-wheel task. (a) Schematic of left and right stimuli in the task, which correspond to contralateral and ipsilateral stimuli respectively (b) Schematic showing the logic of the "freeze" period, in which movements can occur in the interim, but will not have an effect on stimulus movement. (c) Example neuron with significant choice-independent stimulus selectivity in the steering-wheel task. (d) A different example neuron from a different session with stimulus-triggered activity during passive stimuli presentation, with choice-independent stimulus selectivity in the steering-wheel task.

Within-task assessment of choice-independent stimulus selectivity

I then calculated the within-task proportions of choice-independent stimulus selective neurons in each task (Figure 28). Up to 20% of neurons were significantly modulated by stimulus side in the steering-wheel task. A sizable percentage of the T-maze neurons were also significantly stimulus selective, up to 38%.

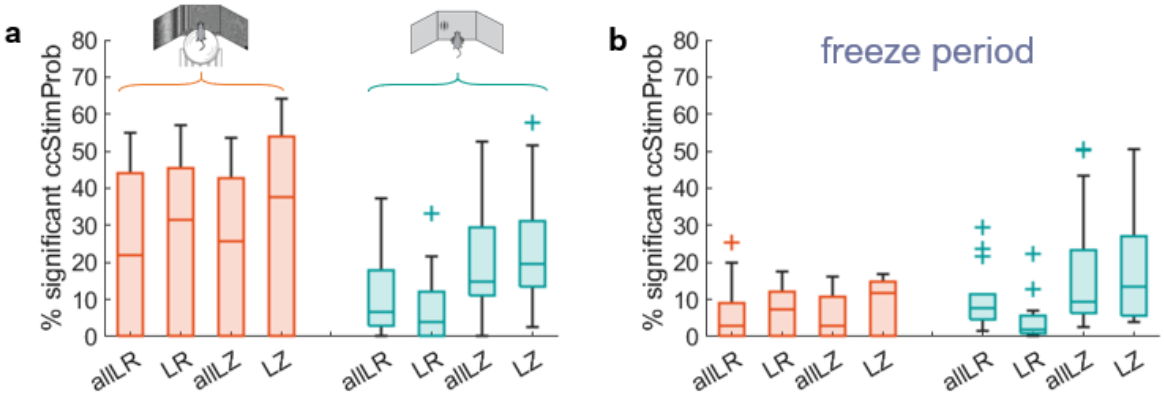

Figure 28. Within-task quantification of % significantly stimulus selective out of all neurons with an isolation distance of at least 0.05. LR = comparing left and right high-contrast stimuli; LZ = comparing left high contrast and 0% contrast; all = all contrast values. (a) Median % stimulus selective 21.8, 31.5, 25.9, 37.6 for the T-maze; 6.1, 4.0, 14.7 and 19.5% for the steering-wheel task from left to right (b) Median % 3.0, 7.4, 2.9, 11.9 for the T-maze; 7.9, 2.0, 9.4, and 13.3% for the steering-wheel task from left to right.

Comparing within-task proportions of stimulus selectivity and choice selectivity

Next, for each task, I tested whether there was a statistically significant difference between the proportion of significantly (choice-independent) stimulus selective neurons and proportions of significantly (stimulus-independent) choice selective neurons, measured from the previous sections (

Figure 24, Figure 28). I used the whole trial epoch so that both stimulus and choice selectivity were estimated using the same time period.

For choice selectivity, I used the ccCP (

Figure 24). For stimulus selectivity, I used the four variants described previously (Figure 28), "allLR", comparing left vs right stimuli of all contrasts; "LR", comparing left vs right stimuli of high contrasts 25% and 50%; "allLZ", left stimuli vs zero contrast trials using all left stimuli contrasts; and "LZ", left stimuli vs zero contrast trials using just high contrast left stimuli. Since the proportions were not normally distributed, I used a non-parametric variant of a one-way ANOVA, the Kruskal-Wallis test. P-values were corrected for multiple comparisons.

In the steering wheel task, only one of four measures of stimulus selectivity had a proportion of stimulus selective neurons that was significantly different from the proportion of choice selective neurons: the "LZ" stimulus selectivity using only the high contrast left stimuli and zero contrast trials. Specifically, there were *more "LZ" stimulus selective neurons* (median proportion: 19.5%) than choice selective neurons (median: 9.4%), $p = 0.002$. However, the proportions of stimulus selective neurons using the three other stimulus selectivity measures (allLR, allLZ, and LR) were not significantly different from the proportion of choice selective neurons.

In the T-maze task, in three of the four stimulus selectivity measures, there was a difference between the proportion of stimulus selective and choice selective neurons, in all three cases with *more choice selective neurons* (median: 45.5%) than stimulus selective neurons (median allLR: 21.8%, $p = 0.005$; LR: 31.5%, $p = 0.026$; allLZ: 25.9%, $p = 0.001$). Of the four stimulus selectivity measures, the "LZ" comparison had the highest proportion of stimulus selective neurons (median proportion LZ: 37.6%); since both "LZ" stimulus selective and choice selective neurons were prevalent in the T-maze, there was no significant difference between these proportions.

Across-task comparisons of stimulus selectivity

I had much fewer sessions available for analysis after exclusion of invalid sessions, including reducing some of the sessions with the across-day comparison. As I did not have many pairs to

begin with (only 4), I did not feel confident in drawing conclusions from <4 examples. Further, there remained only 11 sessions available for within-session comparison where both the T-maze and steering-wheel task had sufficient trial counts. Out of these 11, one or two sessions had a significant correlation. However, it is unclear whether on the whole there is more similarity in choice-independent stimulus selectivity than stimulus-independent choice selectivity, given the difference in overall number of sessions available for comparison.

Across-task comparisons of dependent choice and stimulus selectivity

In order to incorporate more sessions, I performed a preliminary analysis in which stimulus and choice could now be dependent. This analysis allows more sessions to be included that previously had too few trials, but specific conclusions about choice vs stimulus selectivity are more limited as choice and stimulus selectivity are no longer independent of the other. Unless described otherwise, I used "whole trial" epochs so that stimulus and choice selectivity could be estimated using the same time period.

Dependent choice selectivity

For calculating "dependent" choice selectivity, I first used trials of all contrasts, comparing all trials of left choices and all trials of right choices. However, choices at high contrasts are particularly confounded with stimulus selectivity, since mice have generally good, if not perfect, performance at high contrasts. Additionally, errors in spite of "easy" high contrasts may result from unusual processes such as disengagement or motor errors, rather than deliberate perceptual decisions.

So, I calculated two more measures of choice selectivity using only low contrast stimuli, where the mouse may be more uncertain and then "think" a stimulus has appeared on the wrong side. These trials also have more balanced numbers of correct choices and errors, and thus are less sensitive to issues arising from unequal sample sizes. For low contrast analyses, I used either 6% contrasts only (the lowest non-zero contrast) or both 6 and 12% contrasts. As I still required at least 10 trials of each choice for comparison, sometimes there were too few low contrast trials in a session, so this analysis was still limited to relatively few sessions compared to the first analysis with all contrast types.

Consistent with stimulus-independent choice selectivity (i.e. ccCP), I found that dependent choice selectivity was not correlated across tasks, whether I used trials of all contrasts, just low contrasts, the whole trial period or just the post-movement period (Figure 29-a). For low contrast trials, there were fewer sessions available that had enough trials for comparison, but no more

than 2/14 of sessions had a significant correlation. A Kruskal-Wallis test, corrected for multiple comparisons, did not find significant differences between these different measures of choice selectivity, suggesting that regardless of precise measure, choice preferences are not shared across tasks. The similarity of results between dependent choice selectivity using low contrast trials and choice selectivity measures using all trials also suggests that the inclusion or exclusion of zero contrast trials does not affect overall conclusions. Therefore, different zero contrast parameters across tasks (the accidental omission of rewards from zero contrast trials in the steering wheel task) does not explain why choice preferences are not correlated, since I reached the same conclusions in analyses that do not use zero contrast trials. Again, given the relatively few available sessions, these results should be treated with caution. To take advantage of low contrast trials, future experiments could present lower contrast trials with higher probability to produce more trials that can be included for estimates of choice selectivity.

Dependent stimulus selectivity

For calculating "dependent" stimulus selectivity, I used the four variants described previously (Figure 28), using high contrast stimuli only (25% and 50%), or all contrasts, and comparing left vs right side stimuli, or left side vs zero contrast trials.

There did seem to be a positive correlation between stimulus selectivity across tasks in some sessions, depending on the measure (Figure 29-b). The median correlation of stimulus selectivity across sessions was not sensitive to the activity threshold, if anything going up with higher thresholds (Figure 29-c). Note that all thresholds for isolation distance used in this thesis are well beyond the "behaviourally plausible" range for activity. Trials of the same choice or stimulus side usually happen at a rate of once every few seconds, whereas isolation distance thresholds exclude inactive cells which may fire a few times in 20 minutes, if at all. Therefore, exclusion of cells with low activity is unlikely to affect estimates of choice or stimulus selectivity.

In summary, there are hints that stimulus selectivity may be more likely to be shared between tasks in the same neurons. However, given the conflatory nature of this analysis with choice, it is difficult to conclude whether shared stimulus selectivity is about stimulus per se, or specifically the interaction of stimulus and choice. Further work is certainly needed to distinguish these possibilities.

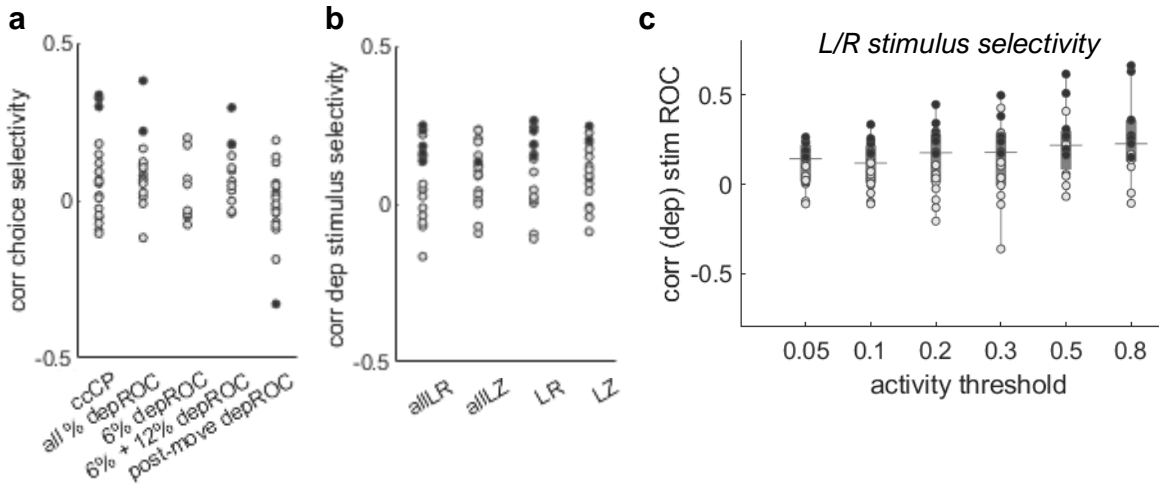

Figure 29. Preliminary analyses for comparing different measures of "dependent" choice selectivity and stimulus selectivity across tasks. Each datapoint reflects the Spearman rank correlation of selectivity across tasks over the neurons within a session. Sessions were excluded if fewer than 10 trials remained. (a) Correlation of choice selectivity across tasks, for dependent choice selectivity and ccCP for comparison. From left to right, $p < 0.05$ in 3/20, 2/21, 0/10, 2/14 and 1/21 sessions. Neurons were included if they had an isolation distance > 0.05 across tasks. (b) Correlation of dependent stimulus selectivity for four measures of stimulus selectivity as described previously. From left to right, $p < 0.05$ in 7/21, 2/20, 8/20, and 3/20 sessions. Neurons were included if they had an isolation distance > 0.05 across tasks. (c) Examining the effects of isolation distance threshold on the correlation between dependent stimulus selectivity for the L/R comparison across tasks.

Discussion

In summary, there is a minority of neurons that seem to be choice selective in either task, however these neurons do not seem to share choice preference across tasks. In the steering-wheel task, there are relatively few neurons that are stimulus-independent choice selective (~9%), and choice selectivity is only moderately correlated in the population between neighboring days in 2/4 of available pairs. In comparison, there is a larger proportion of choice selective neurons in the T-maze (~45%) and choice selectivity in the T-maze is also more consistent across days (correlated in 4/4 pairs). Therefore, these findings suggest that in these tasks, neurons in PPC do not share abstract representations of choice. I find there is some evidence for choice-dependent stimulus-related activity that is shared across tasks, supporting a role of PPC early in the decision-making process. However, further work is necessary to pinpoint the contribution of stimulus vs choice information, ideally with enough trials to compute measures in which choice and stimulus are independent of the other.

Within-task assessment of choice selectivity

In the steering-wheel task, in those neurons that were choice selective, there seemed to be more neurons representing ongoing choice, and few representing upcoming choice. Although precise comparisons of choice windows are limited due to the temporal resolution of calcium imaging, observations of a low proportion of choice-selective neurons and relative prevalence of ongoing vs upcoming choice representations are consistent with findings using Neuropixels probes in a 2AUFC contrast discrimination variant of the steering-wheel task (Steinmetz et al., 2019).

I see more neurons that are choice selective in the T-maze than the steering-wheel task; differences between tasks could be due to the subtlety of the motor report of the choice. Perhaps more complex or vigorous choice movements, such as that seen in the T-maze task, are responsible for driving stronger choice representations. In particular, running is thought to increase the "gain" of neural responses throughout the brain (V1: Niell & Stryker, 2010; but see alternative conclusion in Saleem et al. (2012) and Christensen & Pillow for an opposing result in mouse higher visual areas; brain-wide: Stringer et al., 2019; Musall et al., 2019), and that might explain why here choice representations are stronger. Note that the turn to make a choice in the steering wheel tasks is still quite overt: the mouse is required to turn the wheel 90 degrees (out of 360) to complete the choice. If effort does play a role, this hypothesis could be tested by additionally including a two-alternative task using licks as a motor report, which is even less effortful than a steering wheel turn.

After comparing proportions of choice selective and stimulus selective neurons, I found that in the T-maze there was generally a higher proportion of choice selective than stimulus selective neurons; however, in the steering-wheel task there was generally no difference between the two proportions, with some tendency towards a higher proportion of stimulus selective neurons. Differences in proportions of choice vs stimulus selective neurons in the steering-wheel task were sensitive to the exact measure of stimulus selectivity used, so further work is needed. There is some evidence from other work that in overlapping higher visual areas, stimulus selectivity better describes PPC activity than choice selectivity, when jointly fitting stimulus and choice predictors to Neuropixels data using regression models (Steinmetz et al., 2019). This analysis could be applied here as well in future work, perhaps focusing on sessions that only include one task to maximize trial count for better estimation of feature selectivity.

Across-task comparisons of choice selectivity

Despite observing choice representations in each task, these choice preferences do not seem to be shared across tasks. These results across two tasks with different motor reports complement results of consistency in choice encoding in rodent PPC across different tasks that employ the same actions,but differ in modality of the sensory stimulus (tactile vs visual: Nikbakht et al. 2018; visual vs auditory: Raposo et al. 2014). In these studies, 40-50% of neurons were found to share significant choice selectivity across tasks of different modalities (despite apparent modality-specific effects of perturbations). A relevant difference between these studies and the current results is that the former employ the same means of motor report, whereas here the difference is likely due to "motor-context-specific" choice representations that are particular to choices in the T-maze vs steering wheel context.

These findings are perhaps consistent within the "intentional framework" (Shadlen et al. 2008). Namely, that choices could be unrelated across apparatus because they are literally encoded with respect to the action undertaken, i.e. "left treadmill turns", "right treadmill turns", "left wheel turns", and "right wheel turns". Given the small number of possible actions available across the tasks, i.e. four, it is conceivable that these are sufficient to cache separately, particularly when it is more efficient to do so for action. Indeed if it is behaviorally useful to represent two task contexts distinctly, such as the need to perform different actions (wheel turn vs treadmill running) within each context, it is computationally more advantageous to use distinct subsets, or populations with minimal overlap, to minimize "interference" and aid with efficient retrieval.

In general, the extent to which an embodied representation is provoked is likely species-dependent, perhaps modulated by ecological need — embodied representations are more

efficient and may be more useful for animals which are "prey", such as rodents — or ecological niche — rodents have relatively low spatial acuity so must move to sense and act, whereas primates can sample and decide at long-range.

The involvement of PPC in movements

I observed activity related to ongoing choices left and right, which is not wholly indistinguishable from the physical act of turning a wheel or spinning a spherical treadmill. Indeed both tasks involve rotation of the apparatus, but it is unlikely that motor correlates better account for activity in PPC as in a control analysis, I confirmed that neurons do not share modulation for rotational velocity across task contexts (addressed in Appendix C).

Further, linking back to the inactivation literature, perturbation studies do not show that PPC has a motor-specific role. First, optogenetic inactivation throughout the cortex, including a region that overlaps with parietal areas, suggests that unilateral inactivation of PPC in steering-wheel task variants blinds the contralateral hemisphere (Zatka-Haas, Steinmetz et al., bioRxiv; Coen et al., SfN 2019). Additionally, in one of these studies, as the task was a 2AUFC contrast discrimination task, the authors also observed boosting of ipsilateral choices relative to No-Go trials (Zatka-Haas, Steinmetz et al., bioRxiv). One might expect that if PPC "drove" the motor execution of choices, body rotations or orienting in general, the ability to make choices to either side would be impaired by inactivation. Instead, inactivation of PPC and other visual areas in 2AUFC contrast discrimination and 2AFC visual detection steering wheel tasks do not overtly affect reaction time or wheel velocity trajectory (Zatka-Haas, personal communication; Coen et al., personal communication). So, it does not seem that PPC has a role in movement initiation or execution, at least in the steering-wheel task. In a spherical treadmill-based task, as discussed in the General Introduction, inactivation of PPC does not result in overt motor errors, and impairments can be attributed to disruption of task-relevant sensory evidence in the respective task (Minderer et al., 2019; Pinto et al., 2019).

Finally, other works that require the same movements for tasks of different demands or modalities find differential effects of inactivation across tasks, which would not be predicted by a uniform effect on motor execution (Pinto et al., 2019; Licata et al., 2017). As mentioned in the General Introduction, Licata et al (2017) found that perturbation of PPC affected visual but not auditory decisions, but did not affect reaction times and movement durations for either modality. In both cases the rat has to make the same left vs right orienting movement, so this modality-

specificity would suggest that it is not the ability to make a movement that is affected when perturbing PPC.

Dependent stimulus and choice selectivity

Preliminary analyses showed that there may indeed be some level of shared representation for stimulus information across tasks, which is consistent with the proposed causal role of PPC. The measure of stimulus selectivity used to compare across tasks is not independent of choice selectivity, as I used a "choice-dependent" stimulus selectivity measure due to low trial counts for estimating choice-independent stimulus selectivity. Therefore, further work is certainly needed to determine whether stimulus representations are truly independent of choice, or whether it is the combination of stimulus and choice information that is privileged in PPC and shared across tasks. I have a handful of sessions in which I also recorded during passive presentation of visual stimuli, either playback of the T-maze, or static presentation of gratings. Some of these sessions were not adequate for alignment across tasks, so they did not pass initial inclusion criteria. Further experiments should aim to elucidate whether hints of shared stimulus selectivity across tasks would extend to stimulus selectivity outside of a task, and establish to what extent shared stimulus representations are due to "pure" stimulus selectivity vs a stimulus-choice interaction, using experiments or analyses that allow one to dissociate specific stimulus vs choice contributions. Findings from the literature suggest that the sensorimotor interaction may be the most important characteristic driving PPC neurons.

Limitations

The role of inactive neurons

It may be that even neurons which are apparently non-responsive show some modulation by either choice. Hence, I was careful to check results over a range of thresholds; however, by widening the net to potentially inactive neurons, it is unclear how much observed choice selectivity could be spurious due to potential motor confounds as discussed above.

In any case, there may be yet other neurons that may show task-relevant activity, but perhaps sub-threshold to the number of spikes necessary to invoke a calcium transient. Huang et al. (2019) found that calcium activity at the zoom (500x500um) used here primarily reflects neural activity consisting of more than two APs within a 100-500ms window. If firing rate is lower than this, it might not be possible to detect activity at typical two-photon imaging resolution. These cells might be inactive throughout, or not active for task events, even if they fire extremely rarely

but reliably. This possibility cannot be evaluated in the current dataset, but work from Steinmetz et al. (2019) using Neuropixels probes suggest that the difference between the sensitivity of electrophysiology and two-photon calcium imaging at least does not account for the paucity of "truly choice selective" responses seen here, as I find roughly the same proportion of neurons which have significant choice modulation during ongoing choice (~10%).

Temporal resolution

In the steering-wheel task, the lack of quiescent period in some mice and slow decay of calcium made it difficult to disentangle the temporally overlapping stimulus and choice epochs, particularly as mice tend to respond to the stimulus within 200-500ms. Enforcing a post-stimulus quiescence period, a variant which exists in the lab, may avoid the limitations of the slow decay of the calcium sensor. Alternatively, now that expectations for PPC responses across tasks are established, future work could use chronic Neuropixels probes to record activity across tasks.

Choosing the right window

Finally, for both types of analyses, it is possible I did not examine the right time window within the trial, and some other window would have shown more similarity in feature selectivity across tasks. Further research is needed to address this possibility, ideally using a recording technique with better temporal resolution.

Summary

In this thesis, I asked how populations of single neurons in PPC change their activity as a function of task. I recorded from the same population of neurons as mice performed two variants of a visual detection task: the T-maze and steering-wheel task. These tasks were designed to have similarities in abstract structure, but differed in the visual scene, means of motor report and requirements for navigation. I found that activity in PPC supported a “task-specific” view of its role in decision-making. Many neurons in PPC did not participate in both tasks, but rather were selectively active during performance of one task and were inactive in the other; this was repeatable on the next day. Task selective engagement was upheld even in the absence of a task, following the respective "motor context" of each task, as observed by correlated activity within contexts but uncorrelated activity across contexts. Despite the two contexts differing in the presence or absence of running, task selectivity was not explained by modulation by running.

Although many neurons were not active in both tasks, I wondered whether the subset of neurons active in both tasks shared preference for task features that were present in both tasks. I was able to decode choice from neurons in both tasks, but choice selectivity was uncorrelated between the two tasks. Choice selectivity was consistent on neighboring days within tasks, so the lack of shared choice selectivity across tasks is not due to a random re-organization of task properties across time. However, even within the steering-wheel task alone, choice representations were rare. Instead, within PPC, stimulus representations were generally more prolific, and a representation of stimulus intermixed with choice seemed to be somewhat related across tasks.

In conclusion, at least in these tasks, PPC does not seem to have "abstract" choice representations invariant to task at the level of single neurons. Instead, the activity of PPC seems to be “task-specific”: sensitive to the context in which each task is performed, whereby different subpopulations of neurons are selectively engaged in each context and task-related event-evoked activity is specific not general across task. Next, I discuss potential interpretations of my results.

General discussion

The extent of abstraction may be task dependent

It is very likely that here, PPC was not found to carry "abstract" choice information precisely because there is no need to represent it so abstractly in PPC in these tasks. In both tasks, the choice is deterministic, and the fully-trained mice included in the dataset were likely well aware of the fixed stimulus-response contingencies. Thus, the mouse is able to make its mind up as soon as it sees the stimulus, and the "task" is therefore in perceiving the stimulus, which may occur even within 100ms (Resulaj et al., 2018); this may explain the relative prevalence of stimulus information, observed here and in a similar variant contrast discrimination variant (Steinmetz et al. 2019, Zatka-Haas, Steinmetz et al., bioRxiv). There is then no reason to not immediately pass on sensory information to downstream circuits such as secondary motor area (also known as FOF, M2, ALM) which has been implicated for action in these sorts of tasks (e.g. Erlich et al. 2011; Hanks et al. 2015; Erlich et al. 2015; Zatka-Haas, Steinmetz, et al. bioRxiv; Coen et al., in preparation; and many others).

Choice information may be more necessary to “hold in mind” in task variants which involve ongoing evidence accumulation or a delay period. Indeed studies have found greater effects of inactivation of PPC when directly comparing tasks of these sort to visually-guided tasks with no delay (Pinto et al., 2019; Harvey et al., 2012). However, in visual detection tasks with a delay period, since the stimulus-response contingencies are still fixed, it is still possible that if PPC is a sensory-driven region, that PPC passes this information immediately and memory is deferred to downstream secondary motor regions. Even so, in memory-based stimulus detection and evidence accumulation tasks, it is unclear whether the mouse would "hold in mind" their perception of the sensory stimulus, to later execute an action, or "hold in mind" the choice. Whether parietal activity reflects (accumulation of) sensory evidence or premotor “buildup” of a movement intention is also a strong matter of debate in the macaque LIP literature. A recent study found that accumulation of sensory evidence and premotor “intentional” activity co-exist (e.g. Yates et al., 2017). Note that error trials do not help resolve this matter given that the mouse still acts on their subjective "perception" of the stimulus, which may be incorrect. Different timing of stimulus and choice events help distinguish the two, but it is still unclear whether observed sensory activity is related to perception or the intended choice. In PPC, it is likely the former, given there is more prevalent stimulus than choice information observed here and in other

studies, and the literature on the effects of inactivation at large (reviewed in the General Introduction).

To disentangle these possibilities, a task design is needed that involves deference of the correct motor response until a secondary cue, which would enforce that mice need to "keep in mind" sensory evidence, but cannot plan their movement yet as the correct direction is unknown. Tasks of these types have been developed in rats and mice (Akrami et al. 2018; Condylis et al. 2020; Wu et al. 2020), although not using visual sensory evidence, so further work should expand on these to test for the role of PPC in processing visual sensory evidence vs a motor plan.

Comparison to primate studies

To fully understand a complex neural process such as decision-making, one should operate in a loop, learning from large-scale recordings in rodent studies to shape targeted hypotheses to then re-explore in primate species. As mentioned in the Introduction, the homology between rodent and primate cortex is unclear given the wide evolutionary gap (Belmonte et al., 2015, Sereno et al., 2014). However, rodent studies have been useful in informing work in primate species, given the ease of sampling broadly in an unbiased manner, and therefore the ability to perform within-subject, within-session comparisons.

The ability to sample broadly in rodent neural recordings means that researchers are no longer limited to searching for the "best" neurons on the basis of their response properties, which are biased to finding the sorts of neurons that are expected to be found (discussed further in Implications). Here we have learnt that neurons do not just have different response properties across tasks, but participate in separate ensembles corresponding to each task. Thanks to the unbiased sampling, I know that the neurons I recorded are indeed largely representative of PPC as a whole.

Additionally, in conventional electrophysiology in primates, neurons are often pooled across days, given the low numbers of recorded neurons. This procedure may result in accidental re-sampling of the same neurons across time, and therefore over-estimating the prevalence of the response properties of those neurons found again and again. Alternatively, neurons could change their response properties over days. Here, by having the ability to sample widely within a single session, I am able to restrict my analyses only within-session, which ensures the statistical independence of the reported results.

Further, while work is ongoing in developing calcium imaging in primates, all work in macaque parietal cortex described in this thesis was performed using electrophysiology. One of the motivations for using calcium imaging in this thesis was that imaging techniques afford more confidence in matching the same neurons across tasks and days, which was a key element of the research question under investigation. A direct result is that I was able to discover neurons which were inactive in either task, whereas in electrophysiology, particularly if it is limited to searching for the "best" neurons, neural silence could be more likely confused with drift or cell death. Lastly, I was able to confirm the validity of my findings by matching the re-appearance of neurons across tasks and days, which would be possible but less reassuring if I had not used an imaging method. Together, the large-scale neural recordings using two-photon calcium imaging has allowed us to find task selective neurons and confirm the validity of these findings. This result will hopefully then shape future work in primates that is better informed regarding what to expect when recording the same neurons across tasks.

Context-dependent sensorimotor processing

The relative prevalence of stimulus information may seem contradictory to the stark differences in activity across motor contexts (the T-maze vs steering-wheel apparatuses). Stimulus information is more prevalent in the population in terms of task-evoked activity (Chapter 4). Also, PPC inactivation primarily affects visual sensory information (as discussed in the General Introduction). This prioritization of stimulus information is perhaps strange given that here I observe that the dominant axis of activity vs inactivity in fact lies along the dimension of motor context (Chapters 2 and 3). How might these two observations be reconciled?

A speculative interpretation is that PPC has found a way to jointly encode the stimulus information with the action that is relevant to the respective task (turning the steering wheel vs running on the spherical treadmill), by multiplexing temporally-aligned stimulus information with a "binary-like" representation of the motor context. Motor context selectivity can thus be hypothesized to serve as a "context gate", diverting sensory information in the population to the relevant subpopulation in downstream neurons, such as in secondary motor cortex, depending on which task is being performed.

Indeed, the joint encoding of sensory and motor information in the service of "sensation for (the relevant) action" is reminiscent of historical characterizations of PPC as a site for neither primary sensory nor primary motor representations alone, but their intersection. An interpretation of PPC as a "hub" has been an attractive metaphor, based on its anatomical location and connectivity

between sensory and motor areas. However, there seems to be truth in this characterization; that is, it is efficient to bind the actual stimulus seen with the information of the relevant repertoire of behaviors (which motor context). This account may then explain why in the literature, despite there being a strong causal role of sensory information in PPC, many studies see prevalent and/or dominant motor-related activity (Diamanti et al., bioRxiv; Minderer et al., 2019; McNaughton et al., 1994; Whitlock et al., 2012; Mimica et al., 2018, and others) and motor-choice information is shared across modalities (Raposo et al., 2014; Nikbakht et al., 2018) despite inactivation having a modality-specific effect.

There are perhaps some relevant findings that there are context-specific representations in PPC. Harvey et al. (2012) found spatially-specific responses in PPC in a virtual T-maze decision task, interpreted as choice sequences, but not in a virtual linear track. Krumin et al. (2018) found in the virtual T-maze that in PPC neurons, decoding of virtual spatial position explained a large proportion of variance, and that virtual spatial position was more informative than correlated motor variables. The ability to decode virtual spatial position was corroborated in another study (Koay et al., bioRxiv) although in their task was not exclusive of decision-related activity. In these tasks, different "contexts" are characterized by different visual scenes as well, but there is even evidence that PPC may be sensitive to context even in visually-identical contexts. Diamanti et al. (bioRxiv) found that PPC and other higher visual areas are sensitive to subjective spatial position in a virtual linear track with two pixel-identical segments; however, this effect was also observed in primary visual cortex (V1), so does not suggest that PPC is "special" in this regard. Finally, a seemingly distant finding from a fear conditioning study suggests PPC could be useful for awareness of context, finding that inactivation of PPC reduced freezing to a conditioned stimulus (CS) in a novel context, suggesting mice did not generalize to the association of the CS with the US (foot shock) in the novel context (Joo et al., 2020). The aforementioned studies differed greatly in their task design and aims, so further work is certainly needed to more precisely characterize the involvement of PPC in context selectivity.

Silent cells in cortex

Some works suggest that there are cases where apparent lack of task-related activity may be slight but may still contribute to population decoding, by increasing the dimensionality and therefore facilitating a simpler linear decoding scheme. This possibility has been discussed in the context of apparently "non-task-responsive" cells. There is indeed evidence from modelling studies that "untuned" neurons can still contribute meaningfully to coding of task-relevant variables (e.g. Leavitt et al 2017; Zylberberg, 2017). Also, a recent study found that even in "non-

classically responsive" neurons (i.e. those without a clear evoked response in the peri-stimulus time histogram) can still carry useful information about task-relevant variables in their inter-spike intervals (Insanally et al., 2019). An ultimate experiment to test whether “silent” cells are behaviorally useful would be an “all-optical” approach (Packer et al., 2017) to inhibit the so-called inactive neurons alone and see whether that has any discernible effects on behavior.

Implications

The importance of unbiased sampling

These results underscore the importance of sampling broadly, both with respect to behavior (i.e., testing multiple tasks) and neural activity (i.e., recording hundreds of neurons simultaneously).

Sampling of neurons

First, these results highlight the importance of unbiased techniques such as two-photon calcium imaging to record hundreds of neurons simultaneously. The effect of biased sampling in limiting our understanding of a given brain region was raised by Oldshausen and Field (2006), who estimate that given sampling biases that favor neurons with large cell bodies, “visually-responsive” activity, and high firing rates, only 10-20% of V1 neurons are typically accounted for in the general literature. This undersampling likely explains why in recent years many studies have found surprising diversity in V1 responses for encoding "non-classical" features (e.g. Stringer et al. 2019; Schuler & Bear, 2006; Saleem et al, 2018; Poort et al, 2015).

In PPC, experiments were historically only able to record from a handful of neurons at a time, and therefore for practical reasons selected candidate neurons for recording based on prior expectations of what neural activity should look like. For example, in classic studies of evidence accumulation in LIP, Shadlen and Newsome (2001) chose neurons for inclusion specifically on the basis of whether they showed persistent activity during the delay period. Indeed, a rough calculation revealed that only a quarter of neurons of LIP passed this criterion (Katz, PhD Thesis). Meister et al. (2013) suggested that the bias to recording from these neurons perhaps mischaracterized the relevant neurons for decision-making, finding that a neuron's persistent activity was only weakly correlated to its choice-related activity.

A recent survey of sampling effects on response properties illustrates the dangers of sampling bias: depending solely on the number of cells included in analysis, Mesa et al. (2020) reached different conclusions about the temporal frequency, orientation and direction tuning of neurons

in visual areas. This result speaks to the importance of selecting neurons independent from the basis of response properties, especially given the modern capacity for large-scale recordings on the order of hundreds or thousands of neurons simultaneously. “Widening the net” is essential to fully understand a region’s role.

Sampling of tasks

Similarly, studies that assess neural activity during a single task are likely underestimating the kinds of neural responses to be found in PPC. A given dataset evaluated using a single task often results in a minority of neurons that are judged as “task responsive” and thus included for analysis. In a virtual navigation task, Harvey et al. (2012) found that 47% of putative cells had >2 transients/min, but the majority (53%) of identified ROIs were inactive. In a 2AUFC contrast discrimination task, Steinmetz et al. (2018) found that in parietal areas A, RL and AM, 20-70% of recorded neurons within the three areas were not responsive to any task events of stimulus, choice, or reward. In a study in rats, only 21% of morphologically-identified neurons were shown to be task-responsive in an auditory evidence accumulation task, meaning the other 79% were not engaged by task events (Scott et al. 2017). If a neural population is examined using only a single task, it is easy to conclude that only certain task-specific properties exist in that population. Therefore, future work should sample broadly across a range of tasks, as studies are starting to do (Pinto et al., 2019).

Spontaneous behaviors are context-dependent

Numerous studies have recorded neural activity during spontaneous behaviors while mice can run freely, and their findings have been extremely productive in challenging the domain-specificity of primary sensory areas (e.g. Stringer et al., 2019). However, results of “motor context selectivity” in task-absent conditions (Chapter 3) make a curious implication; namely, that there is no "spontaneous" state. At least, there is no environment that can adequately capture the range of functions within a given region. Placing a mouse on a spherical treadmill engages a certain set of neurons, and placing the mouse on a steering-wheel apparatus engages a certain set of neurons, and this pattern likely holds for other apparatuses as well. Therefore, in choosing a particular apparatus to study encoding of a given region, as described above, one already is restricting analyses to a defined set of neurons that show activity in that context, because this misses a large proportion of neurons that are not engaged in each context.

Non-independent sampling of neurons across sessions

Although I always performed analyses within the same session, for analyses of anatomical organization of task selective clusters, I attempted to align across imaging planes from sessions in which I did not purposely try to return to the same neurons (described in Appendix A). Surprisingly, I was able to match these different sessions very well, probably due to the narrow anatomical extent of PPC on the cortical surface and the narrow span of layers 2/3 in depth. Together with issues of accidental or intentional sampling bias for certain response properties this finding cautions against blind pooling of neurons across sessions without accounting for the dependence of accidentally resampling the same neurons.

Limitations

Differences in definitions of PPC

The region I defined as PPC (overlapping with higher visual areas A/RL) differs from some other definitions of PPC (overlapping with AM), but this difference is unlikely to account for differences here compared to other studies of PPC in the literature.

At first glance, it is important to precisely target PPC, as the spatial extent of PPC is fairly narrow along the anterior-posterior axis essentially no more than the height of a typical imaging field-of-view (500x500um). Mistargeting the area ends up in primary visual or somatosensory cortices, which traditionally are expected to have different, more primary sensory, response properties. There are also certainly differences in connectivity between overlapping secondary visual areas A, RL and AM as revealed by anterograde and retrograde tracing studies (most recently carried out in mice in Hovde et al. 2019; and Glissen et al., 2020).

However, recent evidence — using the kinds of tasks found here — have typically found that encoding of task features and effects of inactivation are highly similar across posterior cortex, particularly across higher visual areas A, RL and AM that typically define PPC (Koay et al., bioRxiv; Pinto et al., 2019; Minderer et al., 2019; Zatka-Haas, Steinmetz et al., bioRxiv; Coen et al., SfN Abstract, 2019; Diamanti et al., bioRxiv). At two-photon calcium imaging resolution, Minderer et al. (2019) was able to cluster a region consisting of A, RL and AM based on their encoding properties — suggesting at least there is internal similarity in encoding properties within regions broadly considered parietal cortex. Interestingly they were not, in the same analysis, able to cluster AM uniquely. Regarding similarity in encoding and causal role across posterior cortex, Pinto et al. (2019) also make the point that different tasks may differential recruitment

distributed cortical areas. At least in the tasks here, the differences do not seem so stark between neighboring regions of cortex.

Projection-specific differences across layers

Some studies have found functional differences across layers within mouse PPC with regards to choice-related activity in decision making tasks (Koay et al., bioRxiv; Hwang et al., 2019). Hwang et al (2019) reported that projection targets of PPC neurons differ both along the dorsal-ventral axis and anterior-posterior/medial-lateral axes. Specifically, PPC neurons that project to posterior secondary motor cortex tend to be located more superficially, up to 500um in depth, which is the typical range accessible by two-photon imaging. In contrast, PPC neurons that project to striatum are in deeper layers. It is possible that I could be biased still to only sampling a certain functional class of neurons given that I only image in layer 2/3.

Wide-field calcium imaging, two-photon calcium imaging, and electrophysiology likely sample from different cortical layers, making generalization across these recording techniques potentially challenging. However, here, I broadly replicate results from another study using a variant of the steering-wheel task which used Neuropixels probes (Steinmetz et al., 2018), which was also shown to broadly match wide-field activity in their same task (Zatka-Haas, Steinmetz et al., bioRxiv).

Activity does not imply causality

Finally, it is important to be wary of the oft-repeated phrase that correlation does not entail causation. As observed in rat (Erlich et al., 2015), mouse (Goard et al., 2015; Zatka-Haas, Steinmetz et al., bioRxiv) and macaque LIP (Katz), the existence of apparent event-evoked activity does not predict whether inactivation will have a behavioral impact. Therefore, inferences of causal relevance of the activity seen here should be made with caution. Steinmetz et al., (2019) found in their 2AUFC contrast discrimination task that many areas showed both visual and motor related activity, but in another study was able to pinpoint that visual information directly correlated with deficits under inactivation, while motor information did not (Zatka-Haas, Steinmetz et al., bioRxiv).

Preliminary findings from the lab suggest that there is a slight unilateral effect of inactivation in both the T-maze (Krumin et al., SfN Abstract, 2018), and a similar 2AFC steering-wheel task (Coen et al., SfN Abstract, 2019), which imply an effect of inactivation in blinding the contralateral hemifield, consistent with existing studies in the literature.

To directly test for the causal influence of task-specific populations, it is enticing to consider the use of technologies such as "all-optical" techniques that could be used to selectively inhibit sub-groups of neurons determined to be task-selective under two-photon calcium imaging (Packer et al., 2015) or employing the c-Fos/tTA-tagging system to optogenetically inhibit just those neurons active during performance of either task (Chen et al., 2019).

Future directions

Population decoding

I do not find that choice selectivity is shared within single neurons across tasks, perhaps given low numbers of neurons that are "truly" choice selective, as observed in Steinmetz et al. (2019). This number should be near 100% if all choice representations are abstracted from the sensorimotor particulars. Within-task analyses suggest that there is a minority of neurons that seem to be choice selective (~9% in the steering-wheel task, ~45% in the T-maze), just that the preference is not consistent across tasks. Therefore it is possible that PPC manages to represent choice abstractly in the population by re-aligning its choice "readout" axis to differently weigh different neurons across tasks, as some studies have suggested (e.g. Mante et al. 2013; Raposo et al. 2014). Further work should explore this question, and also uncover the dimensionality of this "shared subspace" as has been applied to other work (Stringer et al., 2019; Semedo et al., 2019).

The influence of learning on task selectivity

A question of interest is whether these selective groups are fixed, prior to learning — suggesting there is some role of the physical sensorimotor features of each apparatus — or emerge throughout learning. I did not wish to image during learning as I was not certain that differences across learning could not be confused with differences due to relative anxiety or arousal. However, assuming I could eliminate such confounds, it would be interesting to know whether representations stay abstract and become more specifically embodied in either task once mice learn the task contingencies are deterministic. Najafi et al. (2020) imaged PPC neurons during learning of an auditory-visual rate categorization task, and found that choice representations became stronger during learning.

The manner in which tasks are trained may also be important, with modelling studies using neural networks finding that blocked vs interleaved training can have different implications for the dependence or orthogonality of neural representations when switching between tasks (Yang et al., 2019; Flesch et al., 2018). By assigning different groups of mice to be trained in a blockwise or interleaved fashion, it will be possible to direct test this hypothesis and see whether different training protocols really influence the orthogonality of neural representations.

Outlook

It was not too long ago when it was doubted whether rodents possessed the cognitive abilities to perform complex decision-making tasks, yet now, studies of decision making are prolific. Thanks to the advent of large-scale neural recordings, many studies have shown that diversity in the content of neural representations is more common than not. The next frontier is bridging the gap between cutting-edge technologies for recording and manipulating neural populations, with equally complex behavioral paradigms. Only in concert can we start to understand the true nature of complex cognitive processes and their manifestations in neural activity throughout the brain, and make sense of how we make sense of the world.

Appendix A

Anatomical organization of task-selective neurons

Having observed neurons active in either task, I wondered whether these neurons were restricted to different sub-regions in anatomical space.

Alignment of imaging fields of view across days

In some sessions, I purposely returned to the same population of neurons, and was able to align these sessions using Register S2P. However, in other cases, I did not intend to return to the same imaging plane or could not confidently align due to different angles of the microscope and non-linear warping of the brain. Nevertheless, to estimate anatomical localization of task selective neurons, I attempted to roughly align even disparate planes across days based on control point registration using large landmarks such as blood vessels. I was surprisingly able to align imaging sessions in X-Y anatomical space even across sessions in which there initially seemed to be completely different sets of neurons. On this basis, I employed further sub-pixel registration techniques to more closely align sessions based on the pixel shapes of their ROIs. Figure 30-b shows the outcome of this process.

Results

Task-selective neurons were interspersed, suggesting first that the imaging field-of-view did not cross into another defined area of posterior cortex, such as somatosensory cortex or primary visual cortex. I did not find there were functional "subregions" of PPC. Figure 30 shows an example session and merge over sessions from one mouse. Indeed, in mouse parietal cortex, studies typically do not find anatomical separability of neurons encoding specific task features (Harvey et al., 2012; Pho et al., 2018; Tombaz et al., 2020). The only known exception is a study in rats that found an anterior-posterior gradient of head vs back posture encoding (Mimica et al., 2018), however the same authors did not find anatomical separability in mice of motor behaviors (Tombaz et al., 2020), or turning vs running in rats (Whitlock et al., 2012), so the generality of these results is unclear. Overall, at least in mice, there does not seem to be motor-specific anatomical separability.

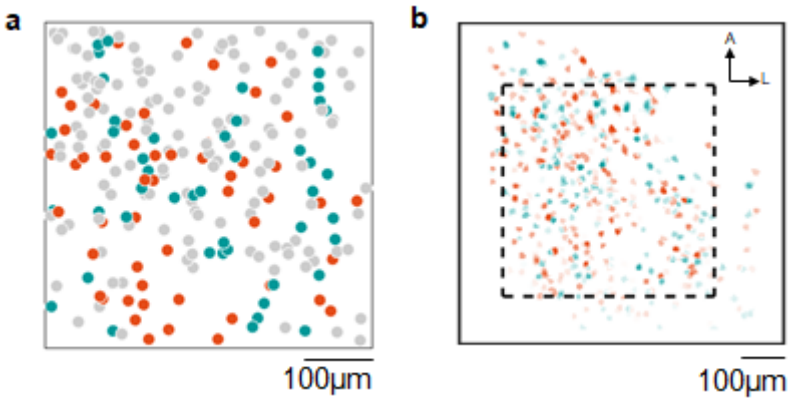

Figure 30. Task selective neurons are anatomically interspersed. (a) Example FOV from one session showing centroid locations of all recorded neurons within this session, colored by whether they were classified as T-maze selective neurons (orange), steering-wheel task selective neurons (blue) or other neurons which were not selective to either task alone (gray). (b) Merge of all seven sessions from one mouse, where the hue is averaged with equal weighting to each session. The dotted box shows the field of view in (a). Over the span of PPC covered in this mouse, there does not seem to be a clear functional border between the two classes of task-selective neurons. The gap in recorded cells to the lateral side was the location of a large blood vessel, so few cells were sampled there.

Appendix B

Comparison of isolation distance to other measures

As mentioned in Chapter 2, isolation distance was found to be the most robust in capturing activity across tasks in different strains of mice with different baseline noise levels. Two example sessions are plotted from different mice, showing activity across tasks using these different measures, showing that isolation distance provides the best measure of activity that is robust across transgenic mice with different speeds of calcium sensor, GCaMP6f and GCaMP6s. While in the GCaMP6f mouse, skewness can be used to reveal different task selective groups, in the GCaMP6s mouse, this measure is very uninformative due to a noisier baseline.

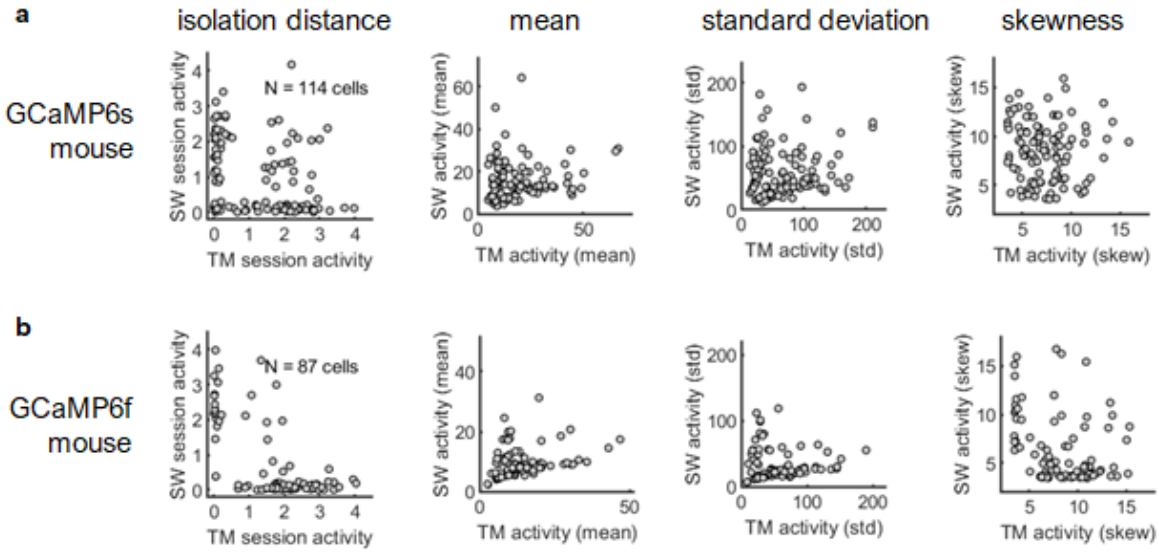

Figure 31. Example sessions comparing task activity measures. (a) Example session from a GCaMP6s mouse. (b) Example session from a GCaMP6f mouse.

Appendix C

Influence of rotational modulation

A behavioral feature which is common across tasks is the rotational movement required to report a choice in both motor apparatuses. In the T-maze, the mouse needs to spin the spherical treadmill to navigate sideways in virtual reality; in the steering wheel task, the mouse needs to spin the steering wheel to move the visual grating. Recent work in rats has suggested that PPC neurons encode three-dimensional posture (Mimica et al., 2018), and other work has found encoding of angular velocity in a potentially overlapping region (near higher visual area A) in a visually-guided locomotion task (Minderer et al. 2019).

In terms of the causal effects of such motor correlates, again few studies have found direct evidence. Minderer et al. (2019) found widespread effects of inactivation in causing decreased angular velocity on a spherical treadmill; however, this deficit was specific to the contralateral side in a task where the mouse had to monitor ongoing visual flow to correct its virtual course, consistent with contralateral blinding, as the authors conclude as well. Another study using a navigation task on a spherical treadmill did not find an increase in overt motor errors during bilateral inactivation of PPC during a visually-guided task (Pinto et al., 2019). In general, a review of perturbation results in rodent parietal areas (as surveyed in the General Introduction) strongly argues against a causal role in late-stage decision-making; there is little or no evidence that inactivation causes impairments at the motor execution stage, nor that perturbations outside tasks cause motor errors or movements per se.

However, given the results from neural recordings, it was still of interest whether shared representations of rotational movements could explain why some neurons are active in both motor contexts.

Again I used the "blank screen" conditions only, seeing as in the T-maze the rotation is highly correlated with the execution of the choice at the juncture of the T. As well, in the tasks, manipulating the apparatus is designed to move the visual scene (except during the ITI), making it hard to disentangle the effects of visual flow vs motion, the interaction of which was pointed out may be important to drive responses in parietal and nearby areas (Minderer et al. 2019).

As with tests for running modulation in section 3.2, I checked for modulation by rotational velocity using correlations on smoothed traces. Here, rather than comparing modulation to task

selectivity (as neurons active in both tasks have a task selectivity ~0 by definition), I compared each neuron's modulation by rotational velocity in each condition.

I only compared neurons active during both tasks. Across different threshold values, I observed a maximum of one session (of 9 to 11 total) that showed a significant relationship between modulation by velocity on the steering-wheel and angular velocity on the spherical treadmill in the "blank" conditions. The median correlation was low, r = 0.05-0.14 across threshold values. Therefore, I can conclude there is not an effect.

Appendix D

Extended methods

Surgery

Surgical procedures were performed according to Home Office Guidelines under aseptic conditions and under isofluorane anaesthesia. For a given mouse, only one surgery was performed, prior to any handling or training, to minimize the number of operations. Rarely a short secondary surgical procedure was performed to add or remove cement around the headplate. Mice were anesthetized with isoflurane (Merial) at 3–5% for induction, and 0.75–1.5% subsequently. Body temperature was maintained at 37 degrees using a heating pad.

Carprofen (5 mg/kg weight, Rimadyl, Pfizer) was administered subcutaneously for systemic analgesia, and dexamethasone (0.5 mg/kg weight, Colvasone, Norbrook) was administered to prevent brain swelling. The scalp was shaved and disinfected, and a local analgesic (Lidocaine, 5% ointment, TEVA UK; or intradermal injection, 6 mg/kg, Hameln Pharmaceuticals Ltd) was applied prior to the incision. The eyes were covered with eye-protective gel (Viscotears, Alcon; or Chloramphenicol, Martindale Pharmaceuticals Ltd). The animal was positioned in a stereotaxic frame (Lidocaine ointment was applied to the ear bars), the skin covering and surrounding the area of interest was removed, and the skull was cleaned of connective tissue. A custom headplate was positioned above the area of interest and attached to the bone with Superbond C and B (Sun Medical). Then, a round craniotomy (3–4 mm diameter) was made with a fine-tipped diamond drill and/or a biopsy punch (Kai Medical).

To provide optical access to the brain, a circular craniotomy of 4mm radius was made over right posterior cortex using a biopsy punch. The craniotomy was approximately centered at stereotaxic coordinates -2mm Anterior-Posterior and 2mm Medial-Lateral with respect to bregma. Given these coordinates and the radius of the craniotomy, 2/3 of V1 and other higher visual areas were usually also visible in the craniotomy, which enabled identification of retinotopic areas for more precise targeting of imaging location (described in the next section).

The craniotomy was covered with glass coverslip (a 5-mm diameter outer coverlip glued to a 4-mm inner coverslip). A circular metal headplate of 7mm radius was attached with dental cement. All recordings were thus made in the right posterior cortex only.

Following surgery, mice were placed in a heated container to recover until they regained consciousness and were ambulatory. Mice were then given carprieve in water as an analgesic and were given at least three days to recover before beginning any handling.

Behavioral details

Experimental apparatus

The mouse was surrounded by three computer screens (Iiyama ProLite E1980SD) at right angles, with the central monitor located ~20cm in front. The three screens spanned the mouse's visual field approximately 270 degrees horizontally and 70-75 degrees vertically. The screens were at a 60Hz refresh rate and Fresnel lenses were mounted in front of the monitors to correct for aberrations in luminance and contrast at steeper viewing angles, and further covered with a scattering window film to prevent specular reflections. A nearby speaker played auditory stimuli associated with task events, i.e. onset tones, reward tones, and incorrect noise bursts. A water spout was positioned near the mouth of the mouse. A piezoelectric film was affixed to the spout such that deflections of the spout would be registered as an analog electrical signal. Water delivery was controlled by a valve which was muffled in a block of foam, but retained an audible click on reward delivery.

Handling, habituation, and water restriction

Training and habituation protocols were tailored to each mouse to help learning and well-being. Mice were habituated slowly to the apparatuses following recovery from surgery. First, mice were handled in their home cage, then slowly introduced to longer periods of head fixation. Once mice were comfortable on the rig, two-photon imaging and wide-field retinotopy were acquired and examined to ensure adequate imaging quality.

If these criteria were passed, mice were water restricted so that water could be used as a reward. Body weight was monitored to ensure no lower than 80% of their initial body weight i.e. restricted to 40mL/kg weight per day as per the Project License and Home Office Guidelines.

After at least two days of water restriction to ensure a stable weight and no adverse effects, mice were slowly introduced to elements of the task. Initial training was occasionally assisted by Miles Wells, Laura Funnell and Hamish Forrest.

To help with shaping, contrasts were initially restricted to including only high contrast subsets and 100% contrast, and larger rewards were given (3-4µl). A shorter ITI was also employed to prevent disengagement by waiting too long in between trials.

Occasionally, the same trial was repeated if mice did not perform them correctly. In testing sessions, this parameter differed across sessions depending on individual mice's biases; however, repeated trials were never included in analyses of choice.

Reward

In some mice, the remaining water requirement was topped up using hydrogel, and in later mice it was topped up using water. Later mice also sometimes received sucrose water in training to make the reward more appealing. However, sucrose at training did not seem to affect performance at the test phase, and they still readily performed for water reward alone once switched to the testing rig.

References

Akrami, A., Kopec, C. D., Diamond, M. E., & Brody, C. D. (2018). Posterior parietal cortex represents sensory history and mediates its effects on behaviour. Nature, 554(7692), 368–372. https://doi.org/10.1038/nature25510

Andermann, M. L., Kerlin, A. M., Roumis, D. K., Glickfeld, L. L., & Reid, R. C. (2011). Functional specialization of mouse higher visual cortical areas. Neuron, 72(6), 1025–1039. https://doi.org/10.1016/j.neuron.2011.11.013

Andersen, R. A., & Buneo, C. A. (2002). Intentional Maps in Posterior Parietal Cortex. Annual Review of Neuroscience, 25(1), 189–220. https://doi.org/10.1146/annurev.neuro.25.112701.142922

Aronov, D., & Tank, D. W. (2014). Engagement of neural circuits underlying 2D spatial navigation in a rodent virtual reality system. Neuron, 84(2), 442–456. https://doi.org/10.1016/j.neuron.2014.08.042

Attwell, D., & Laughlin, S. B. (2001). An energy budget for signaling in the grey matter of the brain. Journal of Cerebral Blood Flow and Metabolism: Official Journal of the International Society of Cerebral Blood Flow and Metabolism, 21(10), 1133–1145. https://doi.org/10.1097/00004647-200110000-00001

Ayaz, A., Saleem, A. B., Schölvinck, M. L., & Carandini, M. (2013). Locomotion controls spatial integration in mouse visual cortex. Current Biology: CB, 23(10), 890–894. https://doi.org/10.1016/j.cub.2013.04.012

Bálint, & R. (1909). Seelenlähmung des "Schauens", optische Ataxie, räumliche Störung der Aufmerksamkeit. pp. 67–81. European Neurology, 25(1), 67–81. https://doi.org/10.1159/000210465

Bennur, S., & Gold, J. I. (2011). Distinct representations of a perceptual decision and the associated oculomotor plan in the monkey lateral intraparietal area. The Journal of Neuroscience: The Official Journal of the Society for Neuroscience, 31(3), 913–921. https://doi.org/10.1523/JNEUROSCI.4417-10.2011

Berens, P., Freeman, J., Deneux, T., Chenkov, N., McColgan, T., Speiser, A., Macke, J. H., Turaga, S. C., Mineault, P., Rupprecht, P., Gerhard, S., Friedrich, R. W., Friedrich, J., Paninski, L., Pachitariu, M., Harris, K. D., Bolte, B., Machado, T. A., Ringach, D., … Bethge, M. (2018). Community-based benchmarking improves spike rate inference from two-photon calcium imaging data. PLoS Computational Biology, 14(5), e1006157. https://doi.org/10.1371/journal.pcbi.1006157

Bhagat, J., Wells, M. J., Peters, A., Harris, K. D., Carandini, M., & Burgess, C. P. (2019). Rigbox: an Open-Source Toolbox for Probing Neurons and Behavior. In bioRxiv (p. 672204). https://doi.org/10.1101/672204

Joo, B., Koo, J. W., & Lee, S. (2020). Posterior parietal cortex mediates fear renewal in a novel context. *Molecular Brain*, *13*(1), 1-11.

Britten, K. H., Newsome, W. T., Shadlen, M. N., Celebrini, S., & Movshon, J. A. (1996). A relationship between behavioral choice and the visual responses of neurons in macaque MT. Visual Neuroscience, 13(1), 87–100. https://doi.org/10.1017/s095252380000715x

Britten, K. H., Shadlen, M. N., Newsome, W. T., & Movshon, J. A. (1992). The analysis of visual motion: a comparison of neuronal and psychophysical performance. The Journal of Neuroscience: The Official Journal of the Society for Neuroscience, 12(12), 4745–4765. https://www.ncbi.nlm.nih.gov/pubmed/1464765

Brunton, B. W., Botvinick, M. M., & Brody, C. D. (2013). Rats and humans can optimally accumulate evidence for decision-making. Science, 340(6128), 95–98. https://doi.org/10.1126/science.1233912

Burgess, C. P., Lak, A., Steinmetz, N. A., Zatka-Haas, P., Bai Reddy, C., Jacobs, E. A. K., Linden, J. F., Paton, J. J., Ranson, A., Schröder, S., Soares, S., Wells, M. J., Wool, L. E., Harris, K. D., & Carandini, M. (2017). High-Yield Methods for Accurate Two-Alternative Visual Psychophysics in Head-Fixed Mice. Cell Reports, 20(10), 2513–2524. https://doi.org/10.1016/j.celrep.2017.08.047

Busse, L. (2018). The influence of locomotion on sensory processing and its underlying neuronal circuits. Neuroforum, 24(1), 41–51. https://doi.org/10.1515/nf-2017-A046

Busse, L., Cardin, J. A., Chiappe, M. E., Halassa, M. M., McGinley, M. J., Yamashita, T., & Saleem, A. B. (2017). Sensation during active behaviors. Journal of Neuroscience, 37(45), 10826–10834. https://doi.org/10.1523/JNEUROSCI.1828-17.2017

Calton, J. L., & Taube, J. S. (2009). Where am I and how will I get there from here? A role for posterior parietal cortex in the integration of spatial information and route planning. Neurobiology of Learning and Memory, 91(2), 186–196. https://doi.org/10.1016/j.nlm.2008.09.015

Chen, B. K., Murawski, N. J., Cincotta, C., McKissick, O., Finkelstein, A., Hamidi, A. B., Merfeld, E., Doucette, E., Grella, S. L., Shpokayte, M., Zaki, Y., Fortin, A., & Ramirez, S. (2019). Artificially Enhancing and Suppressing Hippocampus-Mediated Memories. Current Biology: CB, 29(11), 1885–1894.e4. https://doi.org/10.1016/j.cub.2019.04.065

Chen, J. L., Pfäffli, O. A., Voigt, F. F., Margolis, D. J., & Helmchen, F. (2013). Online correction of licking-induced brain motion during two-photon imaging with a tunable lens. The Journal of Physiology, 591(19), 4689–4698. https://doi.org/10.1113/jphysiol.2013.259804

Chen, L. L., Lin, L.-H., Barnes, C. A., & McNaughton, B. L. (1994). Head-direction cells in the rat posterior cortex. In Experimental Brain Research (Vol. 101, Issue 1, pp. 24–34). https://doi.org/10.1007/bf00243213

Chen, T.-W., Wardill, T. J., Sun, Y., Pulver, S. R., Renninger, S. L., Baohan, A., Schreiter, E. R., Kerr, R. A., Orger, M. B., Jayaraman, V., Looger, L. L., Svoboda, K., & Kim, D. S. (2013). Ultrasensitive fluorescent proteins for imaging neuronal activity. Nature, 499(7458), 295–300. https://doi.org/10.1038/nature12354

Chen, X., DeAngelis, G. C., & Angelaki, D. E. (2018). Flexible egocentric and allocentric representations of heading signals in parietal cortex. Proceedings of the National Academy of Sciences of the United States of America, 115(14), E3305–E3312. https://doi.org/10.1073/pnas.1715625115

Condylis, C., Lowet, E., Ni, J., Bistrong, K., Ouellette, T., Josephs, N., & Chen, J. L. (2020). Context-Dependent Sensory Processing across Primary and Secondary Somatosensory Cortex. Neuron. https://doi.org/10.1016/j.neuron.2020.02.004

de Vries, S. E. J., Lecoq, J. A., Buice, M. A., Groblewski, P. A., Ocker, G. K., Oliver, M., Feng, D., Cain, N., Ledochowitsch, P., Millman, D., Roll, K., Garrett, M., Keenan, T., Kuan, L., Mihalas, S., Olsen, S., Thompson, C., Wakeman, W., Waters, J., … Koch, C. (2020). A large-scale standardized physiological survey reveals functional organization of the mouse visual cortex. Nature Neuroscience, 23(1), 138–151. https://doi.org/10.1038/s41593-019-0550-9

Diamond, M. E., von Heimendahl, M., Knutsen, P. M., Kleinfeld, D., & Ahissar, E. (2008). "Where" and "what" in the whisker sensorimotor system. Nature Reviews. Neuroscience, 9(8), 601–612. https://doi.org/10.1038/nrn2411

Dombeck, D. A., Khabbaz, A. N., Collman, F., Adelman, T. L., & Tank, D. W. (2007). Imaging large-scale neural activity with cellular resolution in awake, mobile mice. Neuron, 56(1), 43–57. https://doi.org/10.1016/j.neuron.2007.08.003

Driscoll, L. N., Pettit, N. L., Minderer, M., Chettih, S. N., & Harvey, C. D. (2017). Dynamic Reorganization of Neuronal Activity Patterns in Parietal Cortex. Cell, 170(5), 986–999.e16. https://doi.org/10.1016/j.cell.2017.07.021

Duan, C. A., Erlich, J. C., & Brody, C. D. (2015). Requirement of Prefrontal and Midbrain Regions for Rapid Executive Control of Behavior in the Rat. Neuron, 86(6), 1491–1503. https://doi.org/10.1016/j.neuron.2015.05.042

Smith, JET, et al. (2012). Linking Neural Activity to Visual Perception: Separating Sensory and Attentional Contributions. In S. Molotchnikoff (Ed.), Visual Cortex - Current Status and Perspectives. InTech. https://doi.org/10.5772/48806

Erlich, J. C., Bialek, M., & Brody, C. D. (2011). A cortical substrate for memory-guided orienting in the rat. Neuron, 72(2), 330–343. https://doi.org/10.1016/j.neuron.2011.07.010

Erlich, J. C., Brunton, B. W., Duan, C. A., Hanks, T. D., & Brody, C. D. (2015). Distinct effects of prefrontal and parietal cortex inactivations on an accumulation of evidence task in the rat. eLife, 4. https://doi.org/10.7554/eLife.05457

Foroosh, H., Zerubia, J. B., & Berthod, M. (2002). Extension of phase correlation to subpixel registration. IEEE Transactions on Image Processing: A Publication of the IEEE Signal Processing Society, 11(3), 188–200. https://doi.org/10.1109/83.988953

Freedman, D. J., & Assad, J. A. (2009). Distinct encoding of spatial and nonspatial visual information in parietal cortex. The Journal of Neuroscience: The Official Journal of the Society for Neuroscience, 29(17), 5671–5680. https://doi.org/10.1523/JNEUROSCI.2878-08.2009

Freedman, D. J., & Assad, J. A. (2011). A proposed common neural mechanism for categorization and perceptual decisions. Nature Neuroscience, 14(2), 143–146. https://doi.org/10.1038/nn.2740

Freedman, D. J., & Assad, J. A. (2016). Neuronal Mechanisms of Visual Categorization: An Abstract View on Decision Making. Annual Review of Neuroscience, 39, 129–147. https://doi.org/10.1146/annurev-neuro-071714-033919

Friedrich, J., Zhou, P., & Paninski, L. (2017). Fast online deconvolution of calcium imaging data. PLoS Computational Biology, 13(3), e1005423. https://doi.org/10.1371/journal.pcbi.1005423

Garrett, M. E., Nauhaus, I., Marshel, J. H., & Callaway, E. M. (2014). Topography and areal organization of mouse visual cortex. The Journal of Neuroscience: The Official Journal of the Society for Neuroscience, 34(37), 12587–12600. https://doi.org/10.1523/JNEUROSCI.1124-14.2014

Gilissen, S. R. J., Farrow, K., Bonin, V., & Arckens, L. (2020). 1 Reconsidering the border between the visual and posterior parietal 2 cortex of mice. In bioRxiv (p. 2020.03.24.005462). https://doi.org/10.1101/2020.03.24.005462

Glickfeld, L. L., & Olsen, S. R. (2017). Higher-Order Areas of the Mouse Visual Cortex. Annual Review of Vision Science, July, 1–23.

Gnadt, J. W., & Andersen, R. A. (1988). Memory related motor planning activity in posterior parietal cortex of macaque. Experimental Brain Research. Experimentelle Hirnforschung. Experimentation Cerebrale, 70(1), 216–220. https://doi.org/10.1007/BF00271862

Goard, M. J., Pho, G. N., Woodson, J., & Sur, M. (2016). Distinct roles of visual, parietal, and frontal motor cortices in memory-guided sensorimotor decisions. eLife, 5. https://doi.org/10.7554/eLife.13764

Gold, J. I., & Shadlen, M. N. (2007). The neural basis of decision making. Annual Review of Neuroscience, 30, 535–574. https://doi.org/10.1146/annurev.neuro.29.051605.113038

Goldberg, M. E., Colby, C. L., & Duhamel, J. R. (1990). Representation of visuomotor space in the parietal lobe of the monkey. Cold Spring Harbor Symposia on Quantitative Biology, 55, 729–739. https://doi.org/10.1101/sqb.1990.055.01.068

Green, D. M., Swets, J. A., & Others. (1966). Signal detection theory and psychophysics (Vol. 1). Wiley New York. http://andrei.gorea.free.fr/Teaching_fichiers/SDT%20and%20Psytchophysics.pdf

Guo, Z. V., Li, N., Huber, D., Ophir, E., Gutnisky, D., Ting, J. T., Feng, G., & Svoboda, K. (2014). Flow of cortical activity underlying a tactile decision in mice. Neuron, 81(1), 179–194. https://doi.org/10.1016/j.neuron.2013.10.020

Hanks, T. D., Kopec, C. D., Brunton, B. W., Duan, C. A., Erlich, J. C., & Brody, C. D. (2015). Distinct relationships of parietal and prefrontal cortices to evidence accumulation. Nature, 520(7546), 220–223. https://doi.org/10.1038/nature14066

Harris, K. D., & Thiele, A. (2011). Cortical state and attention. Nature Reviews. Neuroscience, 12(9), 509–523. https://doi.org/10.1038/nrn3084

Harvey, C. D., Coen, P., & Tank, D. W. (2012). Choice-specific sequences in parietal cortex during a virtual-navigation decision task. Nature, 484(7392), 62–68. https://doi.org/10.1038/nature10918

Harvey, C. D., Collman, F., Dombeck, D. A., & Tank, D. W. (2009). Intracellular dynamics of hippocampal place cells during virtual navigation. Nature, 461(7266), 941–946. https://doi.org/10.1038/nature08499

Hovde, K., Gianatti, M., Witter, M. P., & Whitlock, J. R. (2019). Architecture and organization of mouse posterior parietal cortex relative to extrastriate areas. The European Journal of Neuroscience, 49(10), 1313–1329. https://doi.org/10.1111/ejn.14280

Huang, L., Knoblich, U., Ledochowitsch, P., Lecoq, J., Reid, R. C., Vries, S. E. J. de, Buice, M. A., Murphy, G. J., Waters, J., Koch, C., Zeng, H., & Li, L. (2019). Relationship between spiking activity and simultaneously recorded fluorescence signals in transgenic mice expressing GCaMP6. bioRxiv, 788802. https://doi.org/10.1101/788802

Huk, A. C., Katz, L. N., & Yates, J. L. (2017). The Role of the Lateral Intraparietal Area in (the Study of) Decision Making. Annual Review of Neuroscience, 40, 349–372. https://doi.org/10.1146/annurev-neuro-072116-031508

Huo, B.-X., Gao, Y.-R., & Drew, P. J. (2015). Quantitative separation of arterial and venous cerebral blood volume increases during voluntary locomotion. NeuroImage, 105, 369–379. https://doi.org/10.1016/j.neuroimage.2014.10.030

Hwang, E. J., Dahlen, J. E., Mukundan, M., & Komiyama, T. (2017). History-based action selection bias in posterior parietal cortex. Nature Communications, 8(1), 1242. https://doi.org/10.1038/s41467-017-01356-z

Hwang, E. J., Link, T. D., Hu, Y. Y., Lu, S., Wang, E. H.-J., Lilascharoen, V., Aronson, S., O'Neil, K., Lim, B. K., & Komiyama, T. (2019). Corticostriatal Flow of Action Selection Bias. Neuron, 104(6), 1126–1140.e6. https://doi.org/10.1016/j.neuron.2019.09.028

Insanally, M. N., Carcea, I., Field, R. E., Rodgers, C. C., DePasquale, B., Rajan, K., DeWeese, M. R., Albanna, B. F., & Froemke, R. C. (2019). Spike-timing-dependent ensemble encoding by non-classically responsive cortical neurons. eLife, 8. https://doi.org/10.7554/eLife.42409

Itokazu, T., Hasegawa, M., Kimura, R., Osaki, H., Albrecht, U.-R., Sohya, K., Chakrabarti, S., Itoh, H., Ito, T., Sato, T. K., & Sato, T. R. (2018). Streamlined sensory motor communication through cortical reciprocal connectivity in a visually guided eye movement task. Nature Communications, 9(1), 338. https://doi.org/10.1038/s41467-017-02501-4

Izpisua Belmonte, J. C., Callaway, E. M., Caddick, S. J., Churchland, P., Feng, G., Homanics, G. E., Lee, K.-F., Leopold, D. A., Miller, C. T., Mitchell, J. F., Mitalipov, S., Moutri, A. R., Movshon, J. A., Okano, H., Reynolds, J. H., Ringach, D., Sejnowski, T. J., Silva, A. C., Strick, P. L., … Zhang, F. (2015). Brains, genes, and primates. Neuron, 86(3), 617–631. https://doi.org/10.1016/j.neuron.2015.03.021

Jacobs, E. A. K., Steinmetz, N. A., Carandini, M., & Harris, K. D. (2018). Cortical state fluctuations during sensory decision making. In bioRxiv (p. 348193). https://doi.org/10.1101/348193

Joo, B., Koo, J. W., & Lee, S. (2020). Posterior parietal cortex mediates fear renewal in a novel context. Molecular Brain, 13(1), 16. https://doi.org/10.1186/s13041-020-0556-y

Katz, L. N., & Others. (2016). Decision-making in the primate brain: formation, location, and causal manipulation.

Katz, L. N., Yates, J. L., Pillow, J. W., & Huk, A. C. (2016). Dissociated functional significance of decision-related activity in the primate dorsal stream. Nature, 535(7611), 285–288. https://doi.org/10.1038/nature18617

Koay, S. A., Thiberge, S. Y., Brody, C. D., & Tank, D. W. (2019). Neural Correlates of Cognition in Primary Visual versus Neighboring Posterior Cortices during Visual Evidence-Accumulation-based Navigation. In bioRxiv (p. 568766). https://doi.org/10.1101/568766

Kolb, B., Sutherland, R. J., & Whishaw, I. Q. (1983). A comparison of the contributions of the frontal and parietal association cortex to spatial localization in rats. Behavioral Neuroscience, 97(1), 13–27. https://doi.org/10.1037//0735-7044.97.1.13

Kolb, B., & Walkey, J. (1987). Behavioural and anatomical studies of the posterior parietal cortex in the rat. Behavioural Brain Research, 23, 127–145. https://doi.org/10.1016/0166-4328(87)90050-7

Krumin, M., Lee, J. J., Harris, K. D., & Carandini, M. (2018). Decision and navigation in mouse parietal cortex. eLife, 7. https://doi.org/10.7554/eLife.42583

La Chioma, A., Bonhoeffer, T., & Hübener, M. (2019). Area-Specific Mapping of Binocular Disparity across Mouse Visual Cortex. Current Biology: CB, 29(17), 2954–2960.e5. https://doi.org/10.1016/j.cub.2019.07.037

Ledochowitsch, P., Huang, L., Knoblich, U., Oliver, M., Lecoq, J., Reid, C., Li, L., Zeng, H., Koch, C., Waters, J., de Vries, S. E. J., & Buice, M. A. (2019). On the correspondence of electrical and optical physiology in in vivo population-scale two-photon calcium imaging. In bioRxiv (p. 800102). https://doi.org/10.1101/800102

Lennie, P. (2003). The cost of cortical computation. Current Biology: CB, 13(6), 493–497. https://doi.org/10.1016/s0960-9822(03)00135-0

Licata, A. M., Kaufman, M. T., Raposo, D., Ryan, M. B., Sheppard, J. P., & Churchland, A. K. (2017). Posterior Parietal Cortex Guides Visual Decisions in Rats. The Journal of Neuroscience: The Official Journal of the Society for Neuroscience, 37(19), 4954–4966. https://doi.org/10.1523/JNEUROSCI.0105-17.2017

Mante, V., Sussillo, D., Shenoy, K. V., & Newsome, W. T. (2013). Context-dependent computation by recurrent dynamics in prefrontal cortex. Nature, 503(7474), 78–84. https://doi.org/10.1038/nature12742

Markowitz, J. E., Gillis, W. F., Beron, C. C., Neufeld, S. Q., Robertson, K., Bhagat, N. D., Peterson, R. E., Peterson, E., Hyun, M., Linderman, S. W., Sabatini, B. L., & Datta, S. R. (2018). The Striatum Organizes 3D Behavior via Moment-to-Moment Action Selection. Cell, 174(1), 44–58.e17. https://doi.org/10.1016/j.cell.2018.04.019

McCloskey, M., & Cohen, N. J. (1989). Catastrophic Interference in Connectionist Networks: The Sequential Learning Problem. In G. H. Bower (Ed.), Psychology of Learning and Motivation (Vol. 24, pp. 109–165). Academic Press. https://doi.org/10.1016/S0079-7421(08)60536-8

McNaughton, B. L., Mizumori, S. J., Barnes, C. A., Leonard, B. J., Marquis, M., & Green, E. J. (1994). Cortical representation of motion during unrestrained spatial navigation in the rat. Cerebral Cortex , 4(1), 27–39. https://doi.org/10.1093/cercor/4.1.27

Meister, M. L. R., Hennig, J. A., & Huk, A. C. (2013). Signal multiplexing and single-neuron computations in lateral intraparietal area during decision-making. The Journal of Neuroscience: The Official Journal of the Society for Neuroscience, 33(6), 2254–2267. https://doi.org/10.1523/JNEUROSCI.2984-12.2013

Mesa, N., Waters, J., & de Vries, S. E. J. (2020). The effect of inclusion criteria on the functional properties reported in mouse visual cortex. In bioRxiv (p. 2020.05.12.091595). https://doi.org/10.1101/2020.05.12.091595

Diamanti, E., Reddy, C., Schröder, S., Harris, K. D., Saleem, A. B., & Carandini, M. (2019). Spatial encoding in the visual pathway arises in cortex and depends on active navigation. In bioRxiv (p. 832915). https://doi.org/10.1101/832915

Mimica, B., Dunn, B. A., Tombaz, T., Bojja, V. P. T. N. C. S., & Whitlock, J. R. (2018). Efficient cortical coding of 3D posture in freely behaving rats. Science, 362(6414), 584–589. https://doi.org/10.1126/science.aau2013

Minderer, M., Brown, K. D., & Harvey, C. D. (2019). The Spatial Structure of Neural Encoding in Mouse Posterior Cortex during Navigation. Neuron, 102(1), 232–248.e11. https://doi.org/10.1016/j.neuron.2019.01.029

Miri, A., Daie, K., Burdine, R. D., Aksay, E., & Tank, D. W. (2011). Regression-based identification of behavior-encoding neurons during large-scale optical imaging of neural activity at cellular resolution. Journal of Neurophysiology, 105(2), 964–980. https://doi.org/10.1152/jn.00702.2010

Morcos, A. S., & Harvey, C. D. (2016). History-dependent variability in population dynamics during evidence accumulation in cortex. Nature Neuroscience, 19(12), 1672–1681. https://doi.org/10.1038/nn.4403

Mountcastle, V. B., Lynch, J. C., Georgopoulos, A., Sakata, H., & Acuna, C. (1975). Posterior parietal association cortex of the monkey: command functions for operations within extrapersonal space. Journal of Neurophysiology, 38(4), 871–908. https://doi.org/10.1152/jn.1975.38.4.871

Murakami, M., Vicente, M. I., Costa, G. M., & Mainen, Z. F. (2014). Neural antecedents of self-initiated actions in secondary motor cortex. Nature Neuroscience, 17(11), 1574–1582. https://doi.org/10.1038/nn.3826

Musall, S., Kaufman, M. T., Juavinett, A. L., Gluf, S., & Churchland, A. K. (2019). Single-trial neural dynamics are dominated by richly varied movements. Nature Neuroscience, 22(10), 1677–1686. https://doi.org/10.1038/s41593-019-0502-4

Najafi, F., Elsayed, G. F., Cao, R., Pnevmatikakis, E., Latham, P. E., Cunningham, J. P., & Churchland, A. K. (2020). Excitatory and Inhibitory Subnetworks Are Equally Selective during Decision-Making and Emerge Simultaneously during Learning. Neuron, 105(1), 165–179.e8. https://doi.org/10.1016/j.neuron.2019.09.045

Niell, C. M., & Stryker, M. P. (2010). Modulation of visual responses by behavioral state in mouse visual cortex. Neuron, 65(4), 472–479. https://doi.org/10.1016/j.neuron.2010.01.033

Nikbakht, N., Tafreshiha, A., Zoccolan, D., & Diamond, M. E. (2018). Supralinear and Supramodal Integration of Visual and Tactile Signals in Rats: Psychophysics and Neuronal Mechanisms. Neuron, 1–14. https://doi.org/10.1016/j.neuron.2018.01.003

Nitz, D. A. (2006). Tracking route progression in the posterior parietal cortex. Neuron, 49(5), 747–756. https://doi.org/10.1016/j.neuron.2006.01.037

Nitz, D. A. (2012). Spaces within spaces: rat parietal cortex neurons register position across three reference frames. Nature Neuroscience, 15(10), 1365–1367. https://doi.org/10.1038/nn.3213

Odoemene, O., Pisupati, S., Nguyen, H., & Churchland, A. K. (2018). Visual Evidence Accumulation Guides Decision-Making in Unrestrained Mice. The Journal of Neuroscience: The Official Journal of the Society for Neuroscience, 38(47), 10143–10155. https://doi.org/10.1523/JNEUROSCI.3478-17.2018

Olsen, G. M., Hovde, K., Kondo, H., Sakshaug, T., Sømme, H. H., Whitlock, J. R., & Witter, M. P. (2019). Organization of Posterior Parietal-Frontal Connections in the Rat. Frontiers in Systems Neuroscience, 13(August), 1–23. https://doi.org/10.3389/fnsys.2019.00038

Olsen, G. M., & Witter, M. P. (2016). The posterior parietal cortex of the rat: architectural delineation and thalamic differentiation. The Journal of Comparative Neurology, 00, 1–36. https://doi.org/10.1002/cne.24032

Olshausen, B. A., & Field, D. J. (2006). What Is the Other 85 Percent of V1 Doing? In 23 Problems in Systems Neuroscience. Oxford University Press. https://doi.org/10.1093/acprof:oso/9780195148220.003.0010

Orban, G. A., Claeys, K., Nelissen, K., Smans, R., Sunaert, S., Todd, J. T., Wardak, C., Durand, J. B., & Vanduffel, W. (2006). Mapping the parietal cortex of human and non-human primates. Neuropsychologia, 44(13), 2647–2667. https://doi.org/10.1016/j.neuropsychologia.2005.11.001

Pachitariu, M., Stringer, C., Dipoppa, M., & Schröder, S. (2017). Suite2p: beyond 10,000 neurons with standard two-photon microscopy. Biorxiv. https://discovery.ucl.ac.uk/id/eprint/10049507/

Pachitariu, M., Stringer, C., & Harris, K. D. (2017). Robustness of spike deconvolution for calcium imaging of neural spiking. In bioRxiv (p. 156786). https://doi.org/10.1101/156786

Pachitariu, M., Stringer, C., & Harris, K. D. (2018). Robustness of Spike Deconvolution for Neuronal Calcium Imaging. The Journal of Neuroscience: The Official Journal of the Society for Neuroscience, 38(37), 7976–7985. https://doi.org/10.1523/JNEUROSCI.3339-17.2018

Packer, A. M., Russell, L. E., Dalgleish, H. W. P., & Häusser, M. (2015). Simultaneous all-optical manipulation and recording of neural circuit activity with cellular resolution in vivo. Nature Methods, 12(2), 140–146. https://doi.org/10.1038/nmeth.3217

Park, I. M., Meister, M. L. R., Huk, A. C., & Pillow, J. W. (2014). Encoding and decoding in parietal cortex during sensorimotor decision-making. Nature Neuroscience, 17(10), 1395–1403. https://doi.org/10.1038/nn.3800

Parker, P. R. L., Brown, M. A., Smear, M. C., & Niell, C. M. (2020). Movement-Related Signals in Sensory Areas: Roles in Natural Behavior. Trends in Neurosciences. https://doi.org/10.1016/j.tins.2020.05.005

Pho, G. N., Goard, M. J., Woodson, J., Crawford, B., & Sur, M. (2018). Task-dependent representations of stimulus and choice in mouse parietal cortex. Nature Communications, 9(1), 2596. https://doi.org/10.1038/s41467-018-05012-y

Pinto, L., Koay, S. A., Engelhard, B., Yoon, A. M., Deverett, B., Thiberge, S. Y., Witten, I. B., Tank, D. W., & Brody, C. D. (2018). An Accumulation-of-Evidence Task Using Visual Pulses for Mice Navigating in Virtual Reality. Frontiers in Behavioral Neuroscience, 12, 36. https://doi.org/10.3389/fnbeh.2018.00036

Pinto, L., Rajan, K., DePasquale, B., Thiberge, S. Y., Tank, D. W., & Brody, C. D. (2019). Task-Dependent Changes in the Large-Scale Dynamics and Necessity of Cortical Regions. Neuron, 104(4), 810–824.e9. https://doi.org/10.1016/j.neuron.2019.08.025

Pologruto, T. A., Sabatini, B. L., & Svoboda, K. (2003). ScanImage: flexible software for operating laser scanning microscopes. Biomedical Engineering Online, 2, 13. https://doi.org/10.1186/1475-925X-2-13

Poort, J., Khan, A. G., Pachitariu, M., Nemri, A., Orsolic, I., Krupic, J., Bauza, M., Sahani, M., Keller, G. B., Mrsic-Flogel, T. D., & Hofer, S. B. (2015). Learning Enhances Sensory and Multiple Non-sensory Representations in Primary Visual Cortex. Neuron, 86(6), 1478–1490. https://doi.org/10.1016/j.neuron.2015.05.037

Raposo, D., Kaufman, M. T., & Churchland, A. K. (2014). A category-free neural population supports evolving demands during decision-making. Nature Neuroscience. https://www.nature.com/neuro/journal/v17/n12/abs/nn.3865.html

Redish, A. D. (2016). Vicarious trial and error. Nature Reviews. Neuroscience, 17(3), 147–159. https://doi.org/10.1038/nrn.2015.30

Resulaj, A., Ruediger, S., Olsen, S. R., & Scanziani, M. (2018). First spikes in visual cortex enable perceptual discrimination. eLife, 7. https://doi.org/10.7554/eLife.34044

Rishel, C. A., Huang, G., & Freedman, D. J. (2013). Independent category and spatial encoding in parietal cortex. Neuron, 77(5), 969–979. https://doi.org/10.1016/j.neuron.2013.01.007

Robinson, D. L., Goldberg, M. E., & Stanton, G. B. (1978). Parietal association cortex in the primate: sensory mechanisms and behavioral modulations. Journal of Neurophysiology, 41(4), 910–932. https://doi.org/10.1152/jn.1978.41.4.910

Rossi, L. F. (2018). *Cortical circuits for visual processing and epileptic activity propagation*. UCL (University College London).

Runyan, C. A., Piasini, E., Panzeri, S., & Harvey, C. D. (2017). Distinct timescales of population coding across cortex. Nature, 548(7665), 92–96. https://doi.org/10.1038/nature23020

Saleem, A. B., Ayaz, A., Jeffery, K. J., Harris, K. D., & Carandini, M. (2013). Integration of visual motion and locomotion in mouse visual cortex. Nature Neuroscience, 16(12), 1864–1869. https://doi.org/10.1038/nn.3567

Saleem, A. B., Diamanti, E. M., Fournier, J., Harris, K. D., & Carandini, M. (2018). Coherent encoding of subjective spatial position in visual cortex and hippocampus. Nature, 562(7725), 124–127. https://doi.org/10.1038/s41586-018-0516-1

Save, E., & Poucet, B. (2000). Involvement of the hippocampus and associative parietal cortex in the use of proximal and distal landmarks for navigation. Behavioural Brain Research, 109(2), 195–206. https://doi.org/10.1016/s0166-4328(99)00173-4

Save, E., & Poucet, B. (2009). Role of the parietal cortex in long-term representation of spatial information in the rat. Neurobiology of Learning and Memory, 91(2), 172–178. https://doi.org/10.1016/j.nlm.2008.08.005

Schall, J. D. (2001). Neural basis of deciding, choosing and acting. Nature Reviews. Neuroscience, 2(1), 33–42. https://doi.org/10.1038/35049054

Scott, B. B., Constantinople, C. M., Akrami, A., Hanks, T. D., Brody, C. D., & Tank, D. W. (2017). Fronto-parietal Cortical Circuits Encode Accumulated Evidence with a Diversity of Timescales. Neuron, 95(2), 385–398.e5. https://doi.org/10.1016/j.neuron.2017.06.013

Semedo, J. D., Zandvakili, A., Machens, C. K., Yu, B. M., & Kohn, A. (2019). Cortical Areas Interact through a Communication Subspace. Neuron, 102(1), 249–259.e4. https://doi.org/10.1016/j.neuron.2019.01.026

Sereno, M. I., McDonald, C. T., & Allman, J. M. (1994). Analysis of retinotopic maps in extrastriate cortex. Cerebral Cortex , 4(6), 601–620. https://doi.org/10.1093/cercor/4.6.601

Shadlen, M. N., Kiani, R., Hanks, T. D., & Churchland, A. K. (2008a). An intentional framework. Better than Conscious, 71–101. https://books.google.com/books?hl=en&lr=&id=JQLg7L-Qto4C&oi=fnd&pg=PA71&dq=shadlen+churchland+neurobiology+of&ots=HwiSMX_b5A&sig=NxXO5zqMt6KEZBN6B-C5wLywLDc

Shadlen, M. N., Kiani, R., Hanks, T. D., & Churchland, A. K. (2008b). Neurobiology of decision making: An intentional framework. Better than Conscious? Decision Making, the Human Mind, and Implications for Institutions., 449, 71–101. https://psycnet.apa.org/fulltext/2007-18938-004.pdf

Shimaoka, D., Harris, K. D., & Carandini, M. (2018). Effects of Arousal on Mouse Sensory Cortex Depend on Modality. Cell Reports, 25(11), 3230. https://doi.org/10.1016/j.celrep.2018.11.105

Shuler, M. G., & Bear, M. F. (2006). Reward timing in the primary visual cortex. Science, 311(5767), 1606–1609. https://doi.org/10.1126/science.1123513

Snyder, L. H., Batista, A. P., & Andersen, R. A. (1997). Coding of intention in the posterior parietal cortex. Nature, 386(6621), 167–170. https://doi.org/10.1038/386167a0

Snyder, L. H., Batista, A. P., & Andersen, R. A. (2000). Intention-related activity in the posterior parietal cortex: a review. Vision Research, 40(10-12), 1433–1441. https://doi.org/10.1016/s0042-6989(00)00052-3

Soma, S., Yoshida, J., Kato, S., Takahashi, Y., Nonomura, S., Sugimura, Y. K., Ríos, A., Kawabata, M., Kobayashi, K., Kato, F., Sakai, Y., & Isomura, Y. (2019). Ipsilateral-Dominant Control of Limb Movements in Rodent Posterior Parietal Cortex. The Journal of Neuroscience: The Official Journal of the Society for Neuroscience, 39(3), 485–502. https://doi.org/10.1523/JNEUROSCI.1584-18.2018

Song, Y.-H., Kim, J.-H., Jeong, H.-W., Choi, I., Jeong, D., Kim, K., & Lee, S.-H. (2017). A Neural Circuit for Auditory Dominance over Visual Perception. Neuron, 93(5), 1236–1237. https://doi.org/10.1016/j.neuron.2017.02.026

Steinmetz, N. A., Buetfering, C., Lecoq, J., Lee, C. R., Peters, A. J., Jacobs, E. A. K., Coen, P., Ollerenshaw, D. R., Valley, M. T., de Vries, S. E. J., Garrett, M., Zhuang, J., Groblewski, P. A., Manavi, S., Miles, J., White, C., Lee, E., Griffin, F., Larkin, J. D., … Harris, K. D. (2017). Aberrant Cortical Activity in Multiple GCaMP6-Expressing Transgenic Mouse Lines. eNeuro, 4(5). https://doi.org/10.1523/ENEURO.0207-17.2017

Steinmetz, N. A., Zatka-Haas, P., Carandini, M., & Harris, K. D. (2019). Distributed coding of choice, action and engagement across the mouse brain. Nature, 576(7786), 266–273. https://doi.org/10.1038/s41586-019-1787-x

Stringer, C. (2018). Discovering structure in multi-neuron recordings through network modelling. UCL (University College London).

Stringer, C., & Pachitariu, M. (2019). Computational processing of neural recordings from calcium imaging data. Current Opinion in Neurobiology, 55, 22–31. https://doi.org/10.1016/j.conb.2018.11.005

Stringer, C., Pachitariu, M., Steinmetz, N., Reddy, C. B., Carandini, M., & Harris, K. D. (2019). Spontaneous behaviors drive multidimensional, brainwide activity. Science, 364(6437), 255. https://doi.org/10.1126/science.aav7893

The International Brain Laboratory, Aguillon-Rodriguez, V., Angelaki, D. E., Bayer, H. M., Bonacchi, N., Carandini, M., Cazettes, F., Chapuis, G. A., Churchland, A. K., Dan, Y., Dewitt, E. E., Faulkner, M., Forrest, H., Haetzel, L. M., Hausser, M., Hofer, S. B., Hu, F., Khanal, A., Krasniak, C. S., … Zador, A. (2020). A standardized and reproducible method to measure decision-making in mice. In bioRxiv (p. 2020.01.17.909838). https://doi.org/10.1101/2020.01.17.909838

Tombaz, T., Dunn, B. A., Hovde, K., Cubero, R. J., Mimica, B., Mamidanna, P., Roudi, Y., & Whitlock, J. R. (2020). Action representation in the mouse parieto-frontal network. Scientific Reports, 10(1), 5559. https://doi.org/10.1038/s41598-020-62089-6

Vogelstein, J. T., Packer, A. M., Machado, T. A., Sippy, T., Babadi, B., Yuste, R., & Paninski, L. (2010). Fast nonnegative deconvolution for spike train inference from population calcium imaging. Journal of Neurophysiology, 104(6), 3691–3704. https://doi.org/10.1152/jn.01073.2009

Wallace, D. G., Gorny, B., & Whishaw, I. Q. (2002). Rats can track odors, other rats, and themselves: implications for the study of spatial behavior. Behavioural Brain Research, 131(1-2), 185–192. https://doi.org/10.1016/s0166-4328(01)00384-9

Wang, Q., & Burkhalter, A. (2007). Area map of mouse visual cortex. The Journal of Comparative Neurology, 502(3), 339–357. https://doi.org/10.1002/cne.21286

Wang, Q., Ding, S.-L., Li, Y., Royall, J., Feng, D., Lesnar, P., Graddis, N., Naeemi, M., Facer, B., Ho, A., Dolbeare, T., Blanchard, B., Dee, N., Wakeman, W., Hirokawa, K. E., Szafer, A., Sunkin, S. M., Oh, S. W., Bernard, A., … Ng, L. (2020). The Allen Mouse Brain Common Coordinate Framework: A 3D Reference Atlas. Cell, 181(4), 936–953.e20. https://doi.org/10.1016/j.cell.2020.04.007

Wang, Q., Gao, E., & Burkhalter, A. (2011). Gateways of ventral and dorsal streams in mouse visual cortex. The Journal of Neuroscience: The Official Journal of the Society for Neuroscience, 31(5), 1905–1918. https://doi.org/10.1523/JNEUROSCI.3488-10.2011

Wekselblatt, J. B., Flister, E. D., Piscopo, D. M., & Niell, C. M. (2016). Large-scale imaging of cortical dynamics during sensory perception and behavior. Journal of Neurophysiology, 115(6), 2852–2866. https://doi.org/10.1152/jn.01056.2015

Whitlock, J. R., Pfuhl, G., Dagslott, N., Moser, M.-B., & Moser, E. I. (2012). Functional split between parietal and entorhinal cortices in the rat. Neuron, 73(4), 789–802. https://doi.org/10.1016/j.neuron.2011.12.028

Wilber, A. A., Clark, B. J., Forster, T. C., Tatsuno, M., & McNaughton, B. L. (2014). Interaction of egocentric and world-centered reference frames in the rat posterior parietal cortex. The Journal of Neuroscience: The Official Journal of the Society for Neuroscience, 34(16), 5431–5446. https://doi.org/10.1523/JNEUROSCI.0511-14.2014

Wilke, M., Kagan, I., & Andersen, R. A. (2012). Functional imaging reveals rapid reorganization of cortical activity after parietal inactivation in monkeys. Proceedings of the National Academy of Sciences of the United States of America, 109(21), 8274–8279. https://doi.org/10.1073/pnas.1204789109

Wu, Z., Litwin-Kumar, A., Shamash, P., Taylor, A., Axel, R., & Shadlen, M. N. (2020). Context-Dependent Decision Making in a Premotor Circuit. Neuron, 106(2), 316–328.e6. https://doi.org/10.1016/j.neuron.2020.01.034

Yang, G. R., Joglekar, M. R., Song, H. F., Newsome, W. T., & Wang, X.-J. (2019). Task representations in neural networks trained to perform many cognitive tasks. Nature Neuroscience, 22(2), 297–306. https://doi.org/10.1038/s41593-018-0310-2

Yates, J. L., Park, I. M., Katz, L. N., Pillow, J. W., & Huk, A. C. (2017). Functional dissection of signal and noise in MT and LIP during decision-making. Nature Neuroscience, 20(9), 1285–1292. https://doi.org/10.1038/nn.4611

Zatka-Haas, P., Steinmetz, N. A., Carandini, M., & Harris, K. D. (2020). A perceptual decision requires sensory but not action coding in mouse cortex. In bioRxiv (p. 501627). https://doi.org/10.1101/501627

Zhong, L., Zhang, Y., Duan, C. A., Deng, J., Pan, J., & Xu, N.-L. (2019). Causal contributions of parietal cortex to perceptual decision-making during stimulus categorization. Nature Neuroscience, 22(6), 963–973. https://doi.org/10.1038/s41593-019-0383-6

Zhuang, J., Ng, L., Williams, D., Valley, M., Li, Y., Garrett, M., & Waters, J. (2017). An extended retinotopic map of mouse cortex. eLife, 6. https://doi.org/10.7554/eLife.18372

Zingg, B., Hintiryan, H., Gou, L., Song, M. Y., Bay, M., Bienkowski, M. S., Foster, N. N., Yamashita, S., Bowman, I., Toga, A. W., & Dong, H.-W. (2014). Neural networks of the mouse neocortex. Cell, 156(5), 1096–1111. https://doi.org/10.1016/j.cell.2014.02.023

Zylberberg, J. (2017). Untuned but not irrelevant: The role of untuned neurons in sensory information coding. In bioRxiv (p. 134379). https://doi.org/10.1101/134379